1974

Dynamics And Control Of A Multistage Fluidized Bed Gas Adsorber

Kyriacos Papadatos

DYNAMICS AND CONTROL OF A MULTISTAGE FLUIDIZED BED GAS ADSORBER

by

Kyriacos Papadatos

Faculty of Engineering Science

Submitted for partial fulfillment of the requirements for the degree of Doctor of Philosophy

Faculty of Graduate Studies

The University of Western Ontario

London, Canada

August 1974

ABSTRACT

The performance of a four-stage gas-solid fluidized bed adsorber with downcomers has been studied. The feedrate of solids into the adsorber was measured by a momentum dissipation type solids flowmeter which was specifically designed for low flowrates (0-2.0 lb./min.). The major improvements of this flowmeter compared to the prior art were the use of strain gages and the use of an inclined tube instead of an inclined plate. When coupled with a proportional-integral controller this flowmeter provided excellent control of solids flowrate to the adsorber.

The steady state solids holdup of the shallow beds was found to be linearly dependent on the flowrate of the overflowing solids. Due to this linear relationship the dynamic response of the tray solids holdup was first order. The effect on the time constant of the gas flowrate, the height and the diameter of the downcomer was determined. For the same type of solids it was found that the gas flowrate had no effect on the time constant; on the contrary, the time constant increased with the weir height and decreased with the weir diameter; specifically, for activated carbon when the weir height was increased from 1 to 3 inches and the column to weir diameter ratio ($\frac{d_b}{d_\omega}$) was 8.8, the time constant increased from about 0.2 to 0.5 minutes. At a ratio ($\frac{d_b}{d_\omega}$) of

4.4 the time constant varied from 0.13 to 0.30 minutes. For a ratio $(\frac{d_b}{d_\omega})$ of 13.6 the holdup to solids flowrate relationship was non-linear.

The effect of the nature of the solids on the time constant in the tray solids holdup dynamics was investigated using sand as the fluidized solids. Under similar experimental conditions the time constant for the sand was 2.3 times that for carbon.

Through the use of a strain gage weighing system it was also found that fluidized solids do not rest on the grid but that they are totally suspended.

A mathematical model for the multistage fluidized bed adsorption process was developed. Using this model the process was simulated and the performance of an effluent composition control scheme was studied. The solids feed was the manipulated variable and the inlet composition was the process load. It was found that the effluent composition can be easily controlled by only a proportional controller.

ACKNOWLEDGEMENTS

The author wishes to express his sincere appreciation to Dr. W. Y. Svrcek for his efficient guidance, his friendly cooperation, and his general understanding throughout this project.

Appreciation is extended to Dr. M. A. Bergougnou for his valuable comments on fluidization problems and to all faculty members that contributed to this work.

Thanks are due to the National Research Council of Canada, to the University of Western Ontario, and to the Ontario Provincial Government for providing financial support to the author.

TABLE OF CONTENTS

PAGE

List of Tables

List of Figures

NOMENCLATURE

A	- constant, cu.ft./lb. or cross section area, sq.ft.
a	- height of downcomer narrow section, in.
b	- distance between plate and bottom of downcomer or width, in.
B	- constant, cu.ft./mol.
C	- constant
c	- length of downcomer section immersed into fluidized bed or thickness, in.
d	- diameter, ft. (or as stated)
E	- constant, ft.
e	- elasticity coefficient
F	- force, (lb.force) or gas flowrate, cu.ft./min.
f	- friction coefficient
g	- gravity acceleration, ft./sec.^{2}
g_c	- unit conversion factor, 32.2 (ft.) (lb.)/(lb.force) (sec.^{2})
H	- height of the bed, in. or holdup, lb.
H'	- holdup deviation from steady state, $H-H_s$, lb.
h	- height of dense phase in downcomer or simply height, in.
I	- impulse, (lb.force) (sec.)
K	- controller gain, or constant
L	- solids flowrate, lb./min.
L'	- solids flowrate, lb./cu.ft. of gas
l	- distance between two consecutive plates or simply length, in.
m	- mass, lb; or equilibrium constant, lb./cu.ft.

$\dot{m}$	- mass flowrate, lb./min.
n	- number of particles
n_1, n_2, n_3	- exponents
ΔP	- pressure drop, (lb.force)/sq.ft.
s	- stress, (lb.force)/sq.in.
S	- recorder output between fluidized and unfluidized state, %
t	- time, min.
Δt	- time interval, min.
u	- velocity, ft./sec.
x	- elevation, in.
X	- concentration in solids phase, mol./lb.
Y	- concentration in gas phase, mol./cu.ft.
z	- width, in.

GREEK LETTERS

α	- constant
ε	- porosity of carbon in the dense phase
θ	- angle, degrees
ρ	- density, lb./cu.ft.
τ	- constant, min.

SUBSCRIPTS

b	- bed, bulk
d	- distributor
do	- downcomer
f	- fluidization
g	- gas
i	- inlet

j	- plate number (j=1,2,3,4)
ℓ	- downcomer large section
m	- minimum
n	- downcomer narrow section
o	- unfluidized solids or initial value
p	- plate, particle
s	- solids or steady state
sd	- solids, dense phase
v	- vertical
ω	- weir

CHAPTER 1

INTRODUCTION

Fluidization was first introduced on a commercial scale by BASF in Germany in 1926 for the gasification of coal. Since then, the technique has assumed an increasing importance and numerous applications have been reported during the last thirty years (1)(2).

Fluidization is a unit operation in which fine solids are transformed into a fluid-like state through contacting with a gas or liquid. Fluidized beds present several advantages when compared to fixed beds. The most important of these are as follows:

1. Isothermal operating conditions due to vigorous mixing of solids.
2. High value of mass transfer, heat transfer, and reaction rate coefficient due to the large surface to volume value resulting from the use of small particles.
3. Continuous operation and ease of regulating the flowrate of circulating solids and solids holdup.
4. Substantial reduction in the diameter of the column due to higher permissible gas velocities.

Fluidized beds also have some disadvantages when compared to fixed beds and the most serious of these are as follows:

1. Reduction of the process driving force due to the axial mixing of solids and to a lesser extent of gases.
2. Formation of bubbles which coalesce growing larger in size as the bed height increases. The resulting channelling of bubbles up the middle of the bed results in mechanical disturbances and lower conversions.

Both of these disadvantages can be eliminated by using a number of shallow beds instead of a single one. This approach is known as multistage fluidization and is currently being used for a number of processes such as ore reduction, chlorination of ilmenite, drying of some granular materials, calcining of limestone, adsorptions, etc.(2).

Adsorption of organic vapors on activated carbon in multistage fluidized bed gas adsorbers has been recently used in air pollution control. Although such adsorbers may be designed without downcomers(3) using dowcomers seems to be more attractive from an industrial point of view. Rowson(4) reported that a five stage fluidized bed adsorber, 38 feet in diameter, has been used for recovery of CS_2 (0.1% in air) by using activated carbon with an efficiency of 90-95%. In another similar unit, 40 feet in diameter, for the recovery of acetone, Avery and Tracey(5) reported efficiencies of 99%. They also stated that the same process is being used for the recovery of other solvents such as ethanol, ethyl acetate, and mixed hydrocarbons.

Unfortunately there is little in the literature related to control problems for this adsorption process. It seems

that effluent concentrations were not controlled, but rather, set below an upper limit which was easily attained by manual operation. In fact, Rowson(4) reported that the CS_2 effluent concentration varied between 50 and 100 parts per million. The significance of this rather large variation should be evaluated with respect to both the economics of the process and the forthcoming stricter air pollution laws. In the light of the previous comment the objective of the present work was to design a multistage fluidized bed gas adsorber for an air-CS_2 lean mixture with activated carbon as adsorbent and using the incoming flowrate of carbon as the manipulated variable to control the adsorber-CS_2 exit composition. The project was divided into the following parts:

1. Design of a four-stage fluidized bed gas-adsorber.
2. Development of a low range solids flowmeter and application to solids flow control.
3. Dynamics of the tray solids holdup for the four-stage fluidized bed.
4. Development of a process model and application to effluent exit composition control via simulation.

CHAPTER 2

DESIGN OF A MULTISTAGE FLUIDIZED BED GAS ADSORBER

The concept of design in its true interpretation must be interrelated to both technological and economical factors. However, in academic research first priority is given to technology advancement and any limitations imposed by the economics is left as a problem to be solved by industrial research. In the design approach which will be presented here for a multistage fluidized bed gas adsorber only parameters related to the technical aspects will be considered. These parameters are as follows:

1. Diameter of the adsorber.
2. Air distributor and plate open area.
3. Dimensions of downcomers, and
4. Number of beds.

2.1 Adsorber diameter

The criterion which determines the diameter of a fluidized bed is the flowrate of the gas which has to be handled. This quantity should equal the product of the column cross-section area times the gas superficial velocity; that is

$$F = \frac{\pi d_b^2}{4} \times u_g \qquad (2.1)$$

Solving (2.1) for d_b gives:

$$d_b = \left(\frac{4F}{60\pi u_g}\right) \qquad (2.2)$$

The superficial gas velocity u_g is a function of the minimum fluidization velocity u_{mf} which may be computed from fluid and solids characteristics(6) but the best way is to have it determined experimentally. Obviously u_g has to be greater than u_{mf} but how much greater is a matter of optimization depending on many factors. The approach used in this work was to rely on literature information about similar processes. For activated carbon of 1200 microns mean particle diameter, Molodov and Ishkin reported(7) that the minimum fluidization velocity was approximately 1 ft/sec; on the other hand, for attaining good solids mixing, these authors recommended that the superficial gas velocity be 1.5-2.6 times the minimum fluidization velocity. On the basis of this recommendation u_g was set equal to 2 ft/sec; substituting this value into formula (2.2) and using a gas flowrate F = 90 cu.ft/min, resulted in a column diameter approximately equal to 11 inches.

2.2 Design of air distributor and perforated plates

In a fluidized bed column the fluidizing gas has to be discharged through a nozzle of much smaller diameter than the diameter of the column. The flow patterns of the jet then has to be rearranged so that the gas acting on the bed is uniformly distributed or otherwise a part of the bed will

remain unfluidized. The uniform gas flow distribution may be accomplished by placing a grid above the nozzle. The open area of the grid is designed to provide a sufficient pressure drop which in turn will result in a uniform gas distribution.

Unfortunately there is no strict criterion as to how much the above pressure drop should be. For deep beds Agarwall *et al.* (8) recommended that the pressure drop across the distributor be approximately 10% of the pressure drop across the bed with a minimum in all cases of about 35 centimeters water. For a multistage fluidized bed where the air distributor is not in contact with the solids and shallow beds are used a minimum pressure drop of 35 centimeters water was considered as the design basis. Following the approach suggested by Kunii and Levenspiel(6) a distributor with 0.62% open area and 150 holes of 0.09" diameter resulted. A detailed design procedure for gas distributors in fluidized beds can also be found in a work by Rylec and Standart(9).

The design of the perforated plates which are to be used to support the shallow beds, is based on a work by Molodov and Ishkin(7). The authors recommended that an open plate area of 8-10% be used for having stable operation. On the basis of this recommendation the plates were made of aluminum perforated sheets 3/16 of an inch thick and with 10% open area; a staggered pattern with 3/8 of an inch centers and 0.125 of an inch hole diameter was selected. To prevent dumping of solids through the holes, the plates were covered by a fine mesh screen.

2.3 Design of downcomers

Figure 1 is a view of the downcomer designed for the multistage fluidized bed absorber based on the work of Molodov and Ishkin(7). The design procedure was based on the two following criteria. First, in order that the operation be stable the solids flowing through the downcomer should be in a dense phase; this was achieved by enlarging the diameter above the bottom of the downcomer leg. Secondly, the solids should be able to flow freely; this criterion requires a minimum value for the diameter of the downcomer at the gas inlet section. This value can be computed from the following equation:

$$L = L'F = 60 \frac{\pi}{4} d_n^2 u_s \rho_o \qquad (2.3)$$

The carbon velocity u_s and the carbon flowrate L' through the downcomer were assumed (very conservative) as 0.03 ft/sec (7) and 0.0066 lb/(cu.ft. of gas), respectively. The value for the carbon flowrate is double that used in the commercial units described by Rowson(4) and Avery(5). On the other hand the bulk density of carbon powder is about 30 lb/cu.ft. Introducing these values into equation (2.3) the diameter d_n of the lower part of the downcomer was found equal to 1 inch. The computation for the diameter d_1 of the large section was based on the fact that the gas flow through the two different sections of the downcomer must be the same, that is:

$$\varepsilon \frac{\pi}{4} d_n^2 u_n = \varepsilon \frac{\pi}{4} d_1^2 u_1 \qquad (2.4)$$

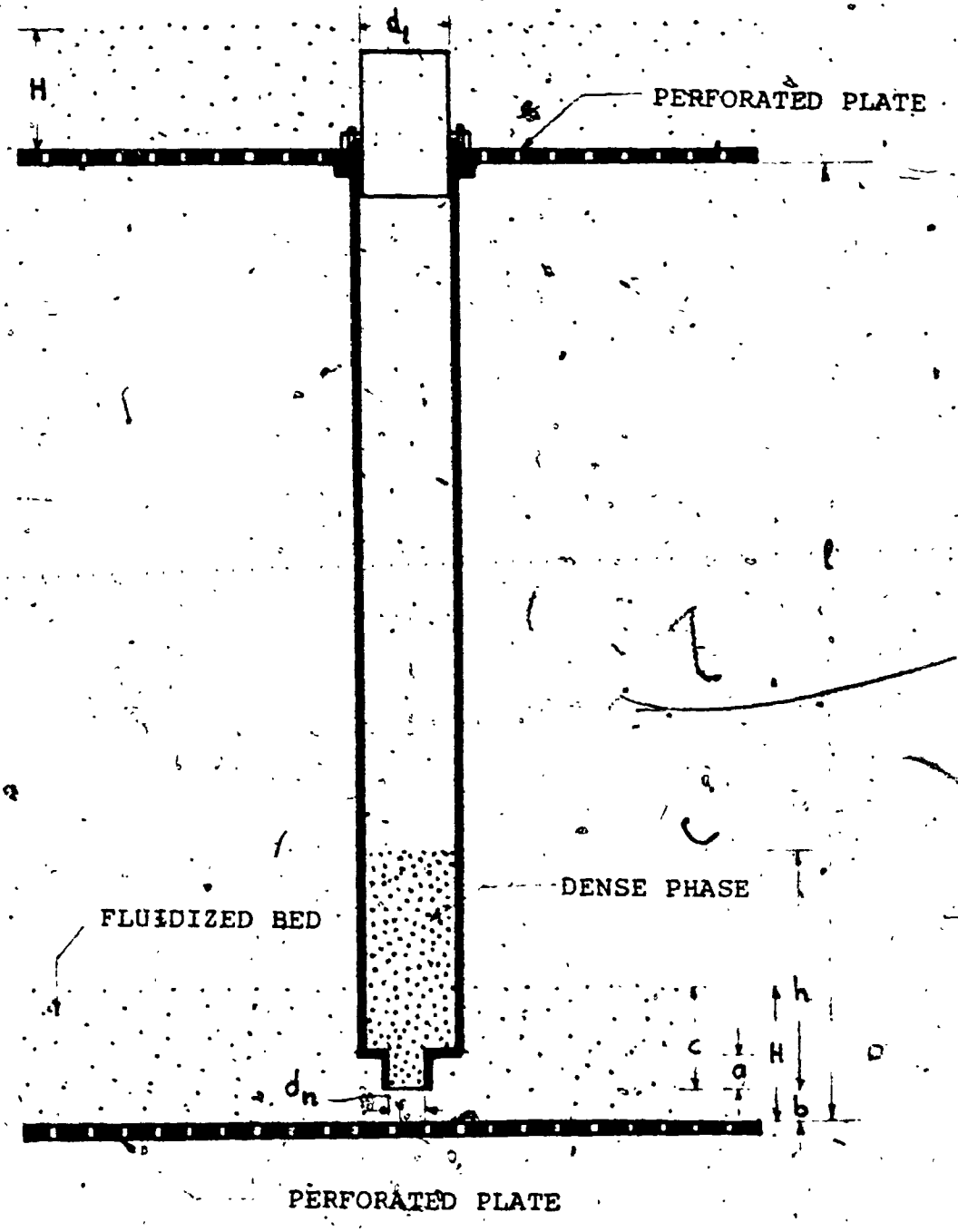

FIGURE 1. VIEW OF DOWNCOMER WITH FLUIDIZED BED IN OPERATION

Molodov and Ishkin assume $u_n = u_g$ (2.5)

Substituting u_n for u_g into equation (2.4) results in the following equation:

$$d_l = d_n \left(\frac{u_g}{u_l}\right)^{\frac{1}{2}} \quad (2.6)$$

To secure a dense phase in the downcomer the ratio (u_g/u_l) was taken equal to 2. Substituting this value into equation (2.6) results in a d_l equal to 1.4 inches.

The height ℓ can be computed from a pressure balance at the bottom of the downcomer

$$h\rho_{sd}\, g = c\rho_b g + H\rho_b g + 12 g_c (\Delta P_p + \Delta P_{do}) \quad (2.7)$$

Equation (2.7) after rearrangement becomes:

$$h = (c + H)\frac{\rho_b}{\rho_{sd}} + 12 g_c \left(\frac{\Delta P_p}{g\rho_{sd}} + \frac{\Delta P_d}{g\rho_{sd}}\right) \quad (2.8)$$

If the superficial gas velocity u_g is not greater than twice the minimum fluidization velocity u_{mf}, then the solids in the downcomer will be unfluidized. This implies that the bulk density of solids ρ_{sd} in the downcomer equals the bulk density of the unfluidized solids ρ_o. On the other hand, between fluidized and unfluidized bed the following relationship is valid.

$$H \rho_b = H_o \rho_o \quad (2.9)$$

Combining equations (2.8) and (2.9), and substituting ρ_{sd} for ρ_o results in:

$$h = K\left[\frac{(H+c)H_o}{H^2} + 12\frac{g_c\Delta P_p}{g\rho_o}\right] \qquad (2.10)$$

where K is a coefficient which takes into account the term $(g_c\Delta P_d/g)$ that results from the resistance of the downcomer to the gas flow. According to Molodov and Ishkin(7), for L = 0.22 lb/min, u_g = 2 ft/sec, and H_o = 1.5 inches it was found that ΔP_p = 1.64 (lb.force)/(sq.ft), H = 4 inches, and K = 1.5. Introducing these values into equation (2.10) and realizing that c = H-b (where b = 1 inch), the height of the dense phase h in the downcomer was found to be 10 inches. Since the above authors recommended a height ℓ for the downcomer 3 to 5 times the value of h it was decided for the present work to take ℓ equal to 3h; in other words to space the plates at 30 inches.

2.4 Number of beds

Computation of the number of beds for the absorber was not carried out and was set arbitrarily at four. Theoretical work on absorption in fluidized beds has been presented by several authors(10),(11),(12),(13). These authors present analytical expressions for mass transfer coefficients and number of transfer units. However, it is the opinion of the author that such expressions should be used only as guidelines and scale-up should be applied for realistic estimates.

Figure 2 shows a schematic and Figure 3 is a photograph of the overall view of the column. It was made of six acrylic sections. The three middle sections are 2 1/2 feet

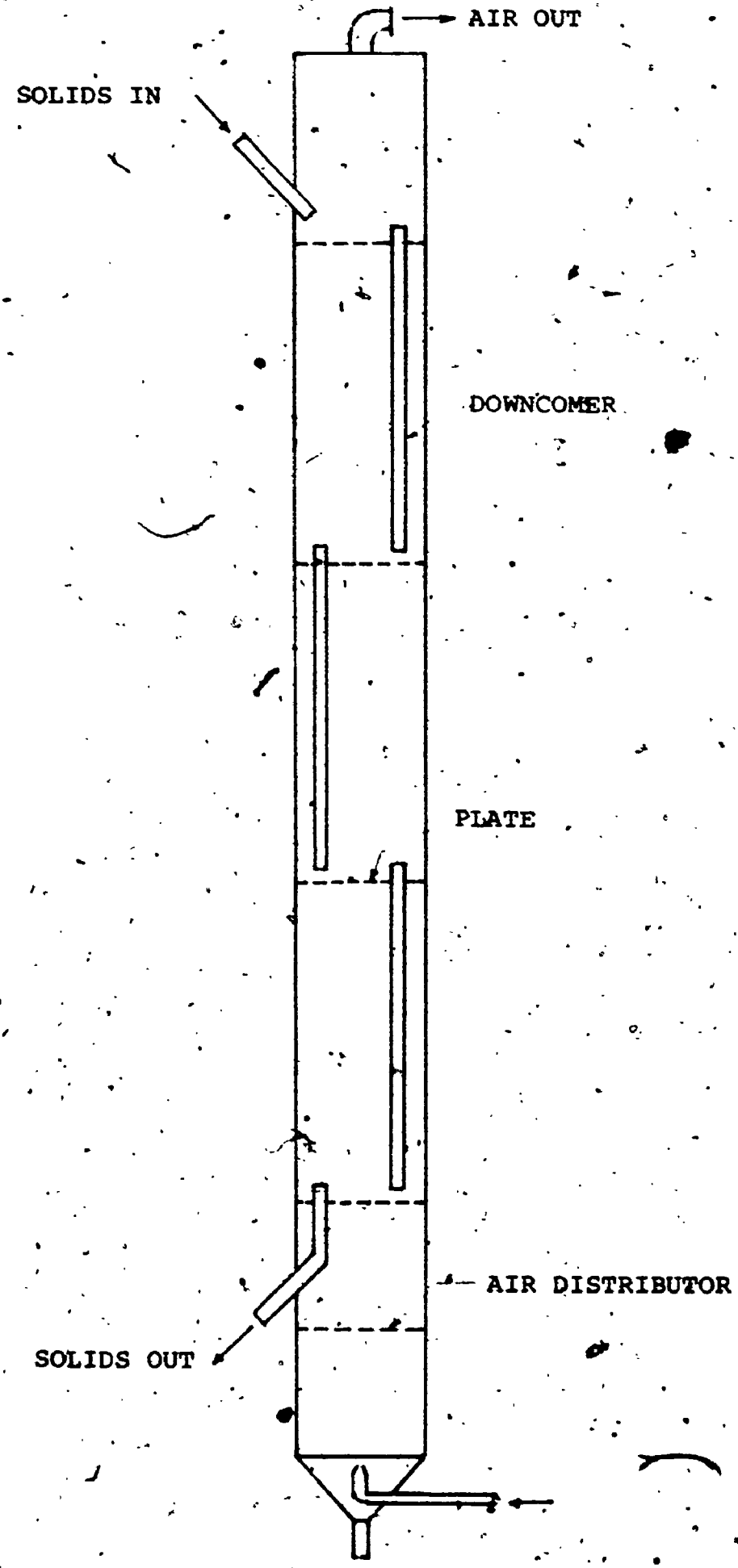
AIR OUT
SOLIDS IN
DOWNCOMER
PLATE
AIR DISTRIBUTOR
SOLIDS OUT

FIGURE 3. OVERALL VIEW OF THE COLUMN

high, the top section is 1 1/2 foot high, and the two lower sections are each 1 foot high. The detailed drawings of these components are presented in Appendix A.

CHAPTER 3

DEVELOPMENT OF A SOLIDS FLOWMETER

The devices available for measuring solids flowrate are based to a large extent on the principle of the momentum change resulting when solids fall from a certain height onto an inclined surface. There are a whole variety of these devices; some have been discussed in the literature while others are already patented and available commercially.

One of the earliest momentum dissipation type solids flowmeters was developed by Dean(14). It consisted essentially of an inclined plate (the sensor), attached to a lever supported half-way by a fulcrum. The free end of the lever deflects due to a changing mass flowrate of solids and this deflection was measured by a force measuring system. The device was claimed to be linear within an accuracy of ±2.5% of the highest reading, and capable of measuring, recording, and controlling the flowrate of granular materials. The operating range in laboratory scale was said to be 4 to 19 pounds per minute and in industrial scale 55 to 234 pounds per minute.

Another similar device was developed by Noble Company(15). The solids fall onto a hemisphere shaped sensor and the impact was transmitted by a lever arm to a spring-scale type force

sensor. The deflection of the force sensor was measured by a linear differential transformer. The meter was claimed to be linear and suitable for automatic control. It is available in ranges from 5 to 4000 pounds per minute.

Another variety of the momentum type solids flowmeter was described by Kumar(16). The solids fall from a height onto an 'impact receiver' (a cone) attached to a lever. The impact force produces a bending moment around a fulcrum. A pointer attached to the other end of the lever was used to indicate the mass flowrate. This device suffers from two disadvantages; (a) it is not linear and (b) measurements are based only on a fraction of the flowing solids. It was operated over a range of 120 g/min to 960 g/min.

A somewhat different, non beam-type solids flowmeter was developed by Nolte(17). The falling particles strike a spring loaded impulse sensor. The position of the impulse sensor is detected by a pneumatic transducer. The device was claimed to be linear for a 30 to 1 turndown but no data was presented.

The Sankyo Impact Line Flowmeter(18) is still another kind of the momentum type flowmeter. It consists of an inclined plate (sensor) and a beam attached to it. The horizontal component of the impact force acts against a compression spring and this is converted to a horizontal movement. Transients are smoothed out by means of a viscous damper and the movement is converted to an electrical signal by a linear differential transformer. Range of operation

was reported as 20 pounds per hour to 10,000 tons per hour. A number of patents associated with the momentum type solids flowmeter have also been issued (19), (20), (21), (22), (23).

Unfortunately, none of the flowmeters reported could provide an operating range of 2 to 20 pounds per hour as was required by the size of the absorber to be used for the experiments. This limitation led to the development of another kind of momentum dissipation solids flowmeter as part of the present work. Its major improvements consist of replacing the inclined plate by an inclined tube and measurement of the impact force by strain gages.

3.1 Theory

Consider a particle of mass m dropped from a height h onto a plate inclined at an angle θ, Figure 4. The particle will strike the plate with a velocity $\vec{u}_1$ and will be deflected off the plate with a velocity $\vec{u}_2$. An impulse I felt by the plate is equal to

$$\vec{I} = \vec{F} \times \Delta t = m \times (\vec{u}_1 - \vec{u}_2) \qquad (3.1)$$

where Δt is the interval of time during which the impact of the particle takes place.

It should be noted that u_1 is a function only of the height h provided that the air resistance is negligible (particle not too small); the velocity u_2 is a function of the height h, the coefficient of friction f between the plate and the particle, and the coefficient of elasticity e of the particle.

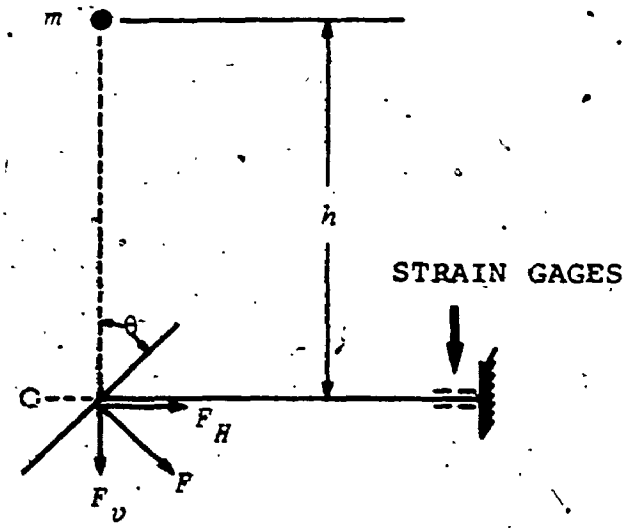

FIGURE 4. PLATE-BEAM COMBINATION FOR SENSING FLOWING SOLIDS

For a continuum of particles equation (3.1) becomes

$$\vec{I} = \Delta t \times \sum_{i=1}^{n} \vec{F}_i = (\vec{u}_1 - \vec{u}_2) \times \sum_{i=1}^{n} m_i \tag{3.2}$$

where Δt now is the interval of time during which the impact of all the particles takes place.

Equation (3.2) may be rewritten as follows:

$$\vec{F} = \vec{k}_1 \times \dot{m} \tag{3.3}$$

where

$$\vec{k}_1 = \vec{u}_1 - \vec{u}_2 \tag{3.4}$$

$$\dot{m} = \frac{\sum_{i=1}^{n} m_i}{\Delta t} \tag{3.5}$$

and

$$\vec{F} = \sum_{i=1}^{n} \vec{F}_i \tag{3.6}$$

The cantilever beam attached to the impact plate was strain gaged, as shown in Figure 4, to sense only the bending moment caused by the component $\vec{F}_v$. Since $\vec{F}_v = \vec{F} \sin \theta$, equation (3.3) may be written as follows:

$$\vec{F}_v = \vec{F} \sin \theta = \vec{k}_1 \times \dot{m} \sin \theta \tag{3.7}$$

or

$$\vec{F}_v = \vec{k}_2 \times \dot{m} \tag{3.8}$$

where

$$\vec{k}_2 = \vec{k}_1 \times \sin\theta$$

The stress caused by the component F_v for a rectangular cross-section beam is given as in equation (3.9).

$$s = \frac{6\, F_v\, l}{b\, e^2} \qquad (3.9)$$

From this relationship it can be seen that for the same value of the force F_v, the stress s is a function of the dimensions of the beam. Common practice is to keep the length l and the width b constant while the thickness e can vary whenever a change of the operating range of the flowmeter is desired.

3.2 Description of the flowmeter and preliminary experiments

Figure 5 is a schematic of the solids flowmeter. It consists of the following parts: (a) a pickup tube, (b) a bracket, (c) a metal mounting block, and (d) a dashpot.

The pickup tube is made of transparent acrylic tube - 1 inch inside diameter, 3 inches long - and it is inclined at an angle θ. The value of the angle θ was determined experimentally based on the following two criteria; (a) the angle should be big enough so that the solids can flow freely and not accumulate in the tube; (b) the angle should be small so that the impact of the solids is maximum. On the basis of these two criteria a value of 30° resulted. As it can be seen from Figure 5, the solids falling in the tube cause a

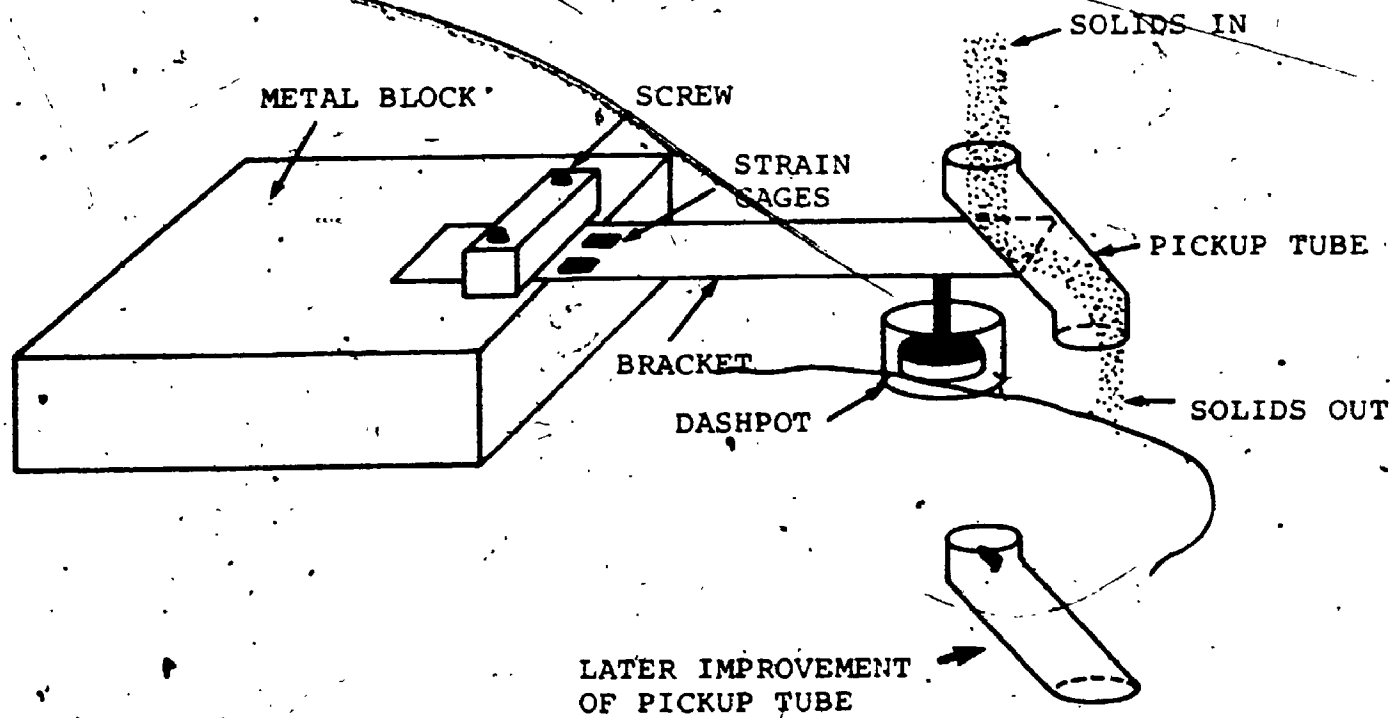

FIGURE 5. SCHEMATIC OF THE SOLIDS FLOWMETER

bending moment on the bracket but they bounce again and strike the lower vertical part of the pickup tube causing a bending moment in the opposite direction. This resulted in a decrease in sensitivity and non-linearity in the output. This problem was solved by eliminating the lower vertical part of the pick-up tube. Figure 6 is a photograph of the solids flowmeter after the above modifications.

The bracket is of aluminum - 4 inches long, 1 inch wide, 1/32 of an inch thick - and is firmly supported on a 6" x 4" x 2" block of steel. The bracket is stressed under the influence of the flowing solids and this stress can be measured by four strain gages. Figure 7 shows how these strain gages were attached to the bracket and how they were connected in a Wheatstone bridge circuitry. The input and the output of the strain gages is supplied by a strain gage amplifier.

The dashpot shown in Figures 5 and 6 was used to damp out the mechanical vibrations of the system. Essentially it consists of a piston immersed in a viscous oil. For thin brackets bending occurs from the weight of the pickup tube and this created some problems in balancing the bridge. To overcome this problem the piston was made of a hollow air sealed cylinder of acrylic and the buoyancy effect was thus utilized to counteract the weight of the pickup tube.

The solids flow device described was to be used for measuring the flow of carbon to the column as part of the solids flow control loop. For this application the flowmeter was enclosed in an air sealed housing box of transparent

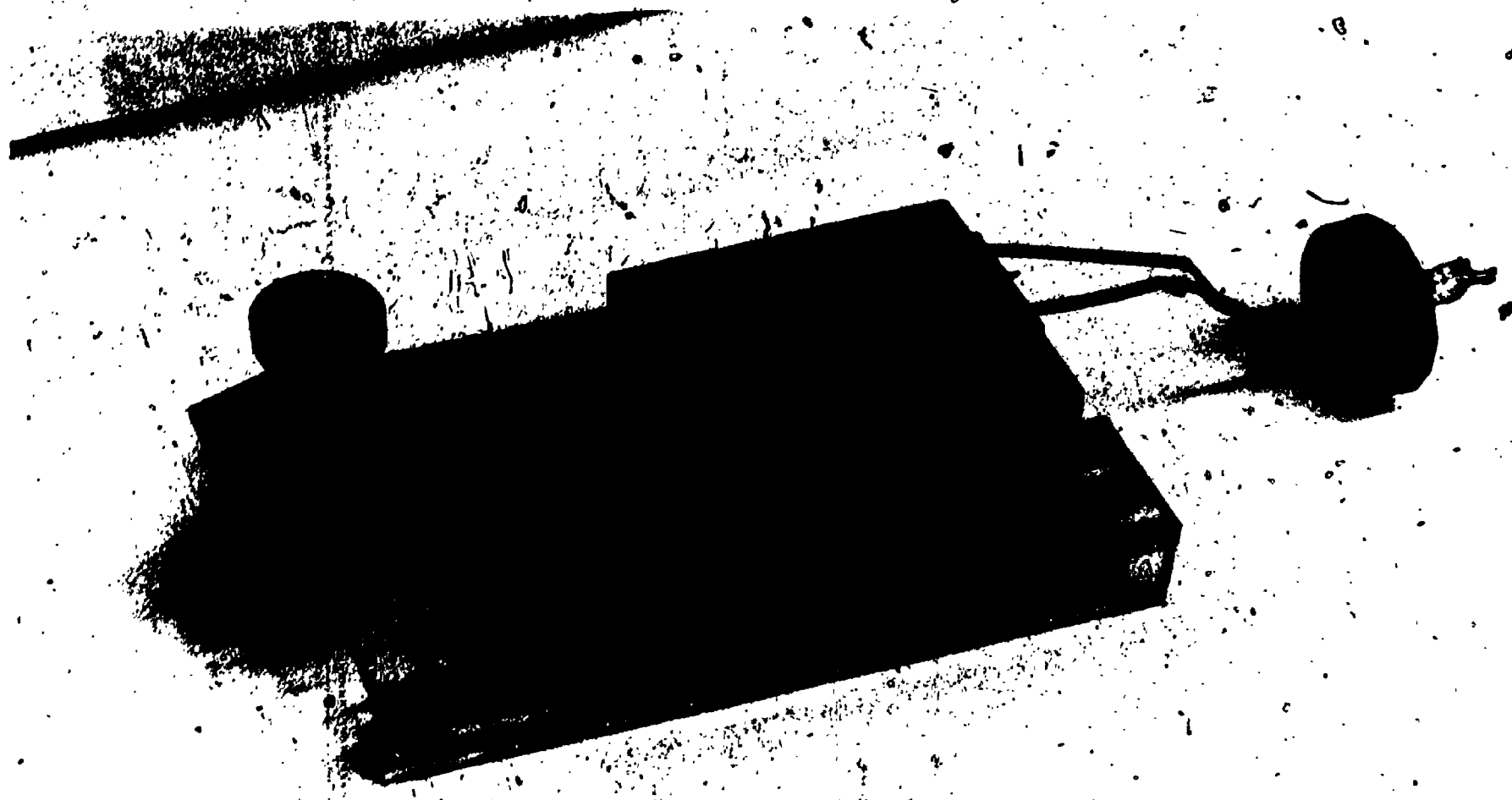

FIGURE 6. THE SOLIDS FLOWMETER AT ITS LAST STAGE OF DEVELOPMENT

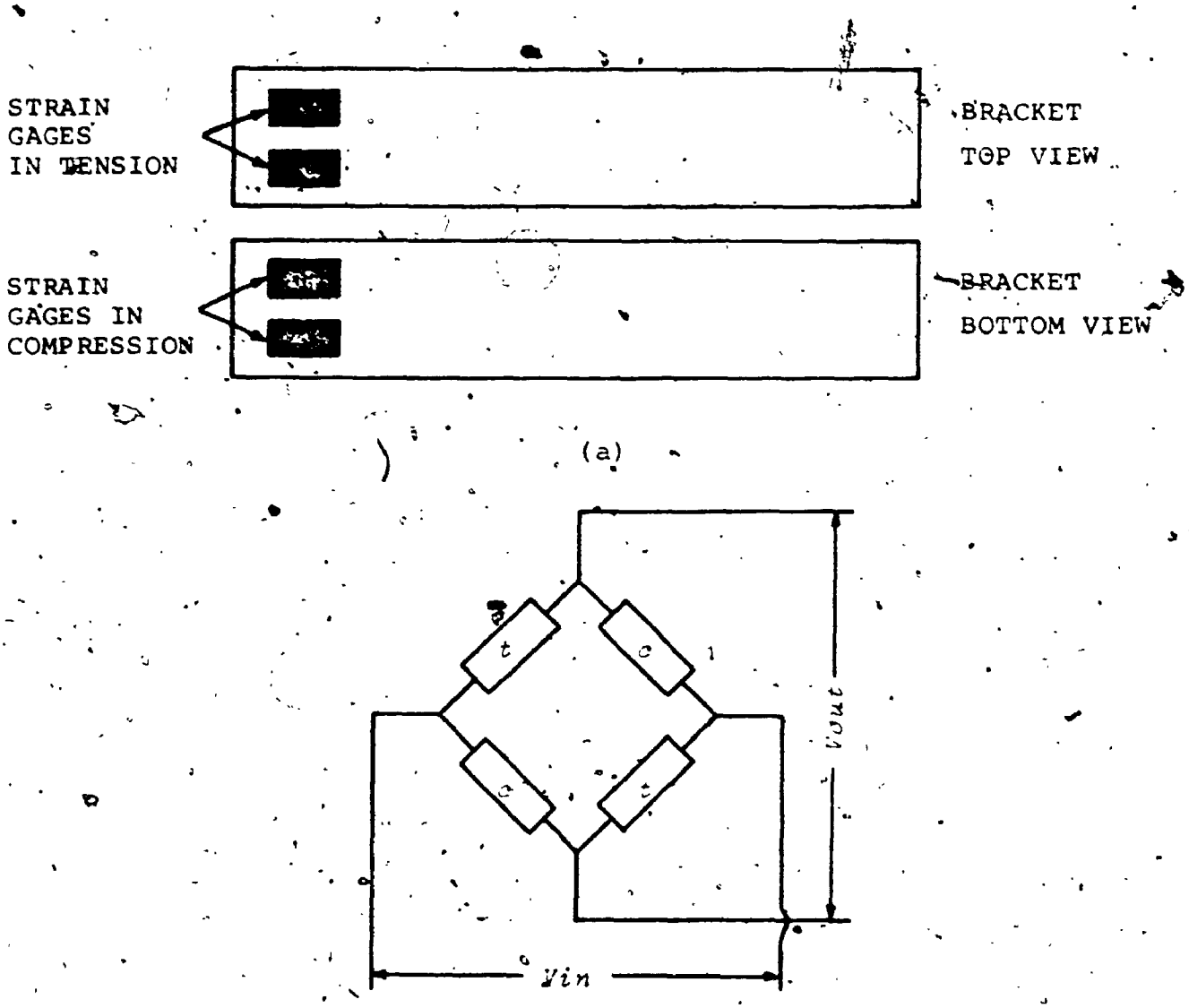

FIGURE 7. STRAIN GAGES SET-UP (a) ATTACHMENT ON THE BRACKET (b) WHEATSTONE BRIDGE CIRCUITRY

acrylic as shown in Figure 8. In order to isolate the flowmeter from vibrations, connections to the solids feeder and to the column were of flexible rubber gaskets.

A problem encountered during the first experiments was the fouling of the bracket and the oil dashpot by carbon dust escaping from the open ends of the pickup tube. This resulted in a zero shift and distortion of the calibration curve for the flowmeter. A first solution was to seal the two open ends of the pickup tube with flexible rubber gaskets. Surprisingly the gaskets prevented free flow of carbon even when there was no air flowing through the fluidized bed column. Gasketing of the open areas between the pickup tube and the carbon supply was abandoned in favour of a regulated stream of air into the housing box of the flow meter (non regulated flow resulted in noisy signal). The air supply was of sufficient pressure to prevent flow of carbon particles into the flowmeter housing. Figure 9 is a photograph of the flowmeter enclosed in the acrylic box.

With these final improvements the solids flowmeter could now be easily used for monitoring and control of continuous flow of solids into a fluidized bed column.

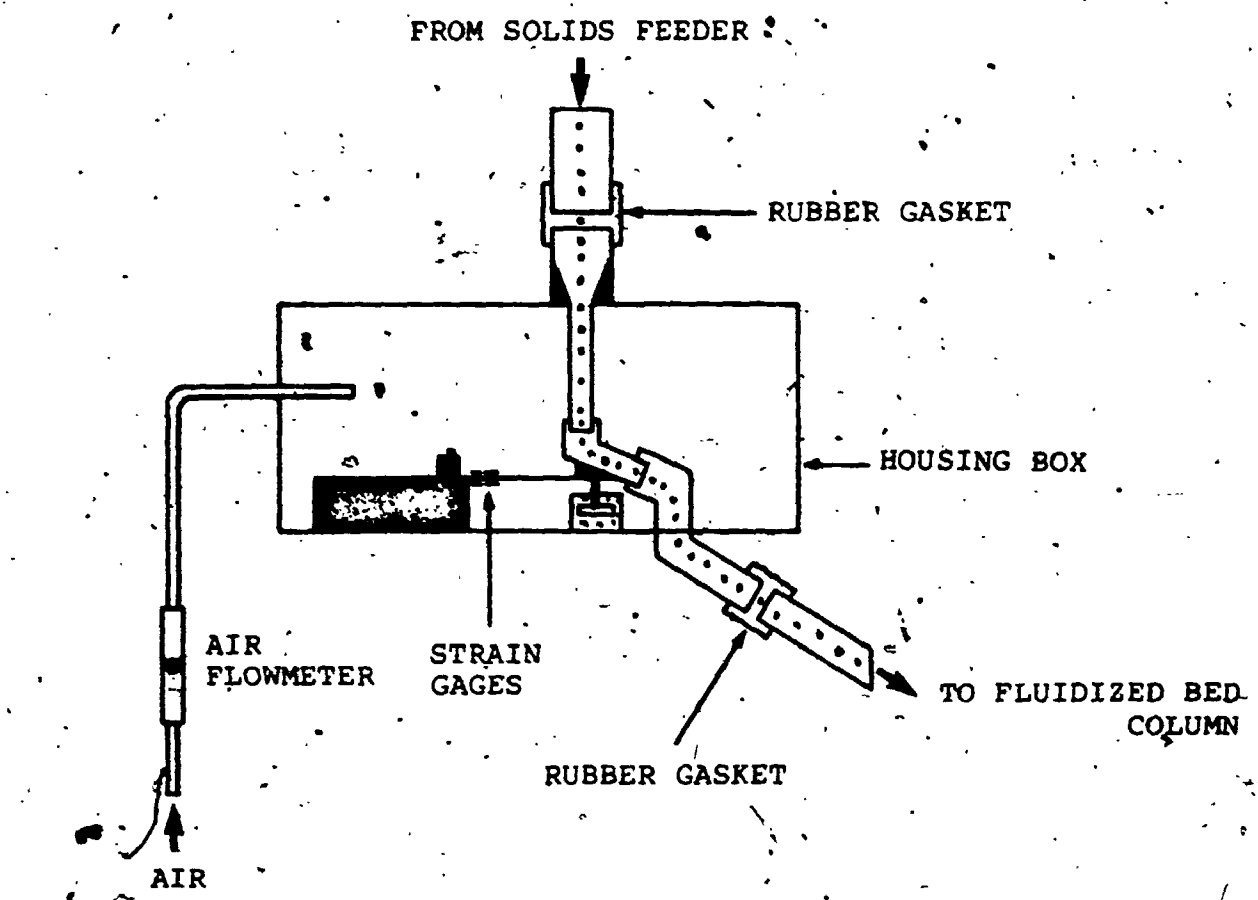

FIGURE 8. SOLIDS FLOWMETER ARRANGEMENT FOR FLUIDIZED BED APPLICATION

FIGURE 9. THE FLOWMETER AND THE HOUSING

CHAPTER 4

DYNAMICS OF THE TRAY SOLIDS HOLDUP FOR THE FOUR-STAGE FLUIDIZED BED

The main objective of this phase was to study the dynamics of solids holdup of each tray as a function of the solids and the gas flowrates. The results of this study in connection with the gas adsorption can then be used in modelling fluidized bed gas adsorbers.

4.1 Description of the adsorber

Figure 10 is a schematic of the four-stage fluidized bed adsorber and the auxiliary equipment used for experimentation.

The fluidizing gas was air. The gas flowrate was adjusted to the desired value and was measured using a rotameter. The air flow operating range was forty to eighty cubic feet per minute corresponding to one to two feet per second fluidization velocities. The gas leaving the column passed through a five inch diameter standard cyclone and then into the exhaust system.

The solids were charged directly onto the top plate of the column by means of a Syntron vibratory feeder. Figure 11 is a photograph of the top part of the column including the solids feeder, the solids flowmeter, and the cyclone. As the solids were passing downward from plate to plate through

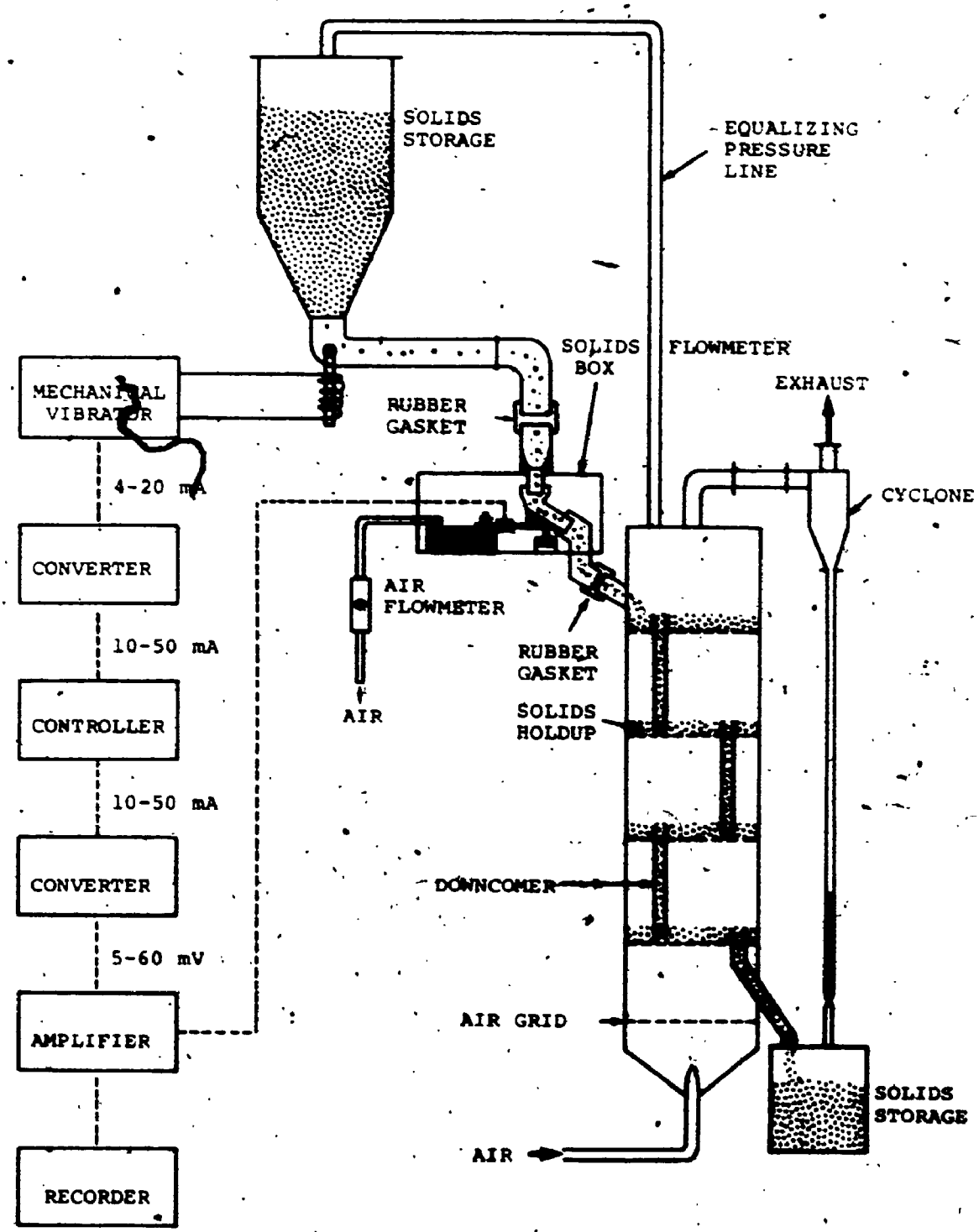

FIGURE 10. SCHEMATIC OF THE ADSORBER WITH AUXILIARY EQUIPMENT

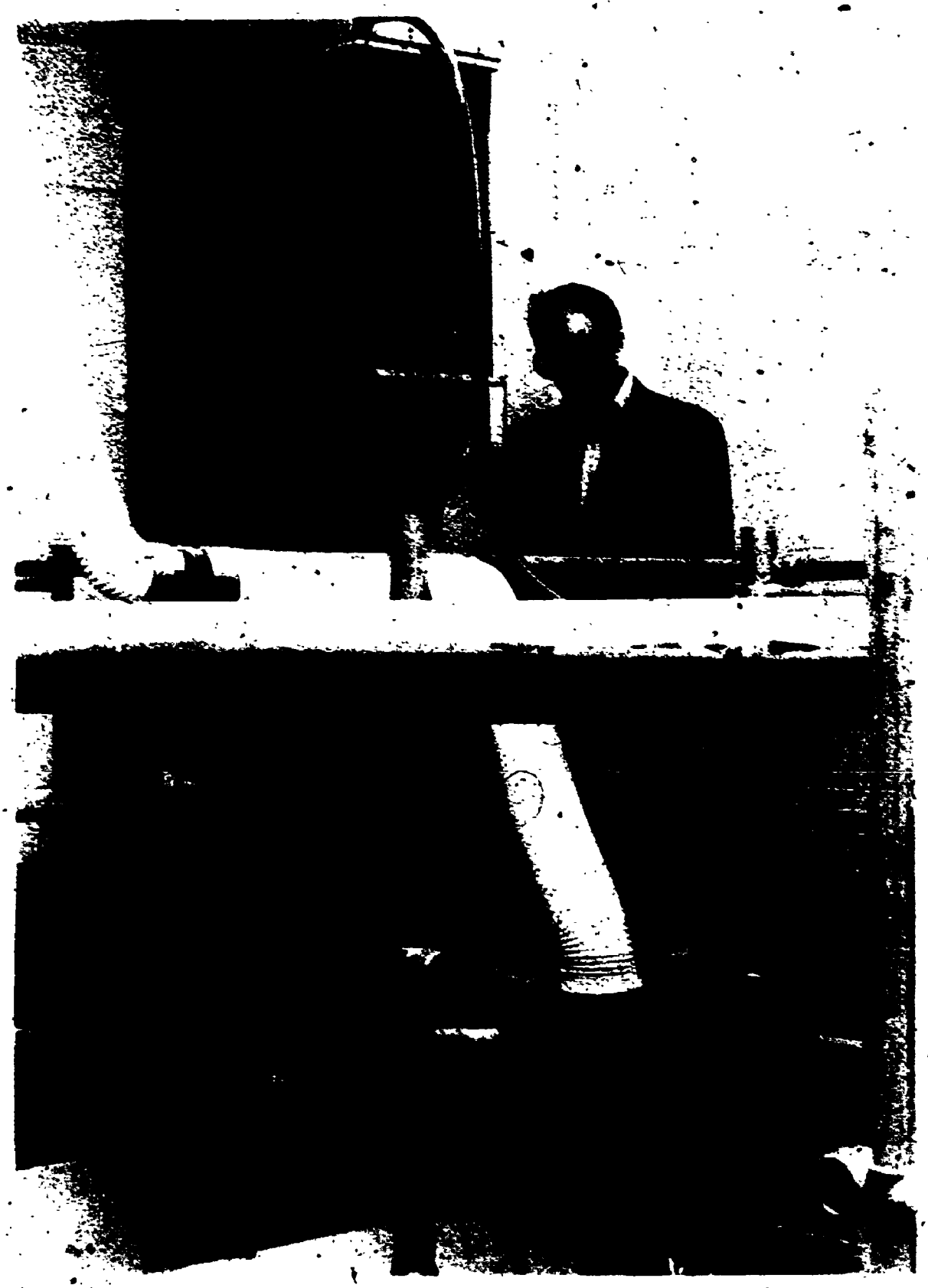

FIGURE 11. THE TOP OF THE COLUMN INCLUDING THE SOLIDS FEEDER, THE SOLIDS FLOWMETER, AND THE CYCLONE

the downcomers they were finally discharged into a storage barrel. On the other hand, the particles collected by the cyclone were accumulated in the dipleg and were discharged into the storage barrel during shut down of the column. The dipleg was valved off during operation to prevent gas flow from the barrel (being at higher pressure) to the cyclone. The solids feed into the column was measured by the flowmeter described in Chapter 3. In order to maintain a constant flow-rate the solids flowmeter was connected in a feedback loop with a proportional-integral controller tuned for flowrates between 0.5 lb/min and 2.25 lb/min.

Figure 12 shows the detailed set-up for measurement of the plate solids holdup. The plates are removable and supported on specially designed holders. These holders are connected to the support structure of the column by means of three light aluminum brackets at 120 degrees angle. In Figure 12 only one bracket is shown. Attached to each bracket there are four strain gages connected in Wheatstone bridge circuits as shown in Figure 7. The three bridges for each plate were connected in parallel so that the force acting on the plate results in the same signal regardless of the force's position on the plate. The input and output for the strain gages is provided by the same amplifier used for the solids flowmeter. Sealing between the plate holders and the column shell was attained by flexible rubber sleeves. Figure 13 is a picture of this arrangement as it was attached to the column including the plate, the plate holder, and the weir of

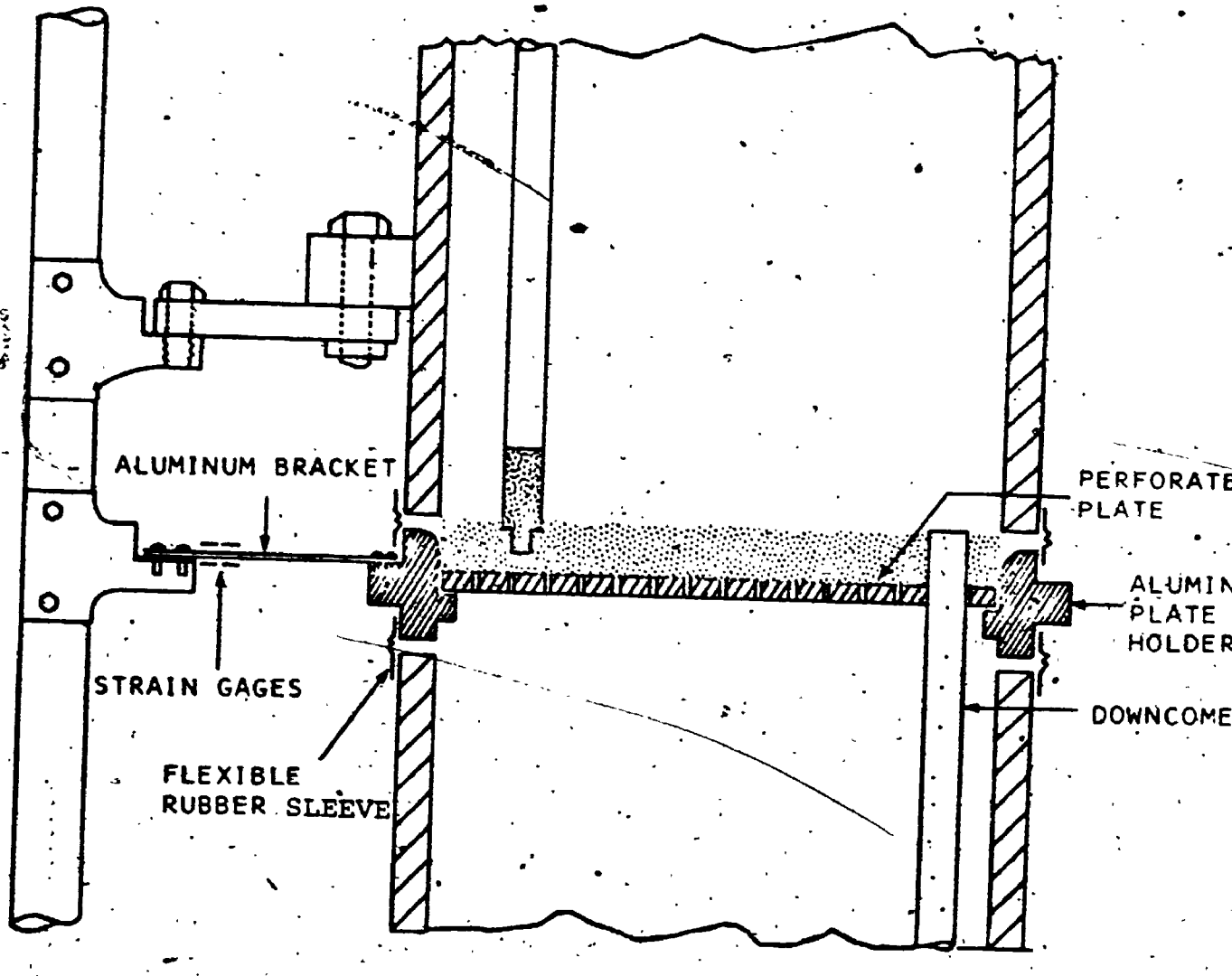

FIGURE 12. PLATE ARRANGEMENT FOR MEASURING THE SOLIDS HOLDUP

FIGURE 13. THE ARRANGEMENT PLATE-PLATE HOLDER AS IT WAS ATTACHED TO THE COLUMN

downcomer. The detailed drawings of the perforated plates, the plate holders and the aluminum brackets can be found in Appendix A.

4.2 Theory of dynamics of solids holdup

The expression 'solids holdup' is used to mean the amount of solids retained on each plate when the fluidized bed column is in operation. Due to many similarities of a multistage fluidized bed adsorber to a distillation column the analysis of the dynamics of the solids holdup will be similar to that for the liquid holdup in distillation columns. In spite of the importance of this subject literature information about experimental work is very restricted and this is of course a reflection of the difficulty of the problem.

An unsteady state mass balance around a tray, Figure 14, at constant gas flowrate results in the following equation:

$$L_i - L = \frac{dH}{dt} \qquad (4.1)$$

This differential equation cannot be solved unless a relationship between solids flowrate L and solids holdup H is known. The usual approach in modelling distillation column tray dynamics is to assume that the Francis formula, $L = K(H')^{1.5}$, for a rectangular weir is valid. For simplicity the linearized form is usually applied (24)(25)(26). Using this same approach the following relationship can be assumed:

$$H = H_s + \tau L \qquad (4.2)$$

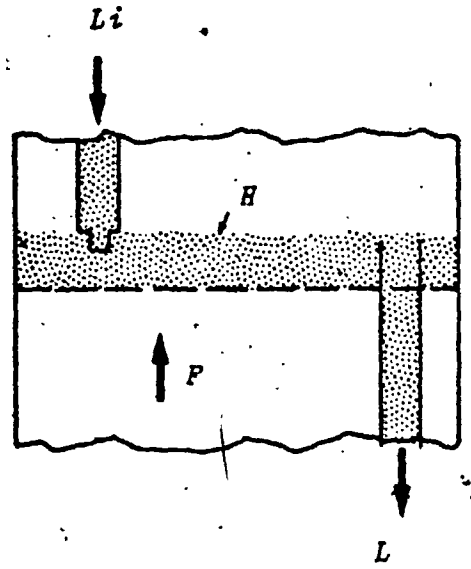

FIGURE 14. TRAY SOLIDS HOLDUP SCHEMATIC

Combining equations (4.1) and (4.2) and in terms of deviation variables results in equation (4.3).

$$\tau \frac{dH'}{dt} + H' = \tau L_i' \qquad (4.3)$$

where $H' = H - H_s$; the deviation variable L_i' is identical to L_i since $L_s = 0$.

Equation (4.3) is a first order differential equation with time constant τ and represents the dynamics of tray solids holdup. The objective of the work at this stage is to verify equation (4.3) experimentally and furthermore to determine the effects of several parameters on the tray time constant. These parameters were selected here to be the gas flowrate (superficial gas velocity), the height of the weir, the diameter of the weir, and the type of solids.

4.3 Solids

The solids which were used for this study were 437 type activated carbon from Barnebey-Cheney. The cumulative size distribution of these solids is shown on Figure 15 on logarithmic probability paper. From earlier experiments it was shown that the particle density was not uniform and resulted in a time dependent holdup when all other conditions were constant. This can be attributed to the different degree of porosity of the particles which results during the production process for the activated carbon. To circumvent this problem the solids were elutriated by passing them through the column at a gas flowrate of fifty cubic feet per minute and removing from top tray the accumulated heavy particles.

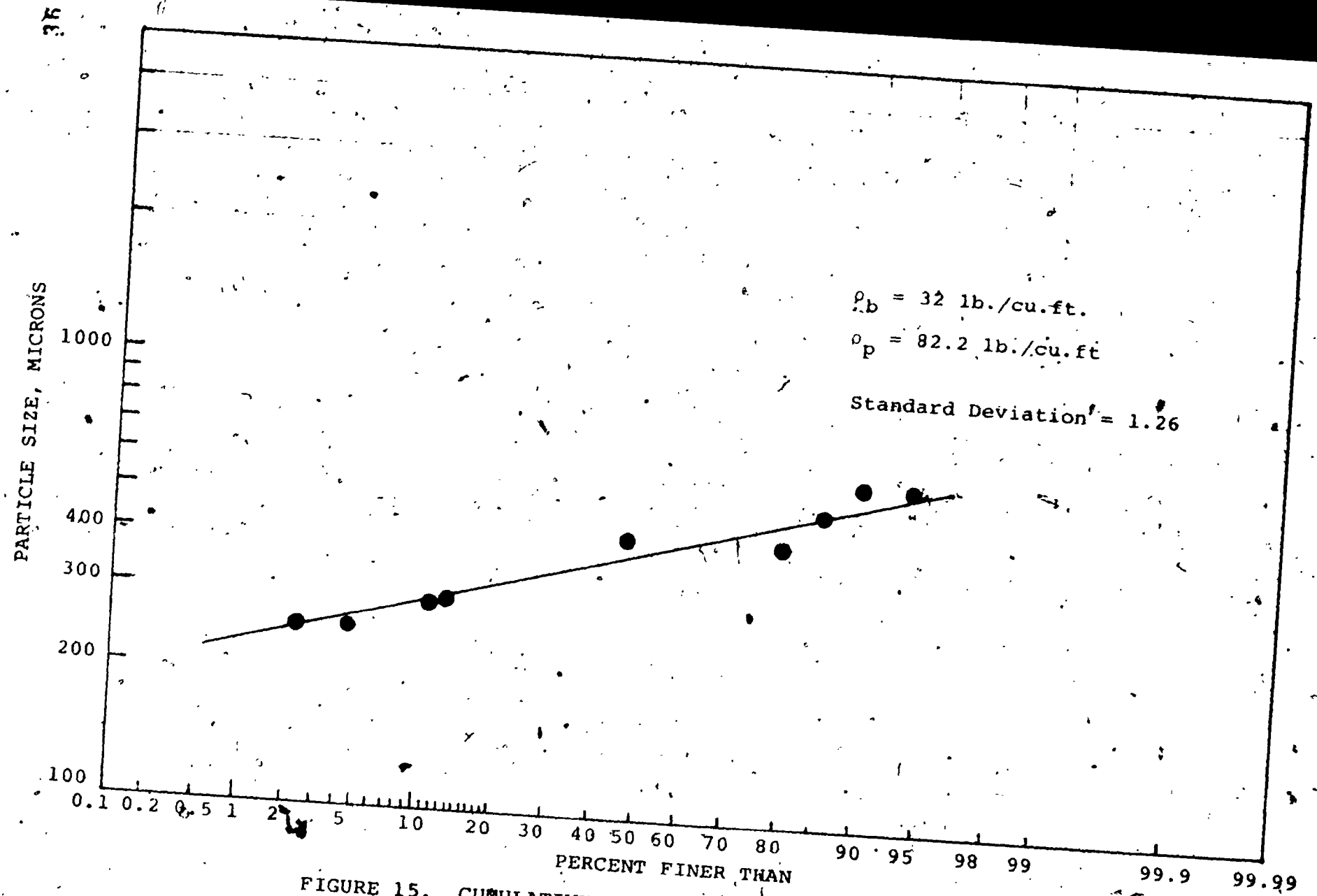

FIGURE 15. CUMULATIVE PARTICLE SIZE DISTRIBUTION FOR 437 TYPE ACTIVATED CARBON

4.4 Results and discussion

(i) Feedback control of solids feed

When solids are discharged from the hopper of a vibratory type feeder their flowrate depends primarily on the amplitude of the vibrations. However, there are several other factors such as compaction, segregation, flushing etc. resulting in bridging at the outlet of the hopper and due to this bridging there are flowrate fluctuations and/or even complete stoppage of the flow (28). Table 1 shows how the flowrate of carbon powder (420 microns mean diameter) varied when the vibratory feeder was used as an open loop system. Under these circumstances a calibration of the vibratory feeder would be meaningless and the direct measurement of solids becomes necessary. This was achieved by using a feedback loop for the feed of solids as shown in Figure 10.

Figure 16 shows the calibration curve for the solids flowmeter. All points but those corresponding to flowrate less than 0.5 lb./min. were obtained by using feedback control. The 0.5 lb./min. value was the lower limit of the flowrate range which the controller was tuned for. Using the least squares method a straight line was fitted to the experimental points resulting in a correlation coefficient and an intercept 0.998, and 0.019 lb., respectively. The high value of the correlation coefficient and the very small value of the intercept suggest that the flowmeter has a linear response to flowrates between 0 and 2.25 lb./min. The sensitivity of the flowmeter as it can be seen from

TABLE I

FLOWRATE FLUCTUATION FROM THE VIBRATORY FEEDER AT SET POINT 55%

NO	TIME, MIN	WEIGHT, LB	FLOWRATE, LB
1	2.6	1.24	0.48
2	2.6	0.97	0.37
3	2.4	1.05	0.44
4	2.1	0.90	0.41
5	2.0	0.95	0.47
6	2.0	0.79	0.40
7	2.0	0.81	0.41
8	2.0	0.81	0.41

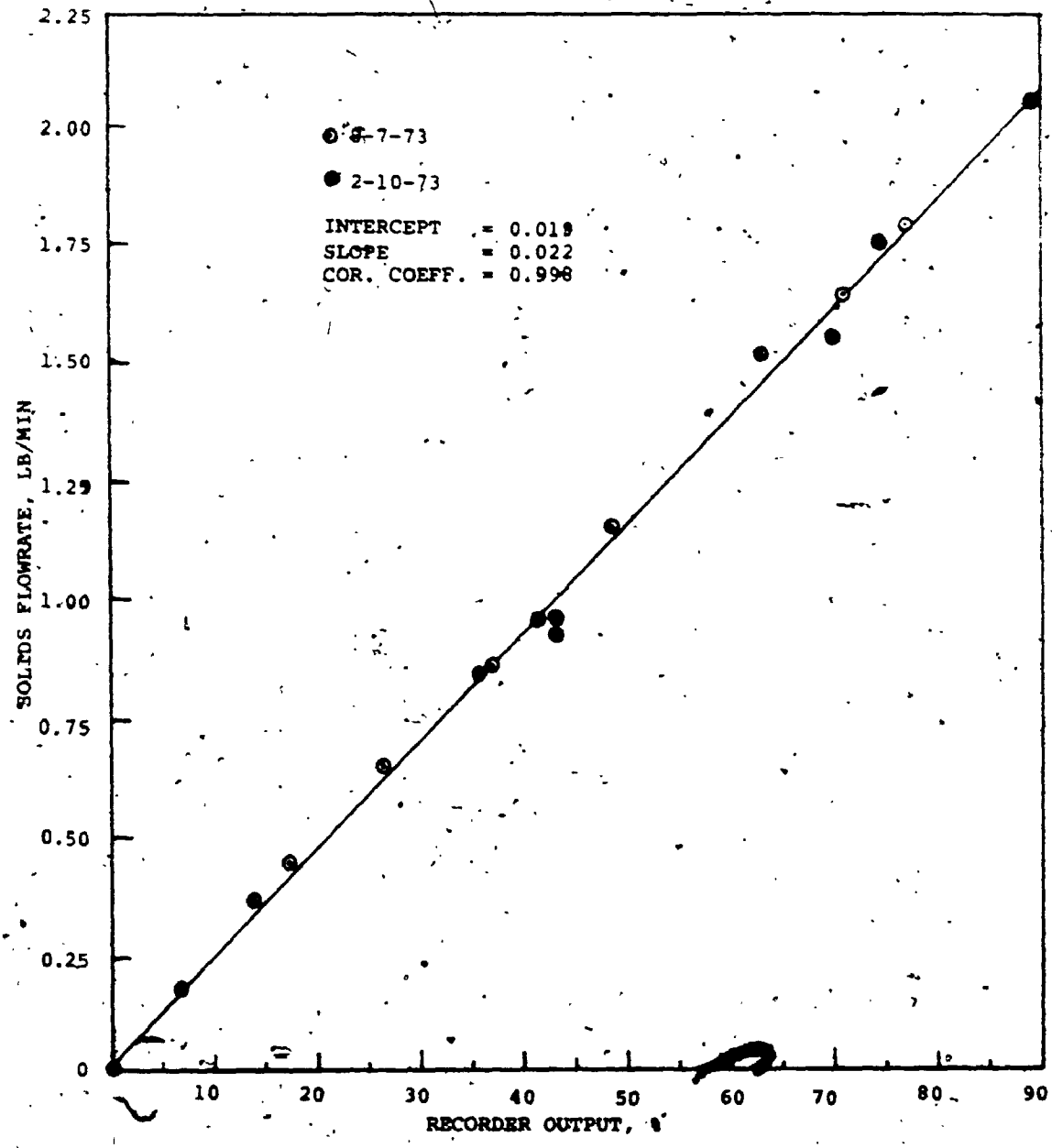

FIGURE 16. CALIBRATION CURVE FOR SOLIDS FLOWMETER

Figure 16, is about 0.05 lb./min. However, by using higher amplification of the flowmeter output signal the sensitivity can be as small as 0.01 lb./min. The high linearity and the high sensitivity make this flowmeter suitable for use in feedback control of solids. The data for the calibration curve of the flowmeter are presented in Appendix B.

Figure 17 shows that the feedback control to the solids flowrate resulted in a fairly constant response while the open loop response varied substantially. The rather large variation of the open loop response is another demonstration showing a limitation of solids feeders; that is, an inability to provide a constant flowrate of solids.

Figure 18 shows the response of the flowrate to a step change of the controller's set point from 40% to 70%. It can be seen that the transition from one steady value to the other takes about 1.75 minutes.

(ii) Solids holdup dynamics.

An experimental proof of equation (4.3) requires the instantaneous weight of solids on a tray. The weighing system used was that depicted in Figure 12. The success of such an experiment depends on the assumption that the weight of fluidized solids can be registered on the supporting tray. To prove whether or not this assumption is correct an experiment was planned and carried out as follows.

A continuous flow of solids was fed to the top tray during operation of the column. By visual inspection of the shallow fluidized beds it was noticed that the solids tray

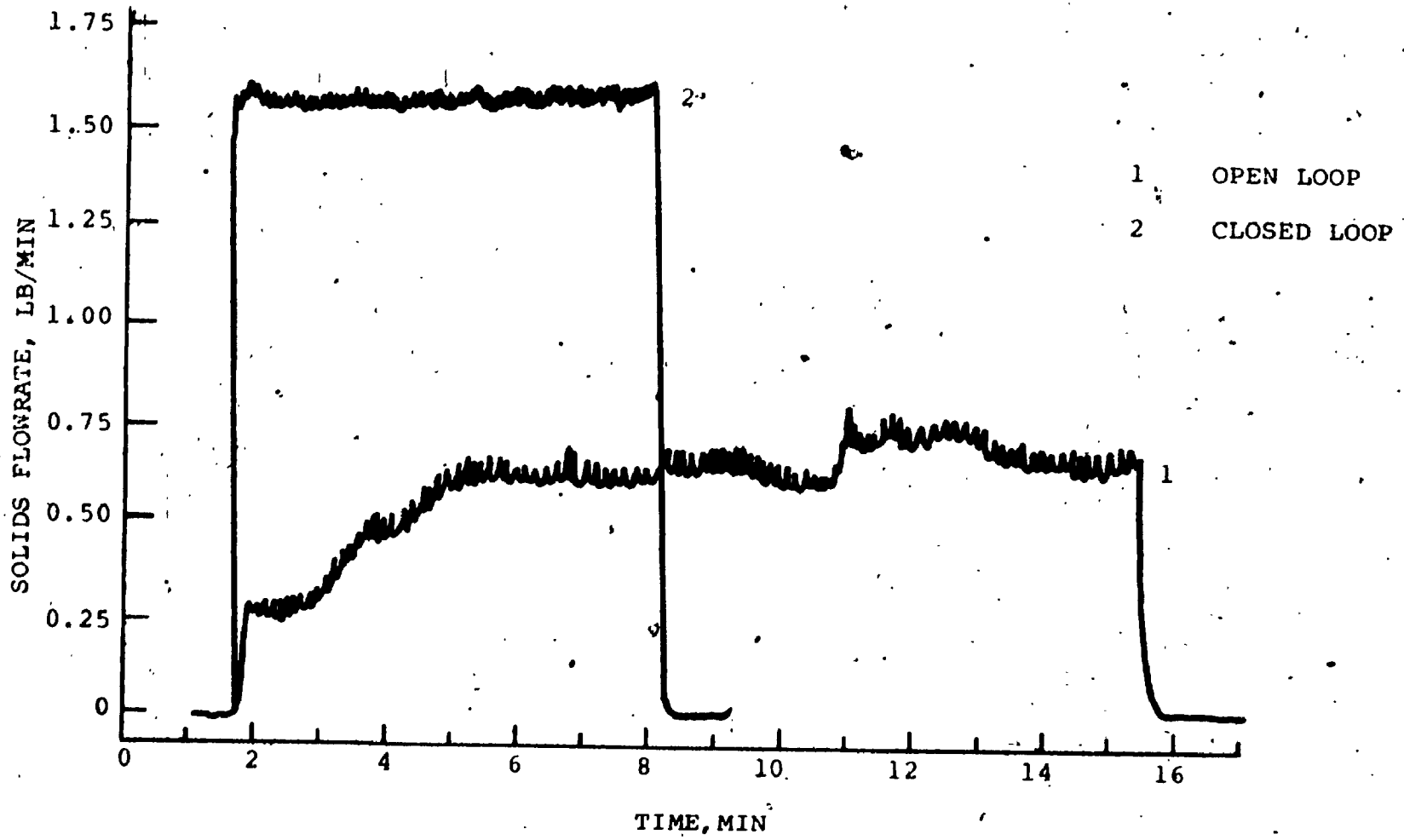

FIGURE 17. SOLIDS FLOWRATE RECORDER TRACING FOR BOTH OPEN AND CLOSED LOOP SYSTEM

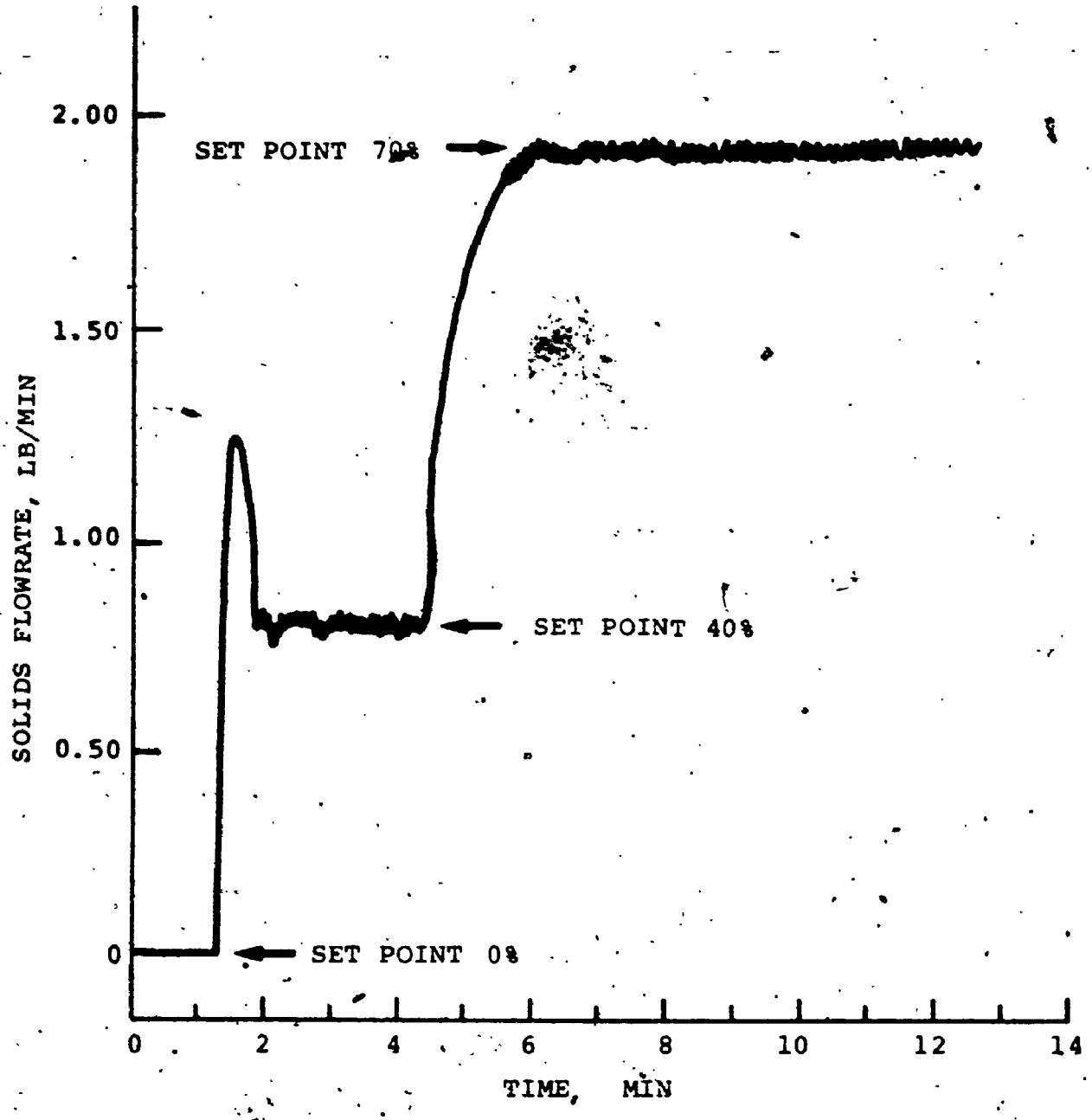

FIGURE 18. FLOWRATE RESPONSE TO A STEP CHANGE IN THE CONTROLLER SET POINT

holdup increased when a step change of the solids flowrate was introduced. However, the strain gages weighing system gave no response to this visual observation. This observation would support the possibility that fluidized solids are suspended hence are not supported by the grid; to check this the following procedure was followed.

The overflow tube of the top tray was covered by a screen so that solids couldn't pass downwards through the downcomer. The solids flow was interrupted and a series of experiments was performed at various gas flowrates for solids tray holdups of 0, 1, 2 and 3 pounds. For each of these experiments the step change response S between fluidized and unfluidized state was recorded. The magnitude of this step named 'recorder output' was related to the sum of the absolute values of both the response due to the pressure drop through the tray S_1 and the response due to the weight of the solids on the tray S_2. Figure 19 shows the typical type of response. It is interesting to note that regardless of whether there are solids or not on the tray the response of the fluidized state with respect to the baseline is always the same for the same gas flowrate and equal to the response due to the pressure drop through the empty tray.

The calibration for the holdup on the top tray was performed by using dead weights and as shown on Figure 20 resulted in a linear response for a range 0 to 4 pounds. Figure 21 shows the four plots A, B, C and D of the 'recorder output' versus gas flowrate for holdups of 0, 1, 2 and 3

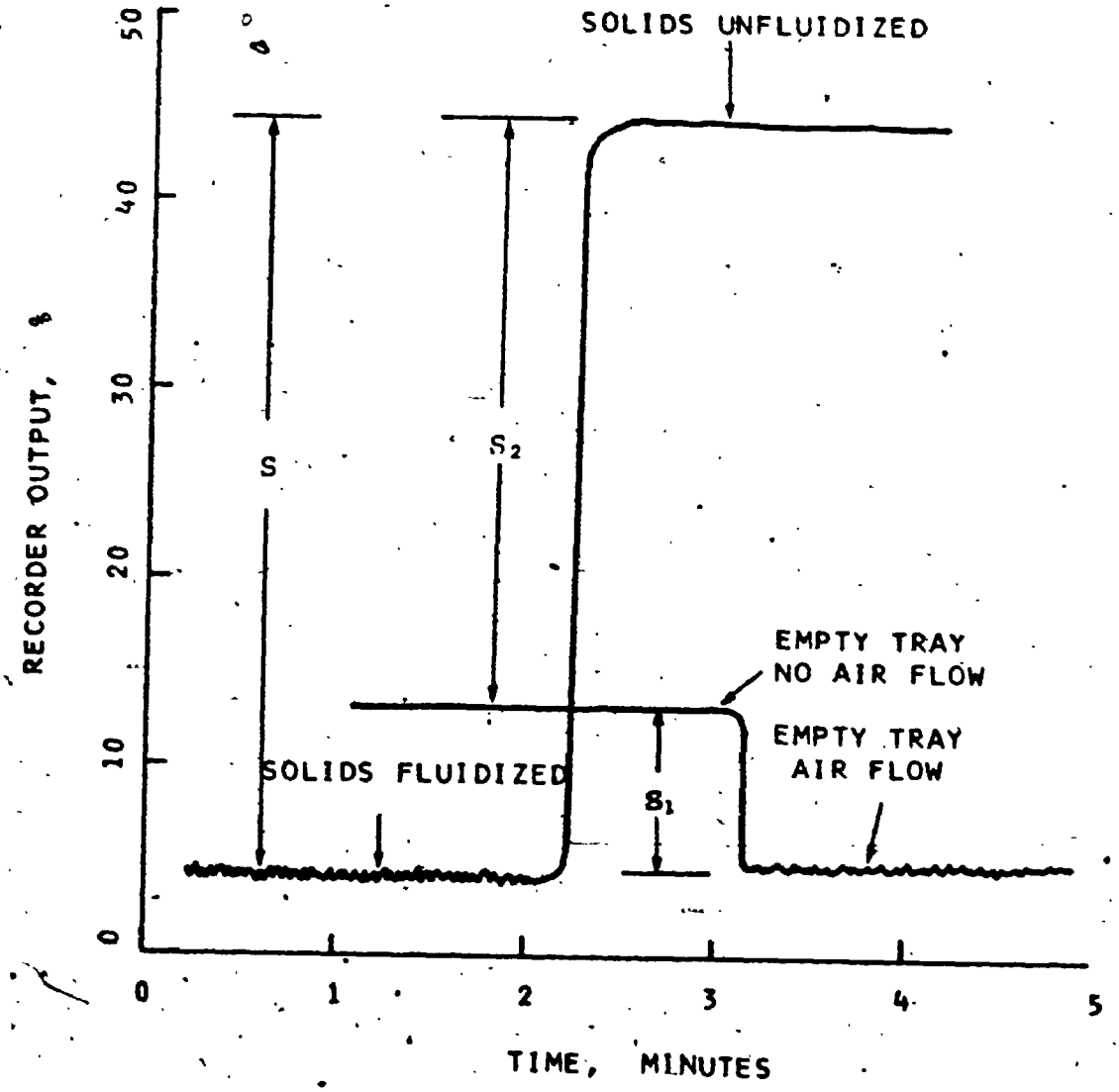

FIGURE 19

RECORDER TRACING OF THE HOLDUP

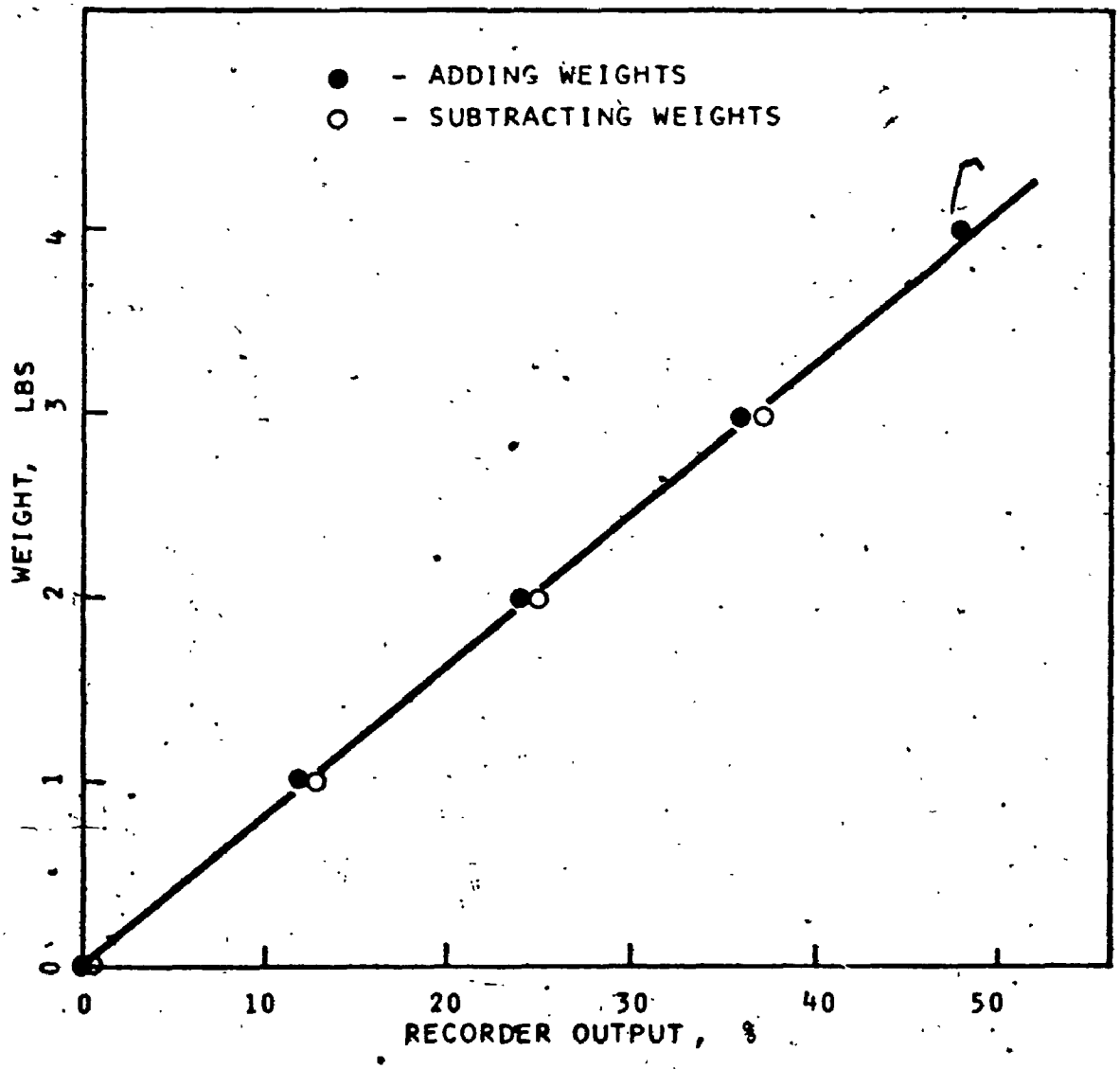

FIGURE 20

CALIBRATION CURVE FOR THE TOP TRAY

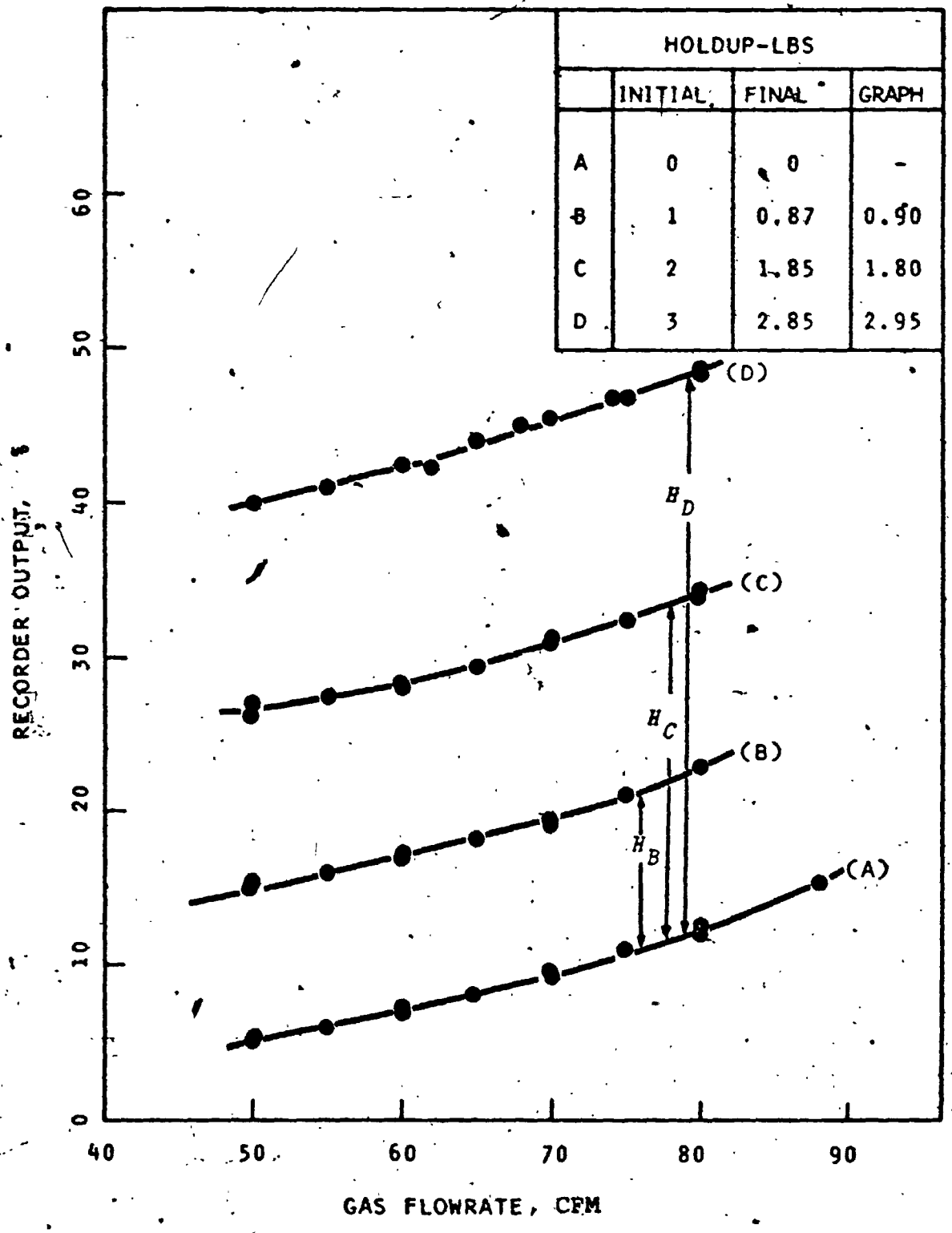

FIGURE 21

HOLDUP MEASUREMENTS

pounds, respectively. If the 'recorder output' is in fact made up of the response due to the weight of the solids plus the response due to the pressure drop through the plate, then the difference of any of the plots B, C, and D from A (empty tray) will give the holdup H_B, H_C, and H_D, respectively. The holdup values obtained with this method are shown at the top of Figure 21 (labelled 'graph holdup') and are evaluated at a gas flowrate of 80 cfm; the 'initial holdup' (actual amount loaded on the tray) and the 'final holdup' (amount of solids at the end of the experiment) are also included. A comparison between 'initial' and 'final' holdup shows a loss of solids of about 0.15 lb. in each case and that was attributed to entrainment and dumping. On the other hand a fairly good agreement was found between 'final' and 'graph' holdup with an error for 1, 2, and 3 pounds of -3.5%, +2.7%, and -3.5%, respectively. The equivalent errors derived at other gas flowrates between 50 and 80 cfm were close to the above values. Within the limits of these errors it can be concluded that the solids were completely fluidized at gas flowrates higher than 50 cfm. Furthermore, when completely fluidized they were totally suspended, and no fraction of their mass is supported on the tray. The only force acting on the tray then, is that due to the pressure drop of the flowing gas through the tray.

This conclusion could also be anticipated theoretically by applying a force balance around the plate as follows (refer to Figure 14):

(Force due to the pressure drop through the plate) + (Force due to the pressure drop through the bed) - (Force due to the weight of the bed) = Net Force (4.4)

or

$$\Delta P_p \times A + \Delta P_B \times A \rightarrow H = \Sigma F \quad (4.5)$$

It is very well known from the theory of fluidization that the pressure drop through the bed of solids equals the weight of the bed divided by its area, that is

$$\Delta P_B = \frac{H}{A} \quad (4.6)$$

Combining equations (4.5) and (4.6) results in equation (4.7)

$$\Delta P_p \times A = \Sigma F \quad (4.7)$$

which says that in a fluidized bed the only force acting on the supporting tray is that due to the pressure drop through the plate. Equation (4.7) is in agreement with the experimental results.

It should be noted that the same analysis applied to aerated liquids (e.g. liquid holdup in distillation columns) leads to equation (4.7). However, an experimental proof in this case is not available.

Figure 22 shows the dynamics of the plate solids holdup to a step change of the solids flowrate from 0.5 lb./min. to zero. Each point shown on Figure 22 was obtained by simultaneously cut-off both the air and the solids flowrate at the indicated time interval. The solids then were collected, weighted, and reused for the next point. It can be seen from Figure 22 that the experimental results are in good

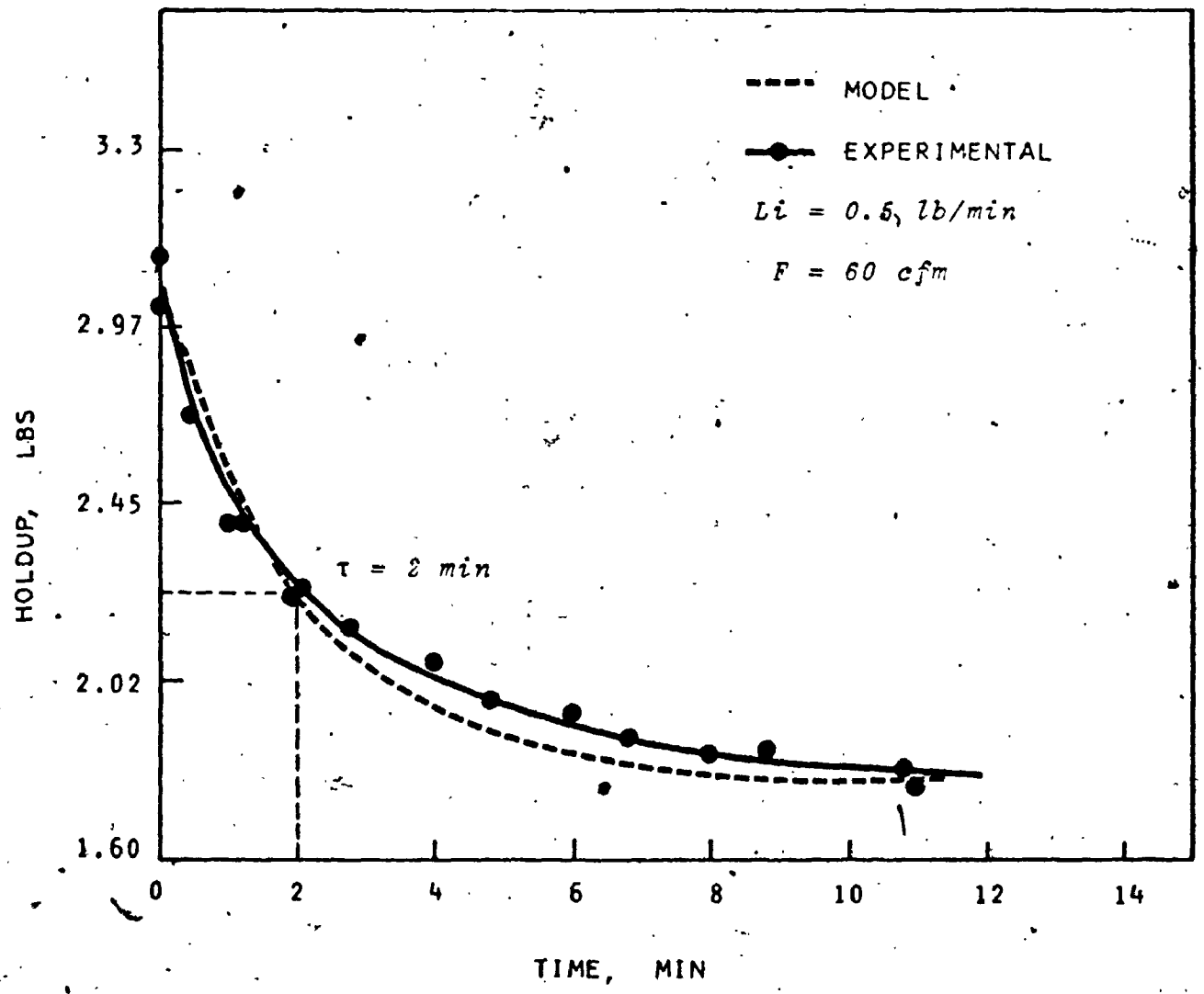

FIGURE 22

SOLIDS HOLDUP DYNAMICS

agreement with the first order differential equation (4.3) with a time constant (63.2% of total response) of about 2 minutes. However, it should be realized that this time constant is valid only for the solids flowrate range 0.5 lb./min. to zero and any extrapolation will be dangerous unless an experimental proof for the linearity of equation (4.2) is provided. This proof study is presented in the following section.

(iii) Steady state holdup

The steady state holdup for the top tray was studied as a function of the carbon flowrate by using the gas flowrate, the height, and the diameter of the weir as parameters. For each experiment the system was allowed to reach equilibrium so that the solids outlet flowrate L_1 from the top tray would be equal to the solids inlet flowrate L_2. The gas and the solids flow then was cut-off simultaneously and the solids were weighed.

Figure 23 shows the relationship between the solids holdup for the top tray and the solids flowrate when a 3 inch high and 1.25 inch diameter weir was used. It can be seen that the relationship is highly linear in the range 0.25 lb./min. to 2.00 lb./min. solids flow. For 1.25, 1.50 and 1.75 ft./sec. superficial gas velocity, the respective time constants were 0:47, 0.48 and 0.50 minutes, and the respective correlation coefficients were 0.984, 0.992, and 0.992. Figure 24 shows another relationship between solids holdup and solids flowrate when a 2 inch high and 1.25 inch

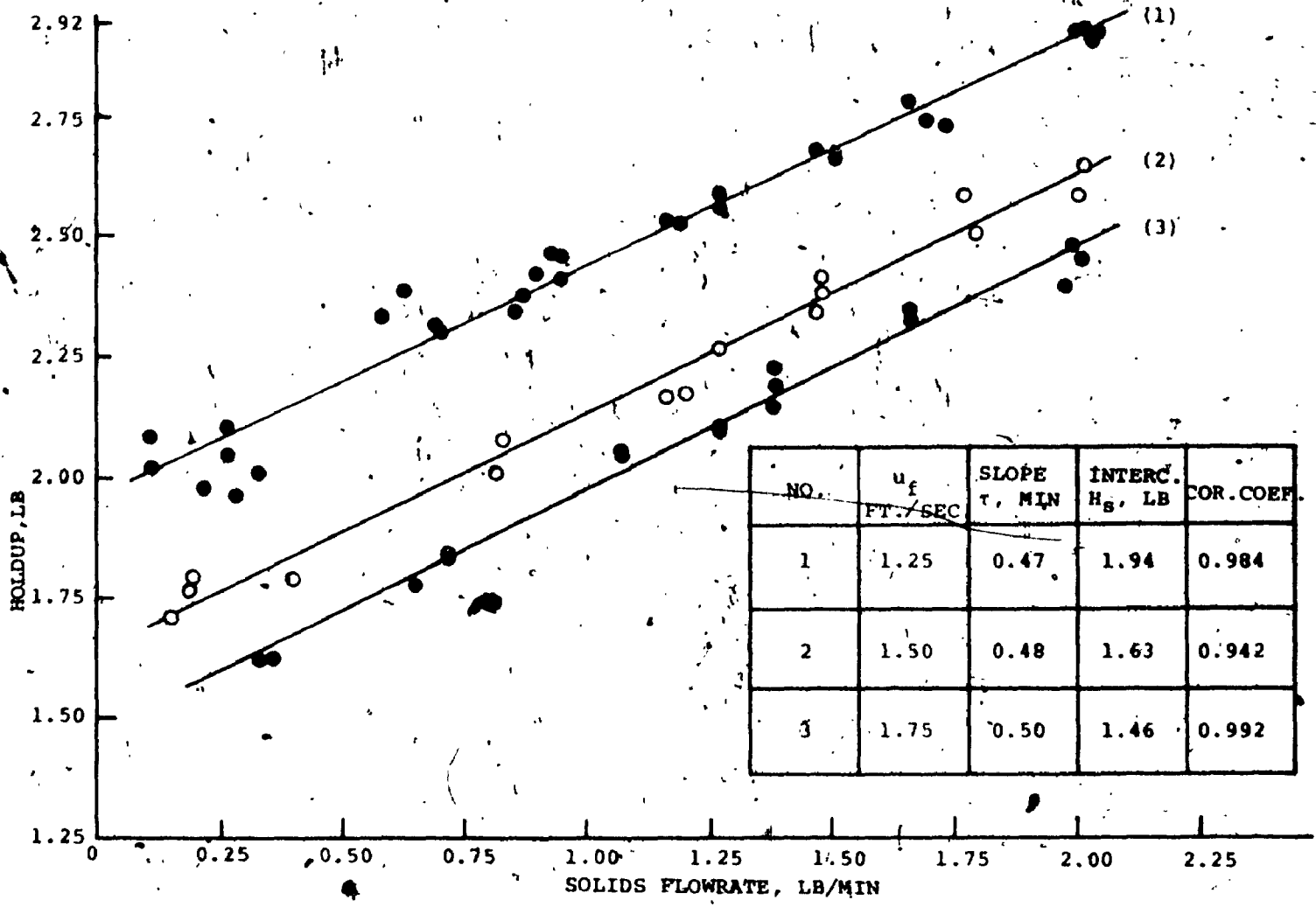

NO.	u_f FT./SEC	SLOPE τ, MIN	INTERC. H_s, LB	COR.COEF.
1	1.25	0.47	1.94	0.984
2	1.50	0.48	1.63	0.942
3	1.75	0.50	1.46	0.992

FIGURE 23. HOLDUP-CARBON FLOWRATE RELATIONSHIP FOR WEIR HEIGHT 3 INCHES AND WEIR DIAMETER 1.25 INCHES

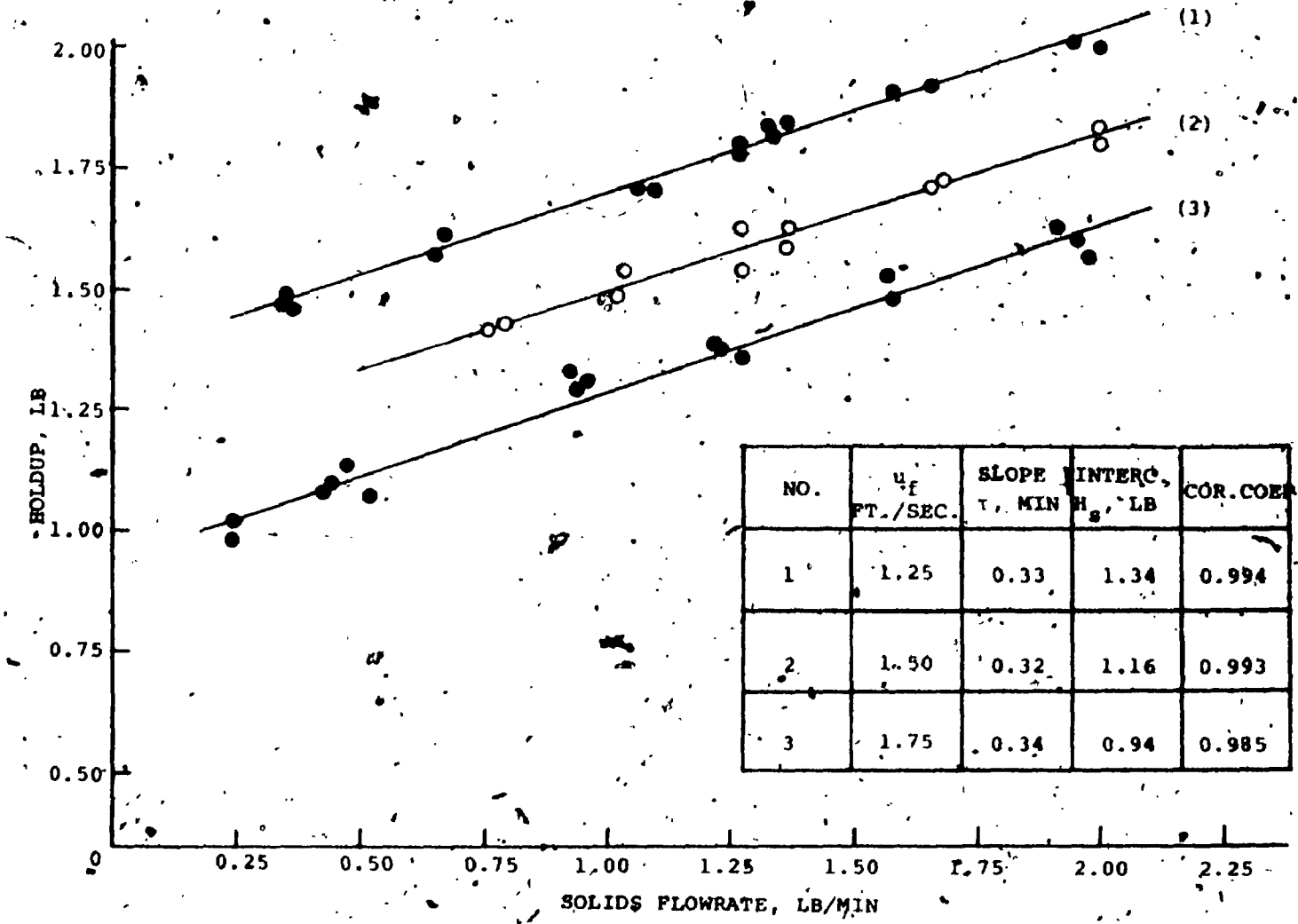

NO.	u_f FT./SEC.	SLOPE, τ, MIN	INTERC., H_g, LB	COR.COEF.
1	1.25	0.33	1.34	0.994
2	1.50	0.32	1.16	0.993
3	1.75	0.34	0.94	0.985

FIGURE 24. HOLDUP-CARBON FLOWRATE RELATIONSHIP FOR WEIR HEIGHT 2 INCHES AND WEIR DIAMETER 1.25 INCHES

diameter weir was used. It can be seen again that this relationship is highly linear with correlation coefficient for 1.25, 1.50 and 1.75 ft./sec. superficial gas velocity, 0.994, 0.993, and 0.985, respectively; the respective time constants were 0.33, 0.32 and 0.34 minutes. When the weir was 1 inch high and retaining the same diameter the solids holdup to the solids flowrate relationship as shown in Figure 25 was again highly linear. For 1.25, and 1.50 ft./sec. superficial gas velocity the correlation coefficient was 0.980, and 0.977, respectively; the respective time constants were 0.18 and 0.19 minutes. When the superficial gas velocity was 1.75 ft./sec. the results, shown on Figure 25, demonstrate that the holdup to the solids flowrate relationship is non-linear. The non-linearity occurred for solids flowrate smaller than 1.25 lb./min. and it might be due to the very shallow bed resulted under these conditions. Figure 26 shows the relationship between solids holdup for the top tray and gas flowrate; here the solids flowrate was kept constant at 1.27 lb./min. while the weir height was used as a parameter. In the range of superficial gas velocity 1.25 to 1.75 ft./sec. this relationship was also linear.

The following series of experiments is intended to determine the effect of weir diameter on the tray time constant. It was found necessary at this stage that the solids flowmeter be cleaned and the oil of the dashpot be replaced with a more viscous one. These changes resulted in a new

NO.	u_f FT./SEC.	SLOPE τ, MIN	INTERC. H_o, LB	COR.COEF.
1	1.25	0.18	0.87	0.980
2	1.50	0.19	0.66	0.977
3	1.75	–	–	–

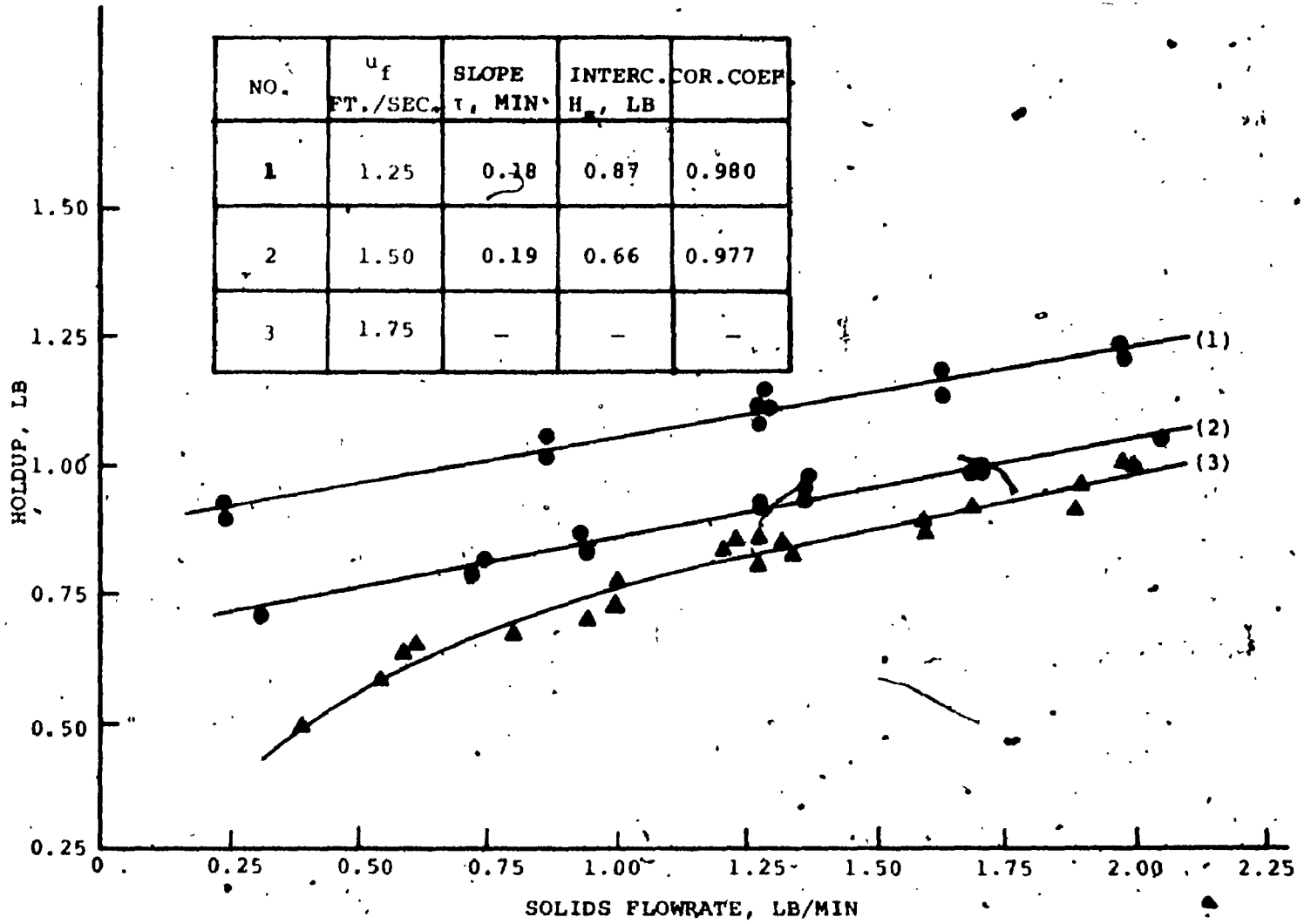

FIGURE 25. HOLDUP-CARBON FLOWRATE RELATIONSHIP FOR WEIR HEIGHT 1 INCH AND WEIR DIAMETER 1.25 INCHES

NO.	WEIR HEIGHT, INCHES	SLOPE, LB/CFM
1	3	-0.024
2	2	-0.022
3	1	-0.013

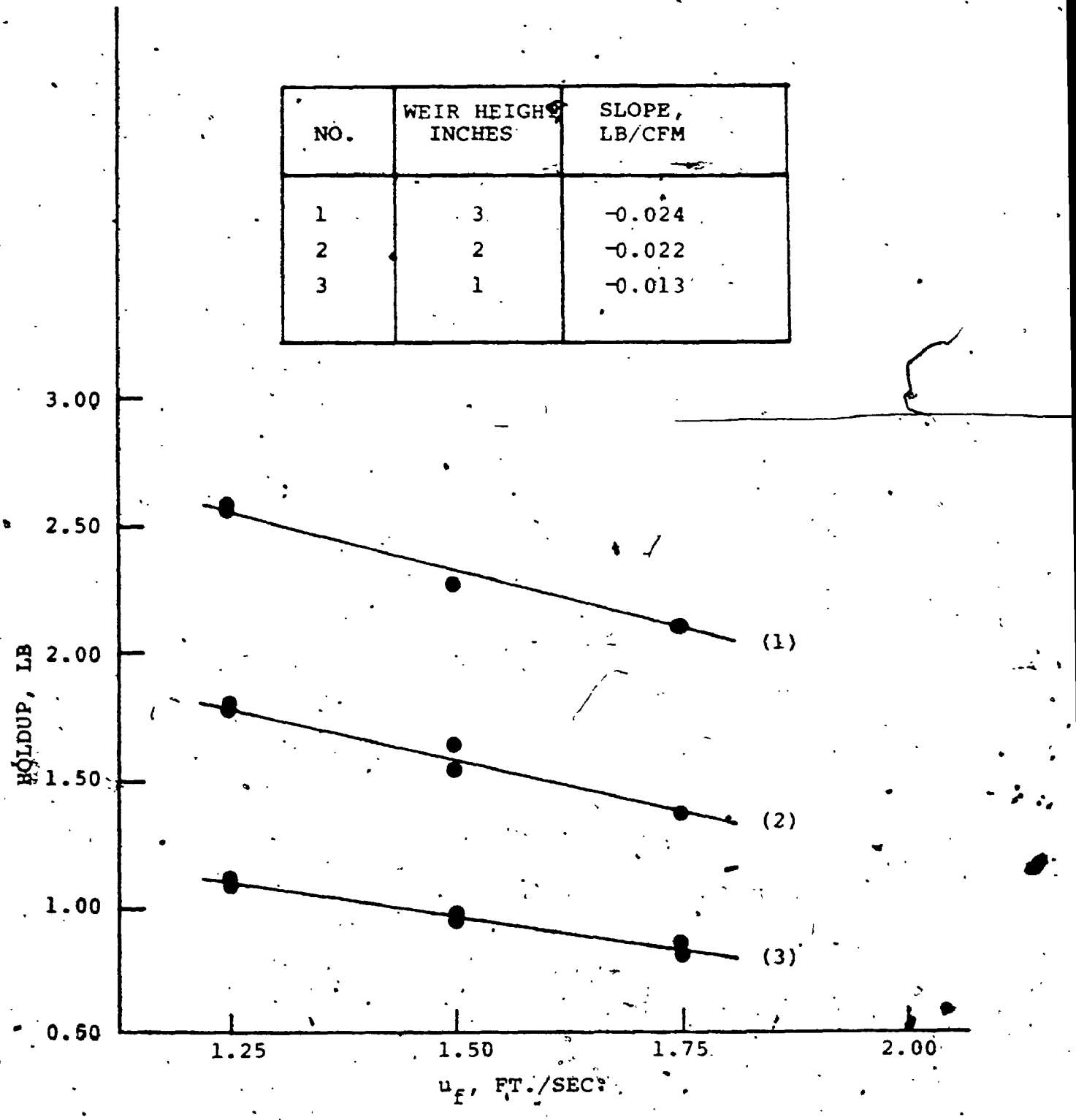

FIGURE 26. HOLDUP-GAS FLOWRATE RELATIONSHIP AT CARBON FLOWRATE 1.27 LB./MIN. AND WEIR DIAMETER 1.25

calibration curve for carbon, Figure 27. Figure 27 also shows a calibration curve for sand (No. 5005, Wedron Company), the size characteristics of which are shown on Table 2. Figure 28 shows the cumulative per cent distribution on logarithmic probability paper.

Figure 29 shows the relationship between the carbon tray holdup and the carbon flowrate when a 2.5 inch diameter weir was used. With 1 inch weir height the time constants at 1.25 and 1.50 ft./sec. superficial gas velocity were 0.15 and 0.11 minutes, respectively; the respective correlation coefficients were 0.961 and 0.926. The trend was again linear at solids flowrates higher than 0.25 lb./min. For 1 inch high weir, superficial velocities higher than 1.50 ft./sec. resulted in a very shallow bed for which the results were scattered and not reproducible.

Figure 30 shows the holdup to solids flowrate relationship when a 2.5 inches in diameter and 2 inches high weir was used. At a superficial gas velocity of 1.25, 1.50, and 1.75 ft./sec., the time constant was 0.23, 0.21, and 0.22 minutes, respectively; the respective correlation coefficients for a linear fit were 0.995, 0.968 and 0.969

Figure 31 is another holdup to solids flowrate relationship with 2.5 inch diameter and 3 inch high weir. At a superficial gas velocity of 1.50 and 1.75 ft./sec., the time constant was 0.32 and 0.28 minutes, respectively; the respective correlation coefficients for a linear fit were 0.985 and 0.986.

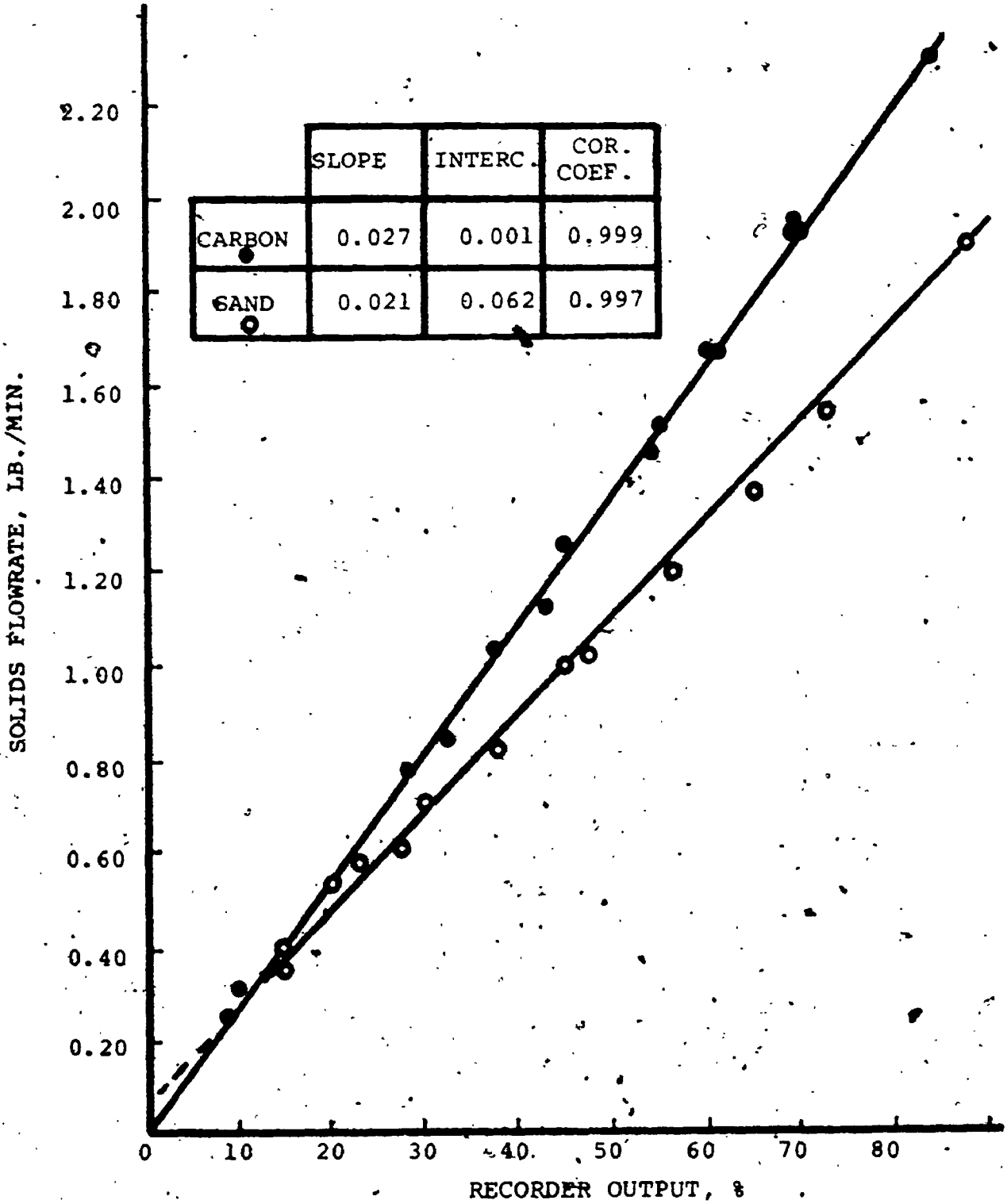

FIGURE 27. RECALIBRATION OF SOLIDS FLOWMETER AFTER CLEANING AND REPLACING THE OIL IN THE DASHPOT

TABLE 2

SIEVE ANALYSIS OF SILICA SAND NO. 5005 FROM WEDRON COMPANY

Retained, %	Size, microns
0.2	420
4.4	297
31.2	210
41.2	149
15.4	105
5.6	74
1.4	53
0.6	44

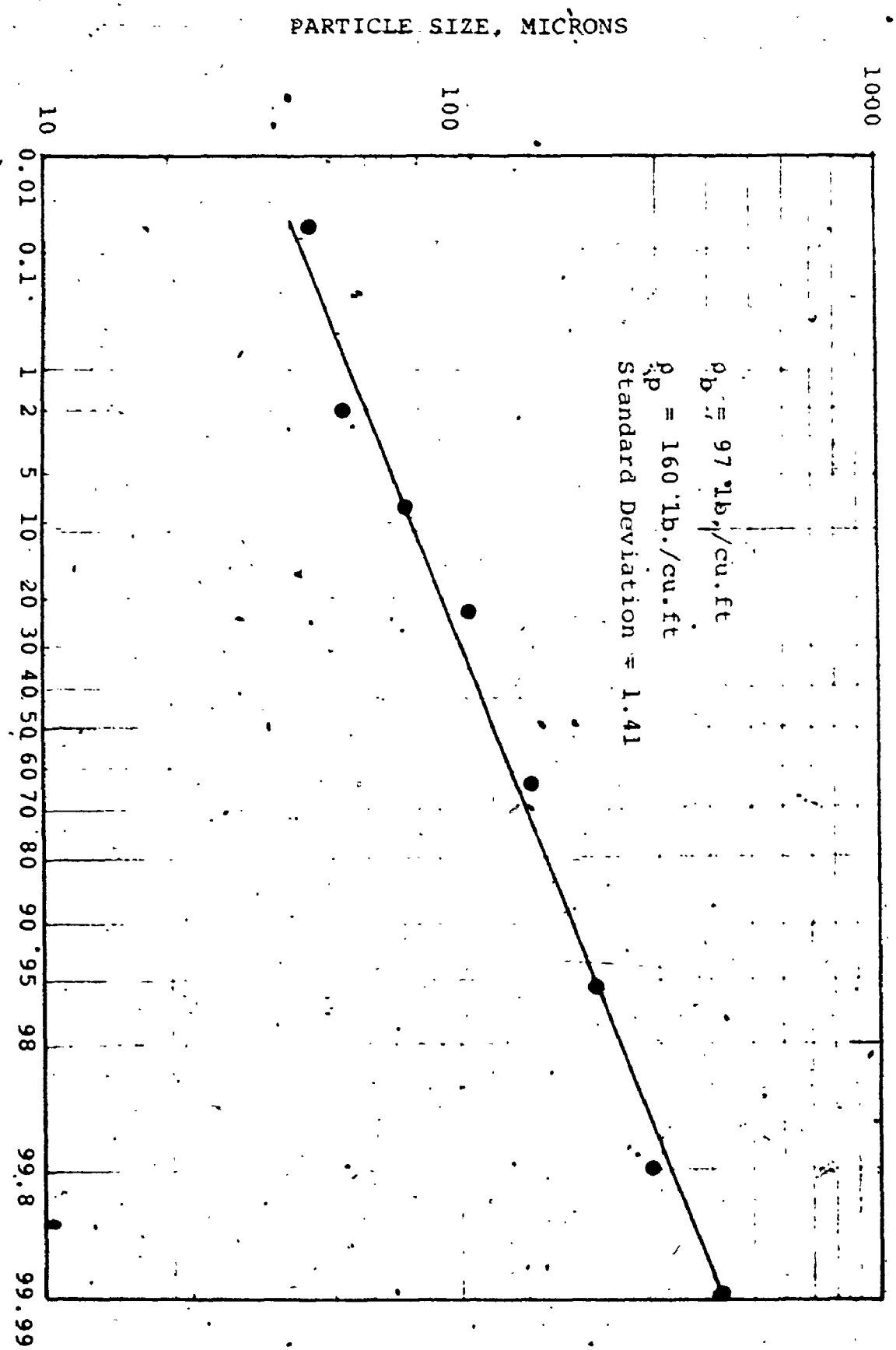

FIGURE 28. CUMULATIVE PARTICLE SIZE DISTRIBUTION FOR 5005 SAND

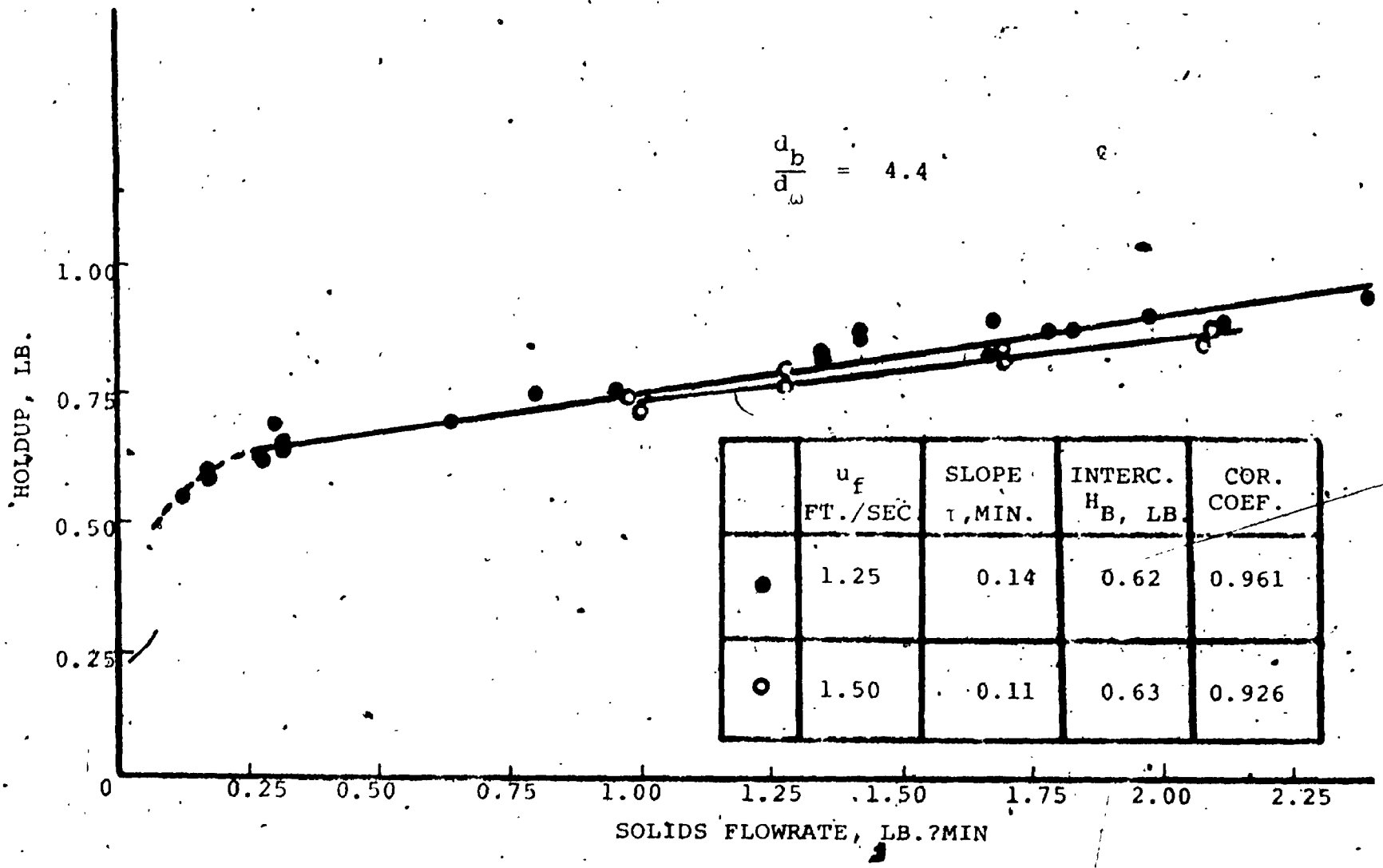

	u_f FT./SEC	SLOPE τ, MIN.	INTERC. H_B, LB.	COR. COEF.
●	1.25	0.14	0.62	0.961
○	1.50	0.11	0.63	0.926

FIGURE 29. HOLDUP-CARBON FLOWRATE RELATIONSHIP FOR WEIR HEIGHT 1 INCH AND WEIR DIAMETER 2.5 INCHES

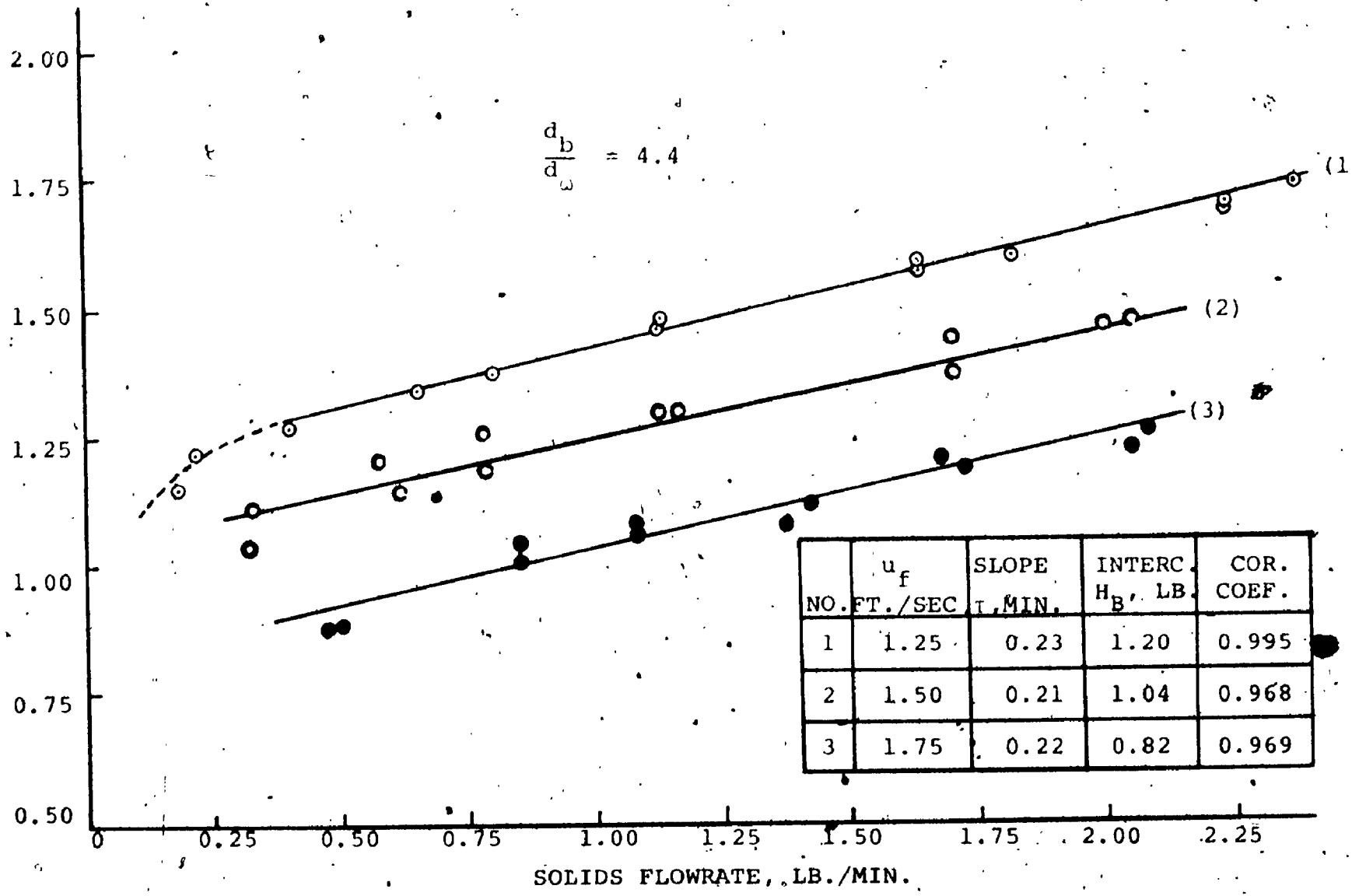

NO.	u_f FT./SEC	SLOPE I, MIN.	INTERC. H_B, LB.	COR. COEF.
1	1.25	0.23	1.20	0.995
2	1.50	0.21	1.04	0.968
3	1.75	0.22	0.82	0.969

FIGURE 30. HOLDUP-CARBON FLOWRATE RELATIONSHIP FOR WEIR HEIGHT 2 INCHES AND WEIR DIAMETER 2.5 INCHES

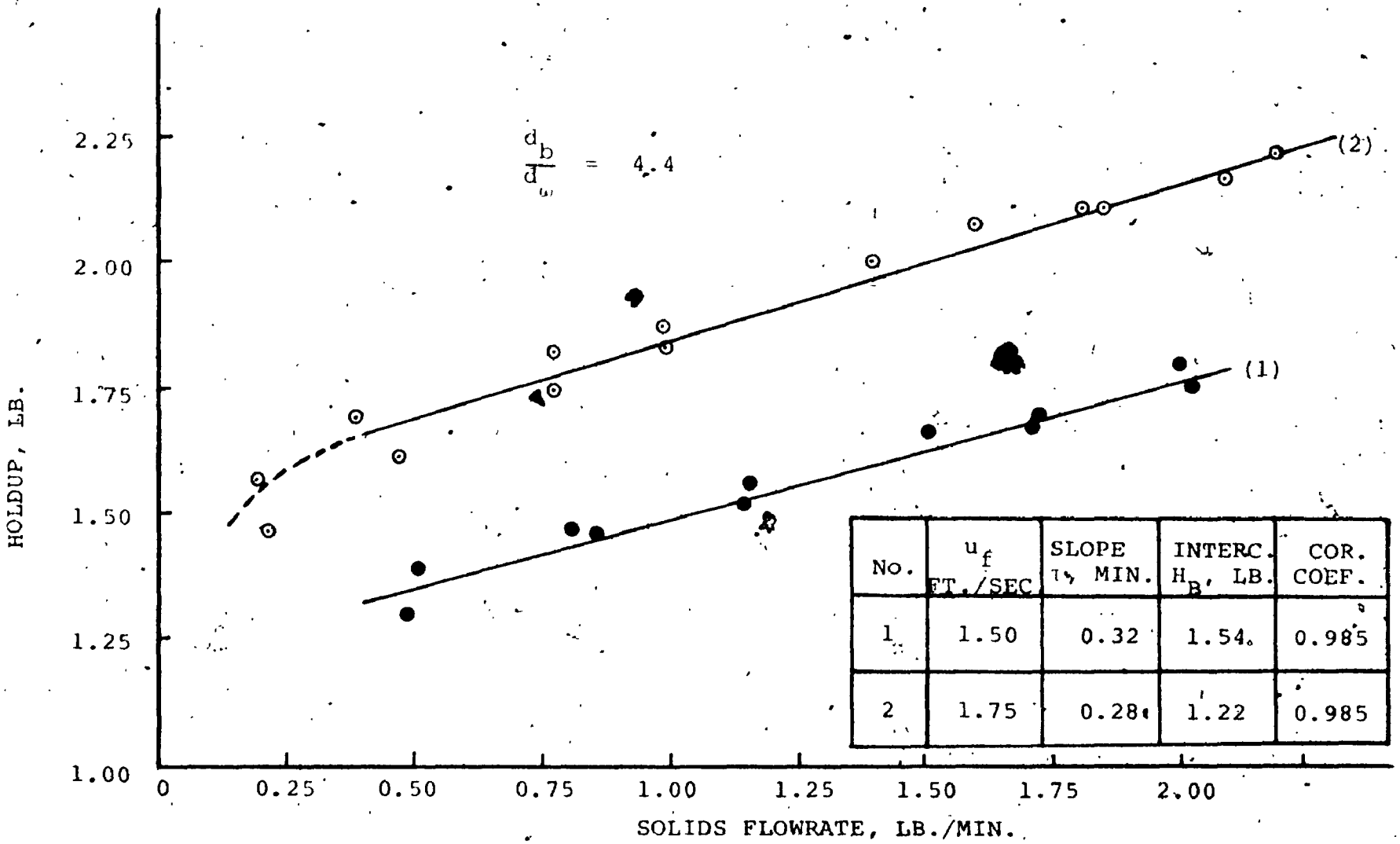

No.	u_f FT./SEC	SLOPE τ, MIN.	INTERC. H_B, LB.	COR. COEF.
1	1.50	0.32	1.54	0.985
2	1.75	0.28	1.22	0.985

FIGURE 31. HOLDUP-CARBON FLOWRATE RELATIONSHIP FOR WEIR HEIGHT 3 INCHES AND WEIR DIAMTER 2.5 INCHES

The linearity of holdup with respect to the solids flowrate which was observed thus far did not occur when a 0.81 inch diameter weir was used. Figure 32 shows that this relationship not only was non-linear but also the trend was different as the weir height varied from 1 to 3 inches.

Figure 33 shows the relationship between the holdup and the weir height at three different weir diameters. The superficial gas velocity and the solids flowrate were kept constant at 1.50 ft./sec., and 1 lb./min., respectively. Within the limits of 1 to 3 inches for the weir height this relationship was also linear.

(iv) Other solids

The superficial gas velocity, u_f, the weir height, h_ω, and the weir diameter, d_ω, were the parameters of which the effects on the tray time constant have thus far been shown. The effects of solids characteristics have not been considered and the question as to whether these have any effect on the tray time constant remains unanswered. To get an insight into this area three other solids were selected; cracking catalyst with a geometric mean of 59 microns, coarse sand of particle size between 420 and 595 microns, and fine sand with particle size between 74 and 297 microns (for the latter a sieve analysis is shown in Table 2 and the cumulative per cent distribution on Figure 28).

Holdup measurement experiments attempted with cracking catalyst presented several problems which were attributed to the design of this particular column. The downcomers,

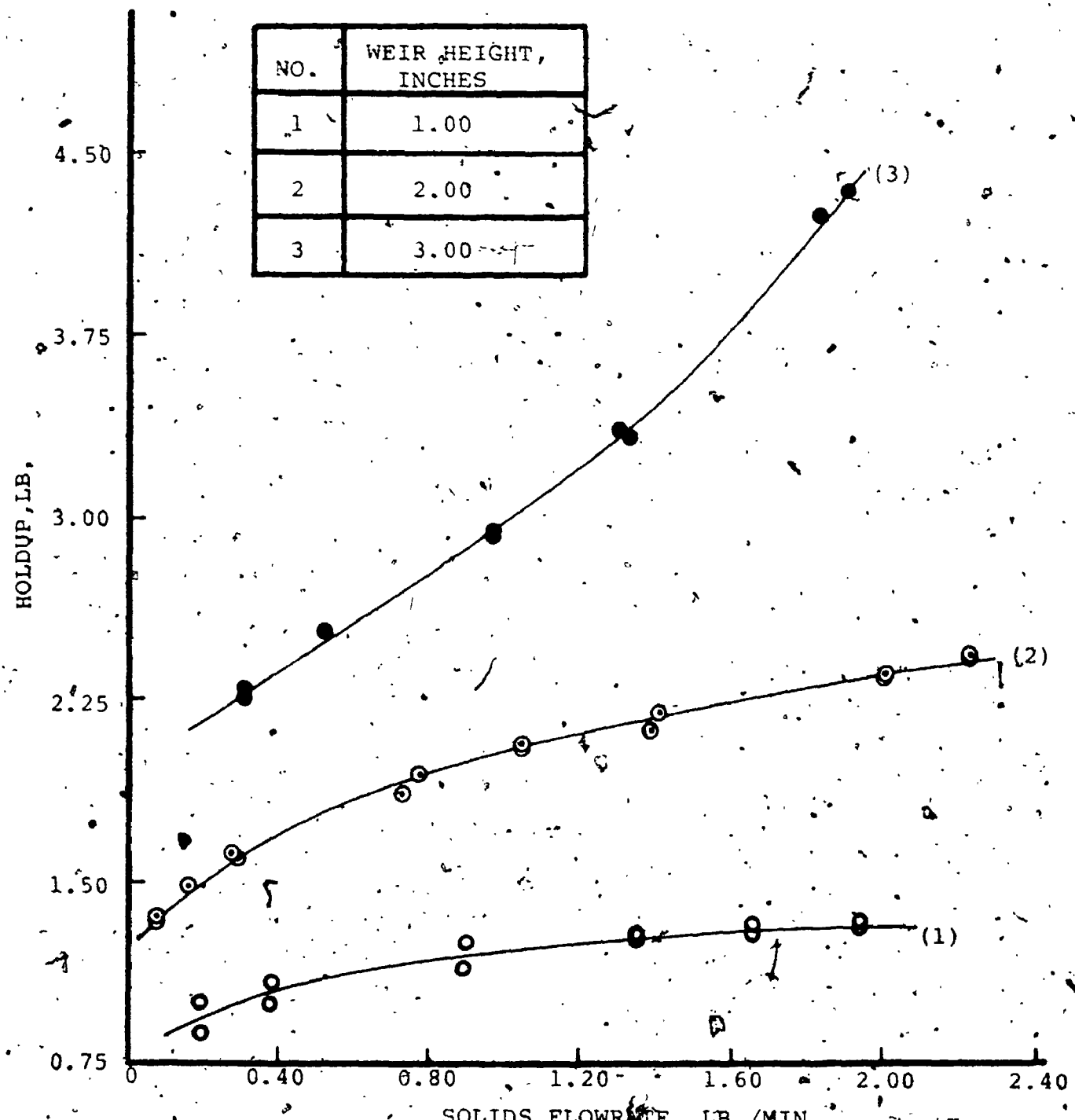

FIGURE 32. HOLDUP-CARBON FLOWRATE RELATIONSHIP FOR WEIR DIAMETER 0.81 OF AN INCH (d_b/d_ω=13.5) AND 1.50 FT./SEC. SUPERFICIAL GAS VELOCITY

NO.	WEIR DIAMETER d_ω, INC.	COLUMN TO WEIR DIAMETER RATIO d_b/d_ω
1	0.81	13.5
2	1.25	8.8
3	2.50	4.4

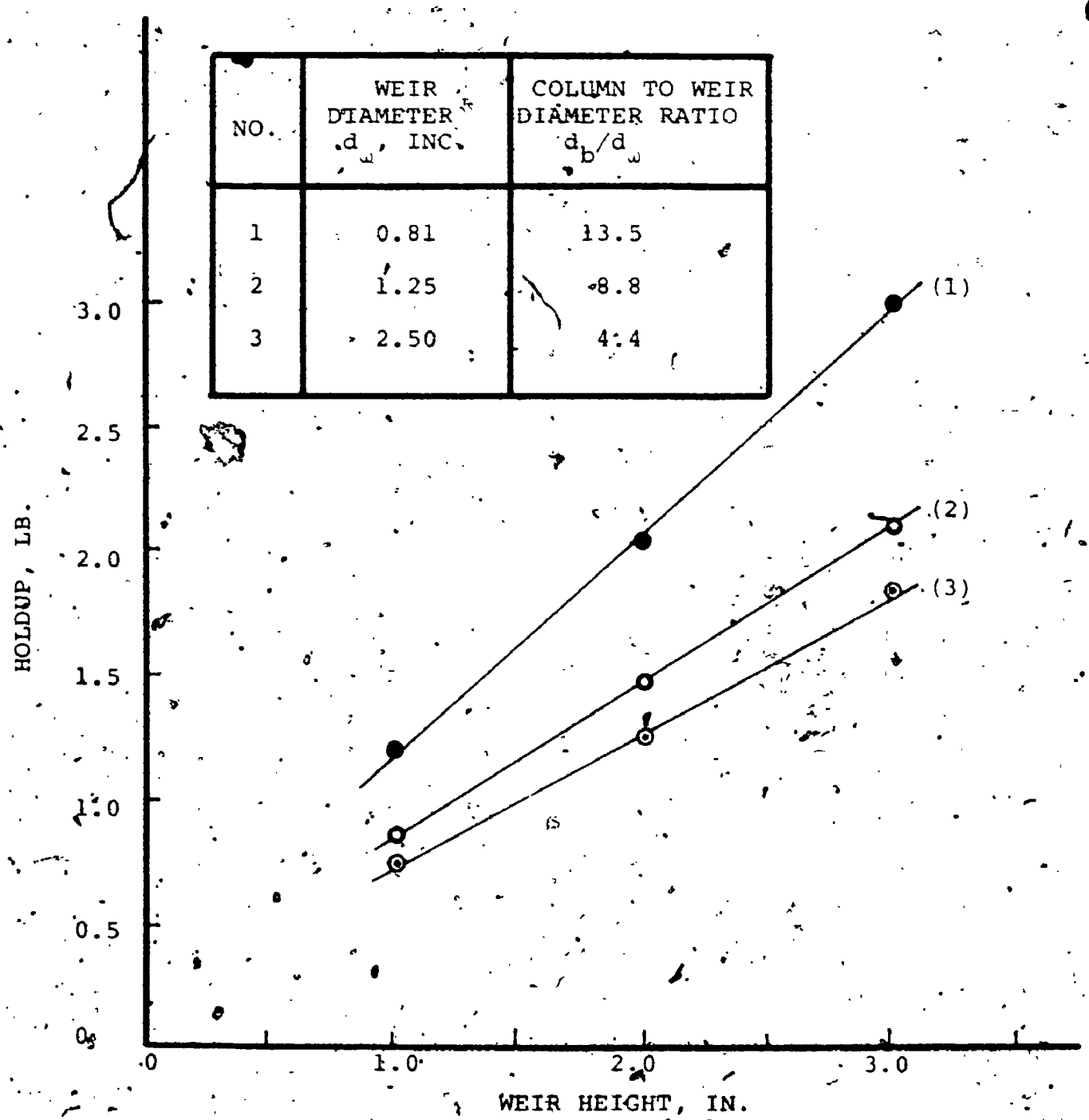

FIGURE 33. HOLDUP VERSUS WEIR HEIGHT AT VARIOUS WEIR DIAMETERS AND 1.50 FT./SEC SUPERFICIAL GAS VELOCITY AT 1 LB./MIN SOLIDS FLOWRATE

for example, designed specifically for activated carbon, did not allow the formation in them of the dense phase of solids which is required for normal operation. Indeed, as has been discussed in chapter 2, uniform and stable fluidization is secured when a dense phase in the downcomer exists during operation; this can be achieved by a proper design of the diameter of the downcomer based on the minimum fluidization velocity of the solids. Other problems that occurred were excessive dumping and entrainment, due to the very fine particles, which made it impossible to make any visual observation and thus to judge the quality of fluidization. At the end of the experiment, when the solids flow and the air flow were simultaneously cut-off, there were very little solids left on the trays. The above problems resulted in abandonment of cracking catalyst as solids for further study.

The coarse sand which was tried as a second choice also presented problems. Due to the large and heavy particles the fluidization was very poor and even at 2.5 ft./sec. superficial gas velocity there was channelling through the shallow beds. On the other hand, higher air velocities resulted in wild fluidization which made it very difficult to achieve reproducible measurements of the tray solids holdup.

The fine sand which was finally tested showed smooth fluidization and in general behaved normally. However, after about five minutes of operation the downcomers were blocked off and the solids flowmeter recording showed excessive

noise (these phenomena were also observed with the coarse sand). In attempting to identify the source of these problems repeated experiments were performed. It was noticed that at the beginning and with fresh sand the flow of sand was quite smooth and resulted in normal operation of the flowmeter. However, after several minutes the sand assumed the characteristic of a rather sticky powder thus causing blocking of the downcomers and an irregular flow (flow in surges) through the solids flowmeter. This phenomenon was attributed to static electrical charge built up by the intense friction on the sand particles. The attraction forces between the charged particles and the opposite charged material of the downcomers and the flowmeter (acrylic) was believed to have caused the sticky characteristic of the sand. To overcome this problem the static electricity had to be kept at a low level. This was achieved by increasing the relative humidity of the fluidizing air. Indeed, with a small flow of steam into the air line the relative humidity increased to 40-60% and under these conditions the downcomers and the solids flowmeter functioned normally.

Figure 34 shows the holdup to solids flowrate relationship for the 5005 sand with a 2 inch high and 1.25 inch diameter weir. At 1.75, 2.00 and 2.25 ft./sec. superficial gas velocity the time constant was 0.80, 0.75, and 0.73 minutes, respectively; the respective correlation coefficients were 0.981, 0.994, and 0.973. The calibration curve for the sand 5005 is shown on Figure 27.

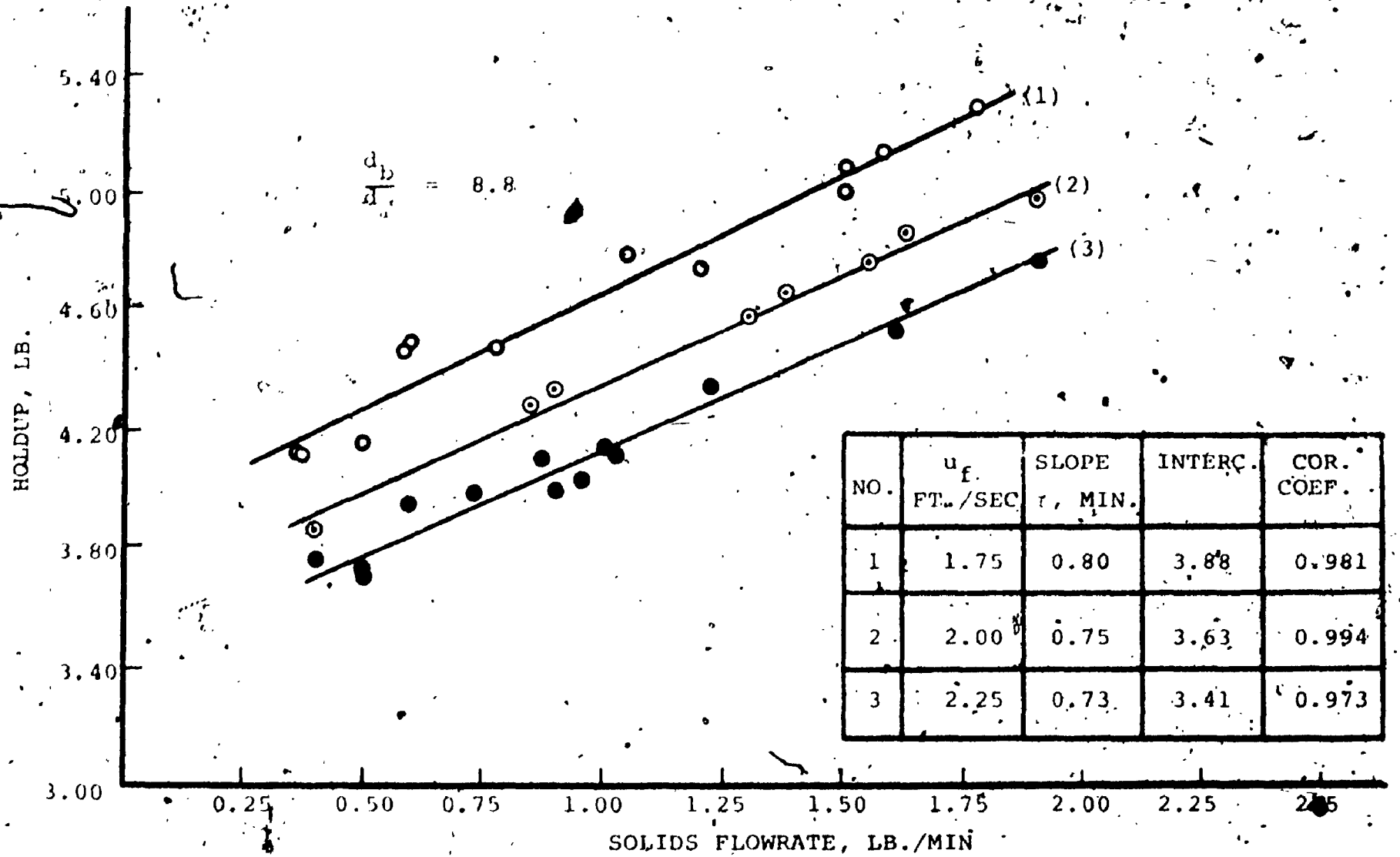

NO.	u_f FT./SEC	SLOPE r, MIN.	INTERC.	COR. COEF.
1	1.75	0.80	3.88	0.981
2	2.00	0.75	3.63	0.994
3	2.25	0.73	3.41	0.973

FIGURE 34. HOLDUP-SOLIDS FLOWRATE RELATIONSHIP OF 5005 SAND WITH WEIR HEIGHT 2 INCHES AND WEIR DIAMETER 1.25 INCHES

General discussion

The plots on Figures 23 through 34 (except Figure 32) were least squares fits to straight lines. A computer program for this purpose and all tables of data related to these Figures are presented in Appendix B. These plots prove that the linear equation (4.2) is indeed valid within a range of solids flowrate of 0.25 to 2.00 lb./min. and a column to weir diameter ratio of 4.4 to 8.8. At zero solids flow the holdup decreased with time due to a continuous removal of solids through the downcomer from bursting bubbles. This is an explanation as to why the time constant of 2 minutes obtained from Figure 22 is not in agreement with the time constants obtained from Figure 23 (both Figure 22 and Figure 23 refer to the same height and diameter of weir). The above plots also showed that the time constant is not a function of the gas flowrate but it depends only on the height of the weir, diameter of the weir, and the type of solids. For column to weir diameter ratio of 4.4 and 8.8 the holdup to the solids flowrate relationship was linear. Figure 35 shows a linear dependence of the time constant on the weir height for the above two diameter ratios. When the column to weir diameter ratio was 13.6 (d_ω=0.81 inches) the holdup to solids flowrate relationship was not linear and this is attributed to a different mechanism of solids overflow.

An explanation of the linear relationship between the holdup and the solids flowrate can be given based on the fact

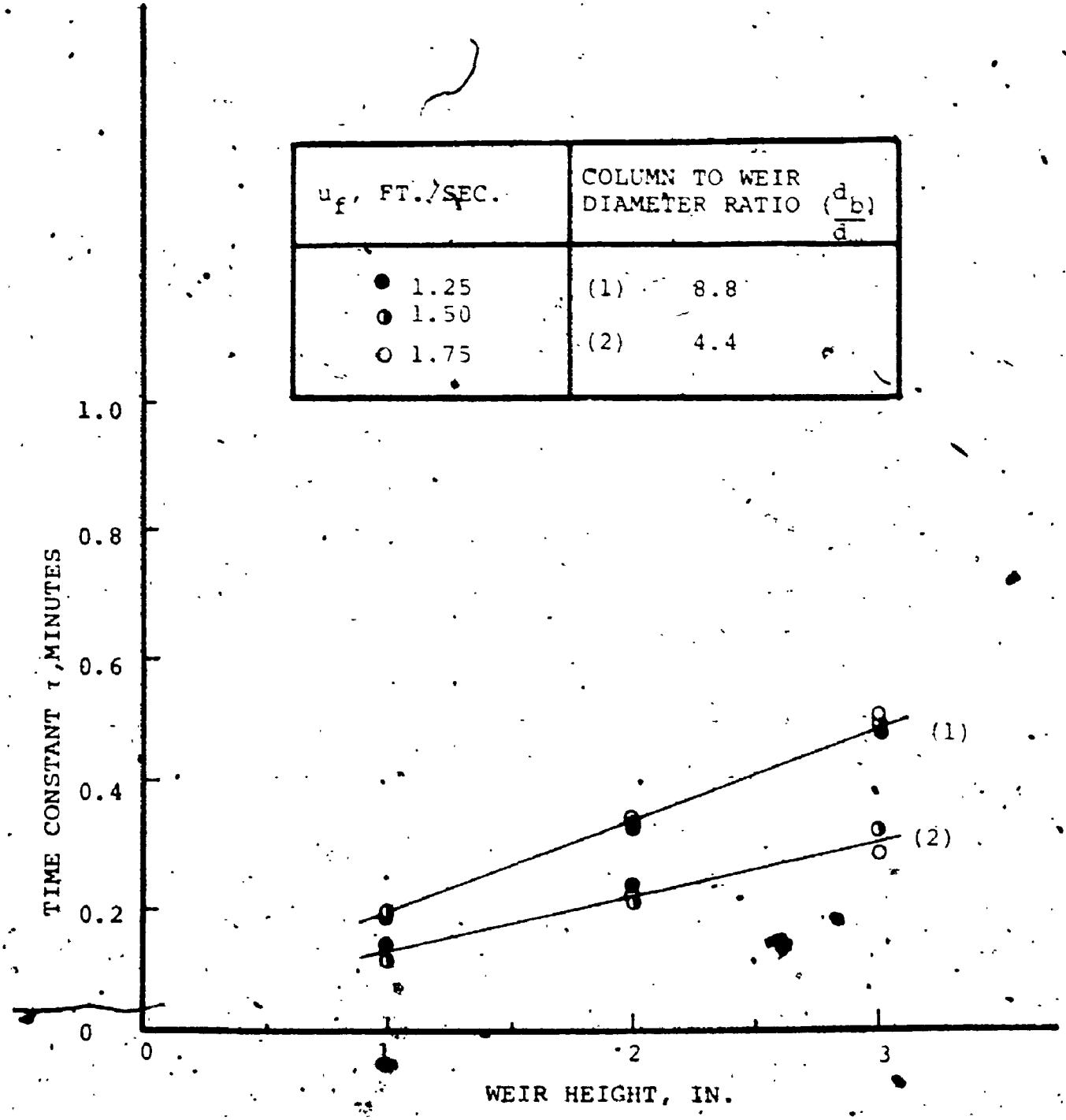

FIGURE 35. DEPENDENCE OF THE TIME CONSTANT ON THE WEIR HEIGHT USING AS PARAMETERS THE WEIR DIAMETER AND THE GAS FLOWRATE

that in a fluidized bed there are two density regions. The lower of these regions is made up of the main bed of uniform density (dense phase) while the upper region is of varying density (dilute phase); this region is formed by the eruption of bubbles at the surface of the bed, thus scattering the solids and resulting in a density gradient (6). Figure 36 is a schematic of this behavior. At this point the following three simplifying assumptions are made:

(a)- The density gradient in the upper region is linear and depends on the distance of the top of the weir from the top of the bed, equation (4.8)

$$\rho = \rho_{bf} - \alpha(h - x) \qquad (4.8)$$

where the slope α is a constant depending on the nature of solids.

(b) The flowrate of solids through the weir is proportional to the bulk density of solids at the elevation of the weir, equation (4.9)

$$L = K\rho \qquad (4.9)$$

where K is a constant depending on the geometry of the weir.

(c) The interface between the lower and the upper region is below the top of the weir.

A change in the solids flowrate ΔL will result in an elevation of the interface of the two regions by a height Δx when equilibrium is reached. This change will affect the density of the upper region at the elevation of the weir by

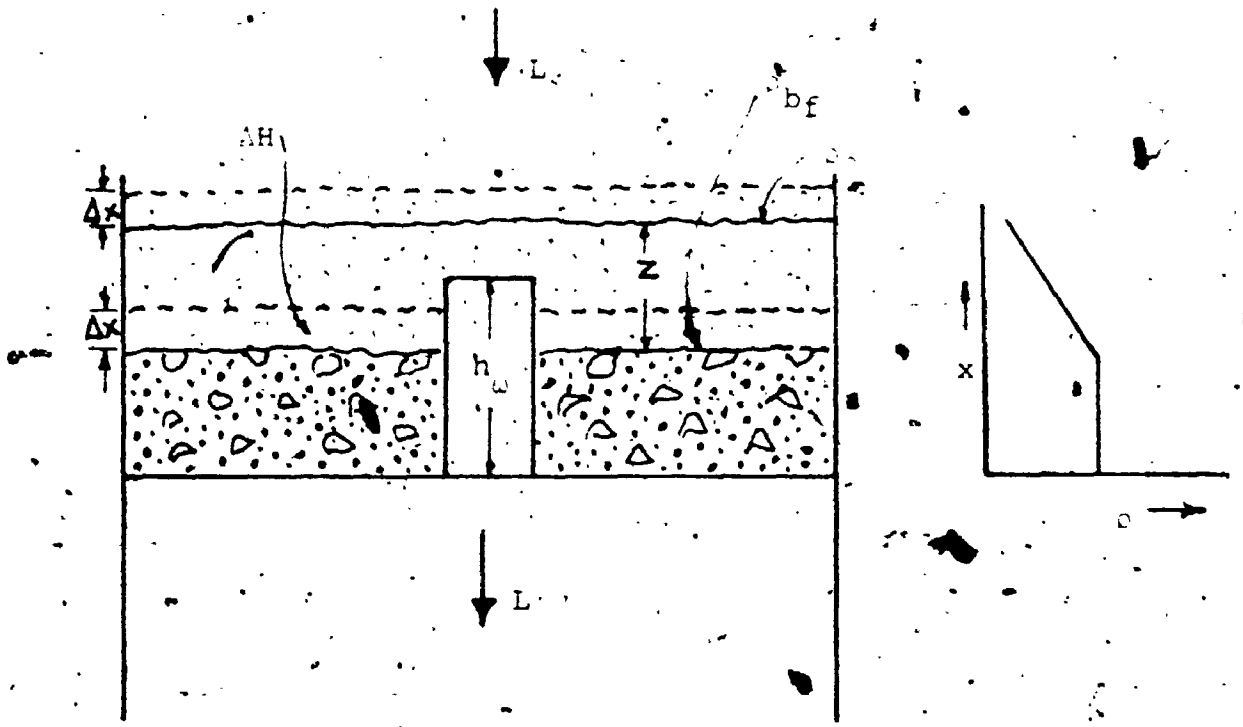

FIGURE 36. MODEL OF A TWO DENSITY REGIONS FLUIDIZED BED.

Then as a result of equation (4.8)

$$\Delta L = K \Delta x \tag{4.10}$$

Due to equation (4.9)

$$\Delta L = K_1 \tag{4.11}$$

Combining equations (4.10) and (4.11) results in equation (4.12)

$$\Delta L = K_1 \Delta x \tag{4.12}$$

Since the density of the solids in the main bed is uniform, an increase of the bed height by Δx will result in a proportional increase of the holdup by ΔH, that is

$$\Delta H = A \rho_{bf} \Delta x \tag{4.13}$$

Dividing equation (4.13) by equation (4.12) results in equation (4.14)

$$\frac{\Delta H}{\Delta L} = \frac{A \rho_{bf}}{K_1} = \tag{4.14}$$

Equation (4.14) shows that the slope of holdup to solids flowrate relationship is constant and depends on the cross-section area of the column A, the density of the fluidized solids ρ_{bf}, the geometry of the weir (reflected in K), and the particle size distribution of solids (reflected in d). This equation is in good agreement with the experimental results where in all but one case the holdup to solids flowrate relationship was linear. The non-linearity observed when the weir diameter was relatively small (refer to Figure 32) thus resulting in a situation where assumption (c) was not met. In fact, a visual inspection showed that when the column to weir diameter ratio was 13.6, the overflow of solids through

the downcomer took place from the lower region of the bed of uniform density.

The average time constant for the sand, as shown on Figure 34, is 0.76 minutes. This value was more than twice the time constant obtained under the same conditions for carbon (Figure 24). This can be attributed to the higher bulk density of sand which is three times that of carbon and according to equation (4.12) the same ratio of time constants for these two materials could be expected. The fact that the ratio of these two time constants, which is equal to 2.3, is different from the ratio of the respective bulk densities, which is equal to 3.0, is due to the higher value of the constant α for sand. In fact, from the particle size distributions of both carbon and sand shown on Figures 15 and 28, respectively, it appears that the standard deviation of carbon is 1.26 compared to 1.41 for sand; this means that sand has a wider particle size distribution and according to assumption (a) the constant α would be larger.

The linear dependancy of the time constant on the weir height, demonstrated in Figure 35, can be explained as follows: In a fluidized bed the bubble size increases linearly with bed height and the frequency of the rising bubbles decreases, due to coalescence, from the center of the bed to the wall (27). However, coalescence starts from a certain height and for shallow beds it can be assumed that the distribution of the bubbles over the bed is uniform. The upper region of the bed has a height which could be related to the

size of bubbles at the surface of the bed. In general, the eruption of a big bubble could be expected to scatter the solids farther than the eruption of a small bubble. Hence, a linear relationship can be assumed between the bed height or weir height h_w and width of the upper region z, that is

$$z = Ch_w + E \qquad (4.15)$$

The boundary conditions for assumption (a) are x=z and $\rho=\rho_{bf}$, thus

$$\rho_{bf} = z + \qquad (4.16)$$

or

$$= \frac{\rho_{bf}-}{z} \qquad (4.17)$$

Combining equations (4.15) and (4.17) results in

$$= \frac{\rho_{bf}-\rho_{}}{Ch_w+E} \qquad (4.18)$$

Substituting for α in equation (4.14) results in equation (4.19)

$$= \frac{C\rho_{bf}}{K(\rho_{bf}-\rho_{})} h_w + \frac{AE\rho_{bf}}{(\rho_{bf}-\rho_{})K} \qquad (4.19)$$

Equation (4.19) demonstrates that the time constant τ is proportional to the weir height h_w and this is in agreement with the experimental results shown on figure 35.

An attempt was made to correlate the tray solids holdup H as a function of the solids flowrate L, the superficial gas velocity u_f, the weir height h_w, the weir diameter d_w, the column diameter d_b, and the particle density ρ_p. By applying dimensional analysis the detailed procedure of which

is presented in Appendix C the following equation was obtained:

$$\left(\frac{H}{d_b^3 \rho_p}\right) = K \cdot \left(\frac{L}{d_b^2 \rho_p u_f}\right)^{n_1} \cdot \left(\frac{h}{d_b}\right)^{n_2} \cdot \left(\frac{d_b}{d}\right)^{n_3} \qquad (4.20)$$

The constants K, n_1, n_2, and n_3 were determined by the least squares method and a program for this purpose is presented in Appendix C. Figure 37, 38, and 39 show the correlation between the actual holdup and the predicted holdup for carbon, sand, and both carbon and sand, respectively. It can be seen that the individual correlations for carbon and sand were satisfactory though the constant K and the exponents n_1, n_2, and n_3 were in general different. The correlation for both carbon and sand was rather poor. This is attributed to lack of considering other variables which possibly affect this correlation. Such variables might be the viscosity of the fluidized solids (6), the shape factor of the particles, the particle size distribution etc.

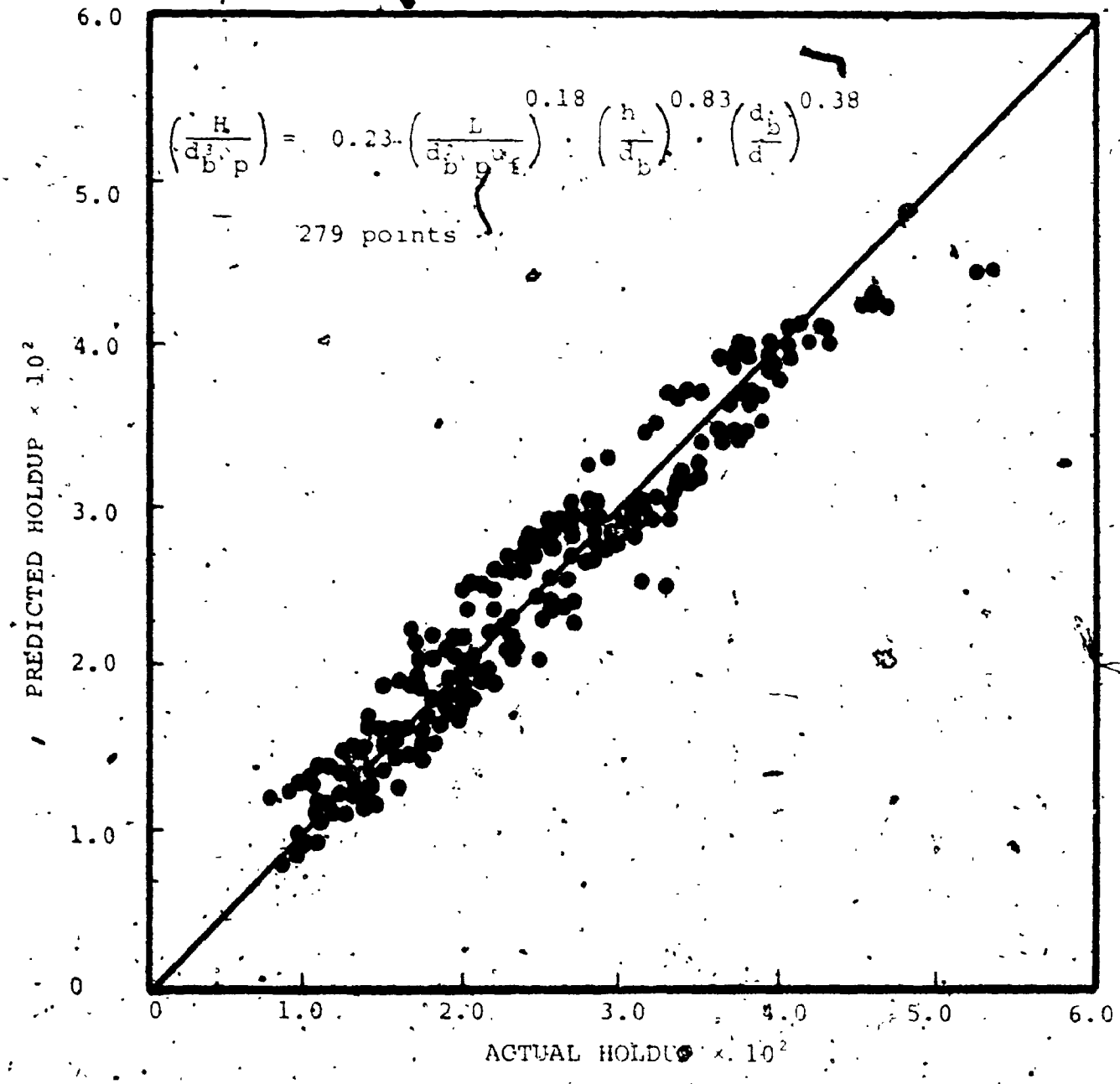

FIGURE 37. CORRELATION OF TRAY SOLIDS HOLDUP FOR CARBON

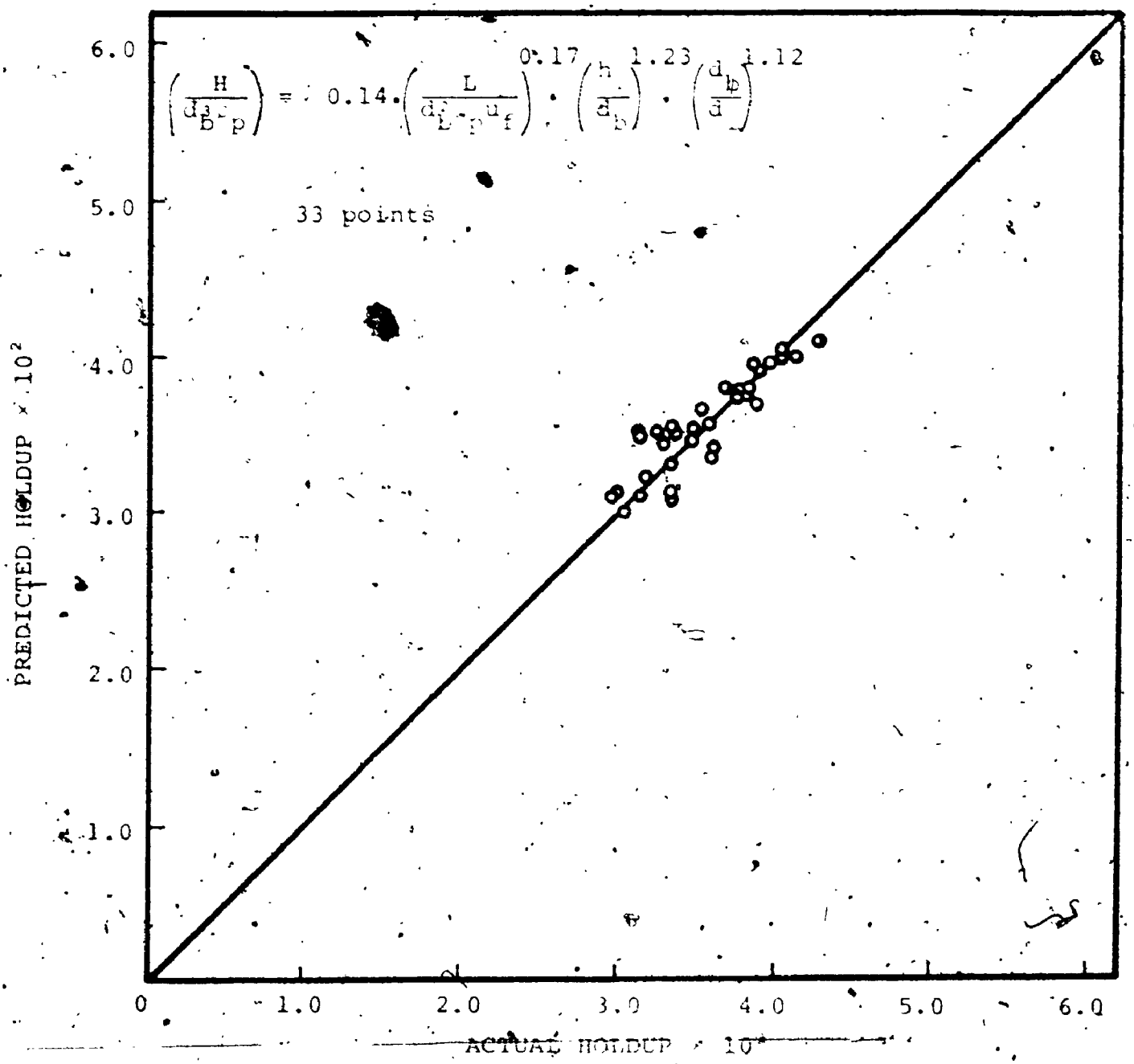

FIGURE 38. CORRELATION OF TRAY SOLIDS HOLDUP FOR SAND

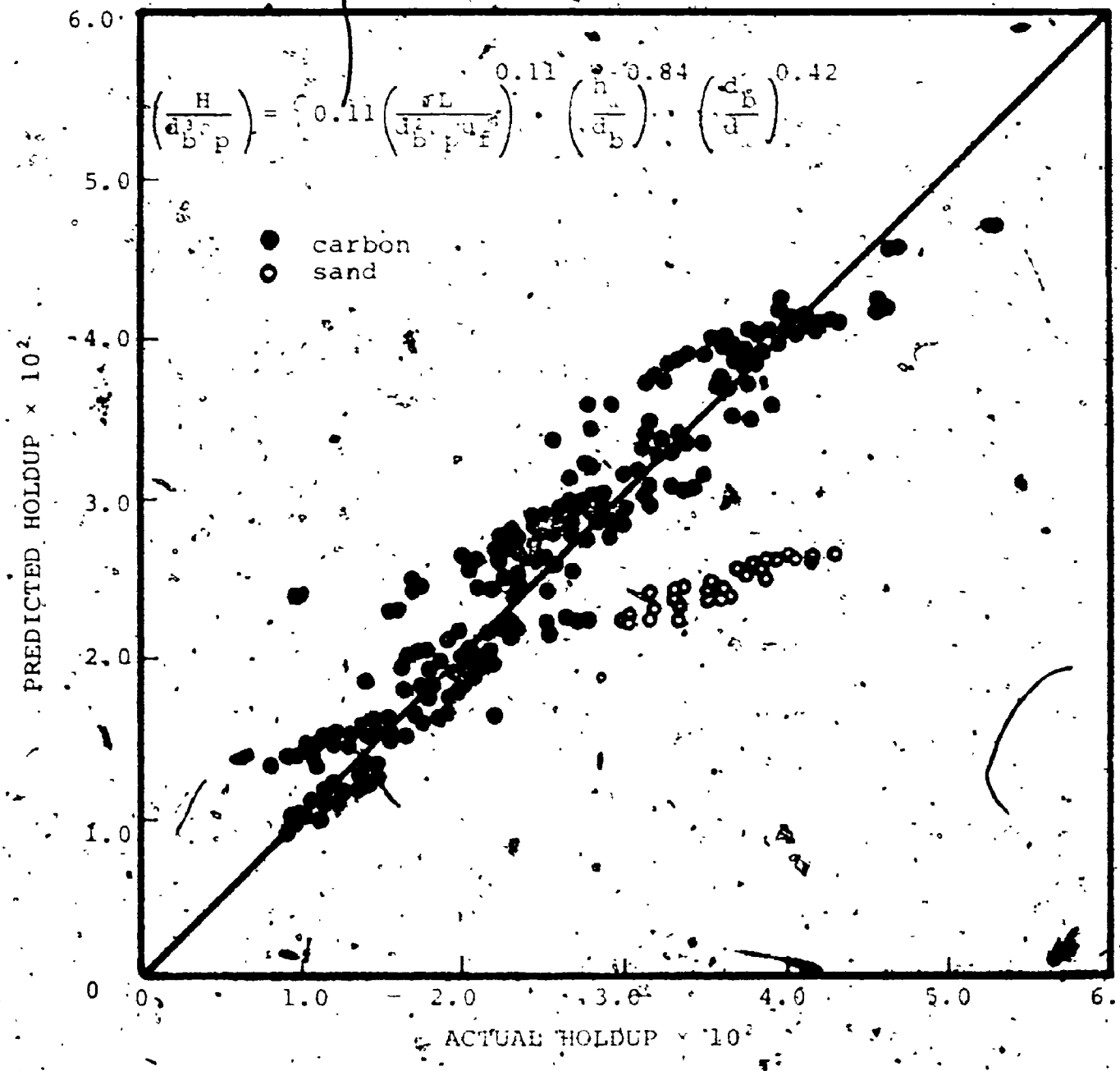

FIGURE 39. CORRELATION OF TRAY SOLIDS HOLDUP FOR BOTH CARBON AND SAND.

2 3

OF/DE

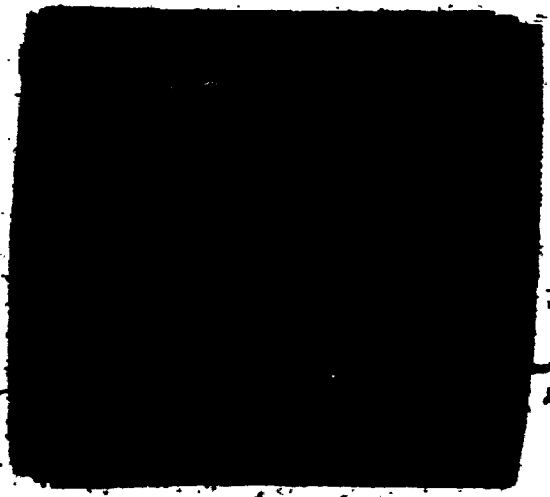

ARC-379

CHAPTER 5

PROCESS MODELING AND COMPUTER SIMULATION

5.1 Mathematical model

Figure 40 is a schematic of the four-state fluidized bed gas adsorber with downcomers. The fluidizing air enters the column at the bottom with flowrate F containing a contaminant (supposedly CS_2) of concentration Y_i. As the mixture passes upwards the concentration of the contaminant, due to adsorption on an adsorbent (activated carbon), is reduced to an exit concentration Y_1. On the other hand, the adsorbent enters the column at the top with a flowrate L_i passing downwards through the colomn and exits at the bottom with a flowrate L_4 and a concentration X_4. The assumptions made in developing the mathematical model are as follows:

(a) Mixing between the gas and solid phases is ideal (lumped parameter model).

(b) Heat of adsorption is negligible, hence the process is assumed to be isothermal.

(c) At low concentrations the relationship between contaminant adsorbed on the solid phase and the contaminant in the gas phase is linear and described by equation (5.1).

$$Y_j = mX_j \qquad (5.1)$$

where $j = 1, 2, 3, 4$

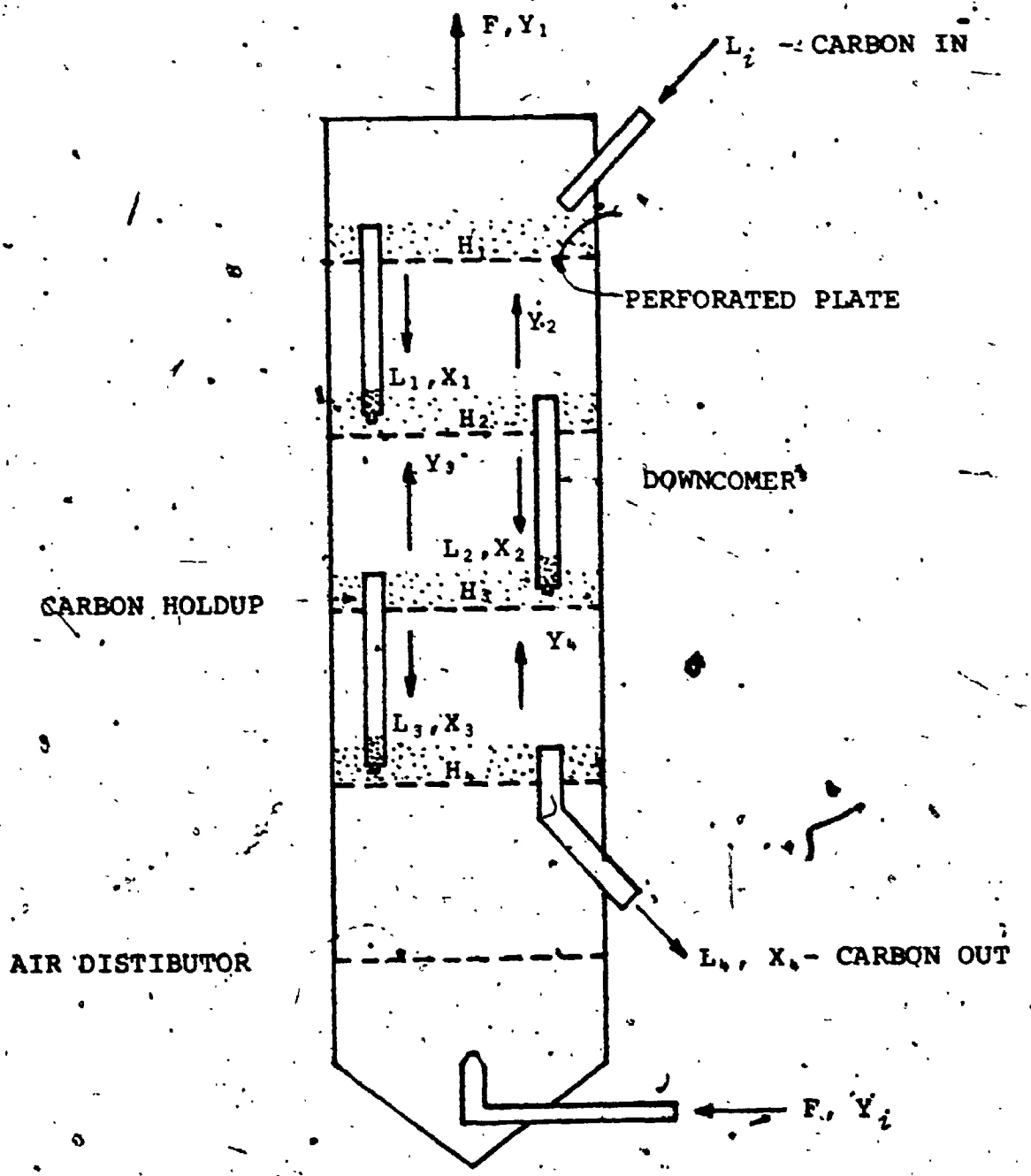

FIGURE 40. SCHEMATIC OF A FOUR-STAGE FLUIDIZED BED GAS ADSORBER

A material balance for the contaminant on plate j results in the following equation:

$$\frac{d(H_j X_j)}{dt} = -(L_j + Fm)\, X_j + L_{j-1}\, X_{j-1} + FmX_{j+1} \qquad (5.2)$$

This equation has the boundary conditions $L_o = L_i$, $X_o = 0$, and $mX_s = Y_i$; equation (5.2) may be rewritten as follows:

$$H_j \frac{dX_j}{dt} + X_j \frac{dH_j}{dt} = -(L_j + Fm)\, X_j + L_{j-1} X_{j-1} + Fm\, X_{j+1} \qquad (5.3)$$

The dynamics of the tray solids holdup may be described by the following equation:

$$\frac{dH_j}{dt} = -L_j + L_{j-1} \qquad (5.4)$$

Multiplying equation (5.4) by X_j and subtracting from equation (5.3) results in equation (5.5)

$$H_j \frac{dX_j}{dt} = -(L_{j-1} + Fm)\, X_j + L_{j-1} X_{j-1} + FmX_{j+1} \qquad (5.5)$$

This is a linear differential equation as the time dependent coefficient L_{j-1} can be obtained from equation (5.4) and the principle of superposition can thus be applied.

The relationship between the solids holdup H_j and the overflow solids L_j, for plate j, was varified in Chapter 4 and is as follows:

$$H_j = H_{js} + tL_j \qquad (5.6)$$

5.2 Computer simulation using the Continuous System Modelling Program for the IBM 1130

This method can be used for solving numerically differential equations of any order by using the second order Runge-Kutta method. The user should be aware, however, that the second order Runge-Kutta, although very convenient for computer work, is a crude method of integration. It generates a large truncation error and unless a proper interval is selected it may lead to instability. The error is a function of the integration interval Δt but is not easy to be estimated (29). For a system of non-linear differential equations analytical determination of the optimum interval Δt for convergence is extremely difficult if not impossible. A practical approach is to change this interval by trial and error until the same results are obtained for two different Δt values.

For the four-stage fluidized bed gas adsorber the set of equations used for simulation are the following:

$$H_1 \frac{dX_1}{dt} = -(L_i + Fm)\, X_1 + FmX_2 \qquad (5.7)$$

$$H_2 \frac{dX_2}{dt} = -(L_1 + Fm)\, X_2 + L_1X_1 + FmX_3 \qquad (5.8)$$

$$H_3 \frac{dX_3}{dt} = -(L_2 + Fm)\, X_3 + L_2X_2 + FmX_4 \qquad (5.9)$$

$$H_4 \frac{dX_4}{dt} = -(L_3 + Fm)\, X_4 + L_3X_3 + FY_i \qquad (5.10)$$

$$\frac{dH_1}{dt} = -L_1 + L_i \qquad (5.11)$$

$$\frac{dH_2}{dt} = -L_2 + L_1 \qquad (5.12)$$

$$\frac{dH_3}{dt} = -L_3 + L_2 \qquad (5.13)$$

$$\frac{dH_4}{dt} = -L_4 + L_3 \qquad (5.14)$$

$$H_1 = H_{1S} + \tau L_1 \qquad (5.15)$$

$$H_2 = H_{2S} + \tau L_2 \qquad (5.16)$$

$$H_3 = H_{3S} + \tau L_3 \qquad (5.17)$$

$$H_4 = H_{4S} + \tau L_4 \qquad (5.18)$$

Figure 41 shows the block diagram representation for equation (5.7) through (5.10). Figure 42 shows the block diagram representation for both equations (5.11) through (5.18) and a proportional controller with its final control element. Table 3 gives the initial conditions for the integrators, and the constants which were used in solving the system of equations (5.9) through (5.18). Table 4 gives the initial conditions and parameters for the controller-final control element system.

5.3 Results and discussion

Figure 43 shows the open loop response of the CS_2 effluent concentration to a step change of the inlet concentration from 0.1% to 0.2%; the carbon flowrate was kept constant at 0.4 lb./min. It can be seen that the response

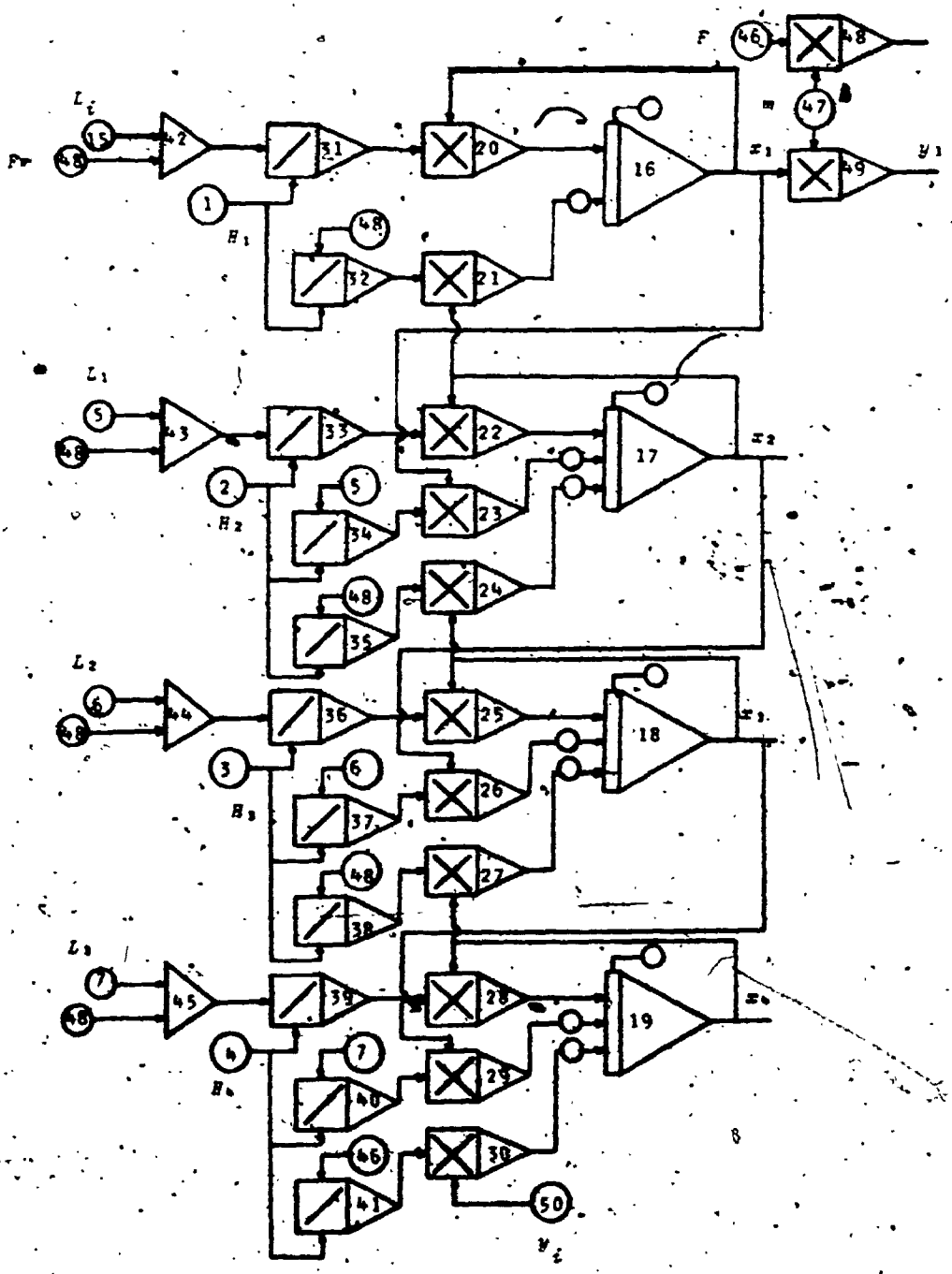

FIGURE 41. BLOCK DIAGRAM FOR EQUATIONS (5.7) THROUGH (5.10)

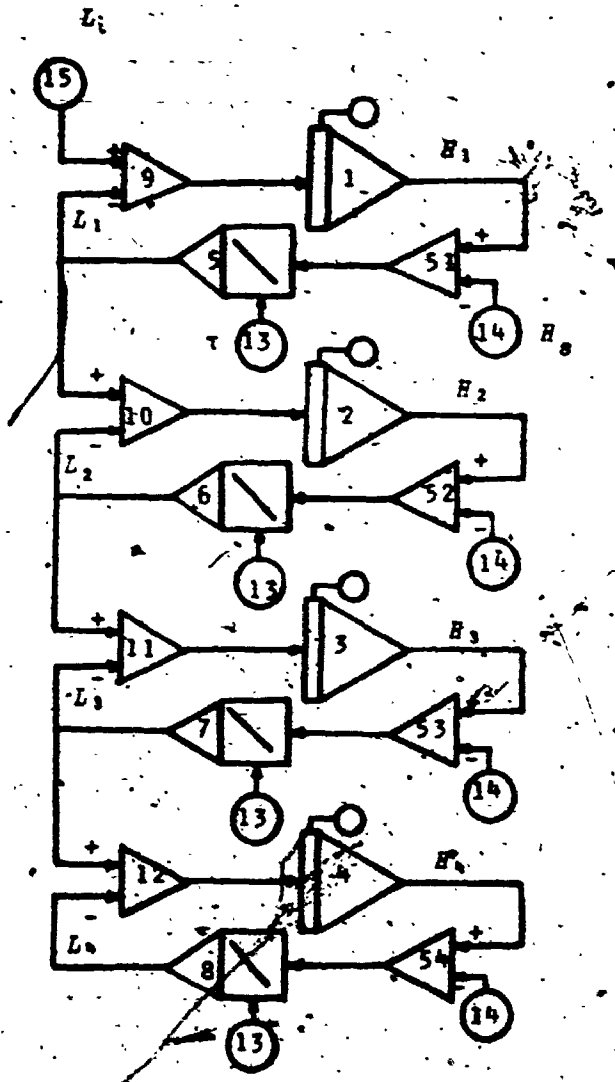

(a)

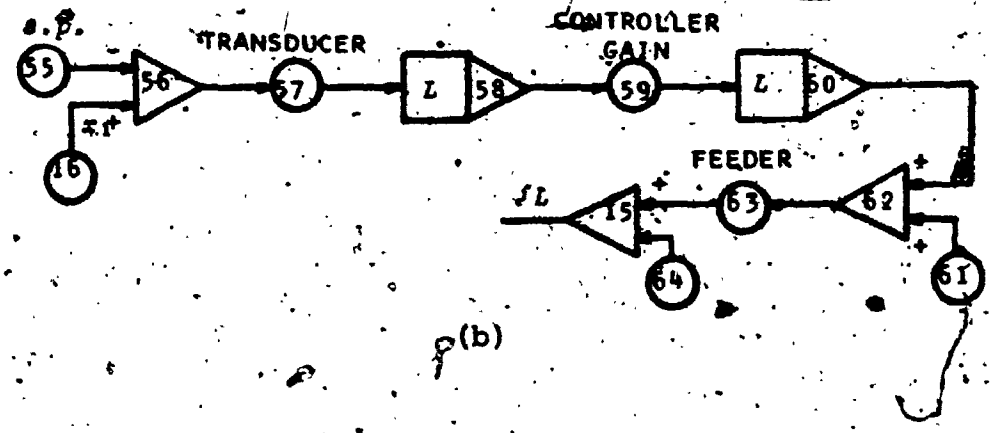

(b)

FIGURE 42. BLOCK DIAGRAM REPRESENTATION (a) EQUATIONS (5.11) THROUGH (5.18); (b) PROPORTIONAL CONTROLLER AND FINAL CONTROL ELEMENT

TABLE 3

INITIAL CONDITIONS AND CONSTANTS

NAME	SYMBOL	VALUE	UNITS
HOLDUP	Hjs	1.9-2.7	$lb.$
TIME CONSTANT	τ	0.2-2.0	$min.$
CARBON INLET FLOWRATE	$L_i=Ljs$	0.4	$lb./min.$
GAS INLET FLOWRATE	G	60.0	cfm
EQUILIBRIUM CONSTANT	m	0.002	$lb./cu.ft.$
CS_2 CONCENTRATION ON PLATE 1	x_1	0.0029	$mol./lb.$
CS_2 CONCENTRATION ON PLATE 2	x_2	0.0125	$mol./lb.$
CS_2 CONCENTRATION ON PLATE 3	x_3	0.0443	$mol./lb.$
CS_2 CONCENTRATION ON PLATE 4	x_4	0.1499	$mol./lb.$
HOLDUP AT NO CARBON FLOWRATE	H_s	1.90	$lb.$
CONTAMINANT INLET CONCENTRATION	Y_i	0.001	$mol./cu.ft.$

TABLE 4

INITIAL CONDITIONS AND PARAMETERS FOR

THE CONTROLLER-FINAL ELEMENT SYSTEM

NAME	VALUE	UNIT
SET POINT	0.0029	$mol./lb$
TRANSDUCER	3000	$psi/(mol./lb.)$
CONTROLLER GAIN	1.0-16.0	
CARBON FEEDER	0.0333	$lb./psi$
CARBON FEEDER CONSTANT	0.1	$lb.$
LIMITER	(-6.0)-(6.0)	psi
CONTROLLER STEADY STATE	9.0	psi

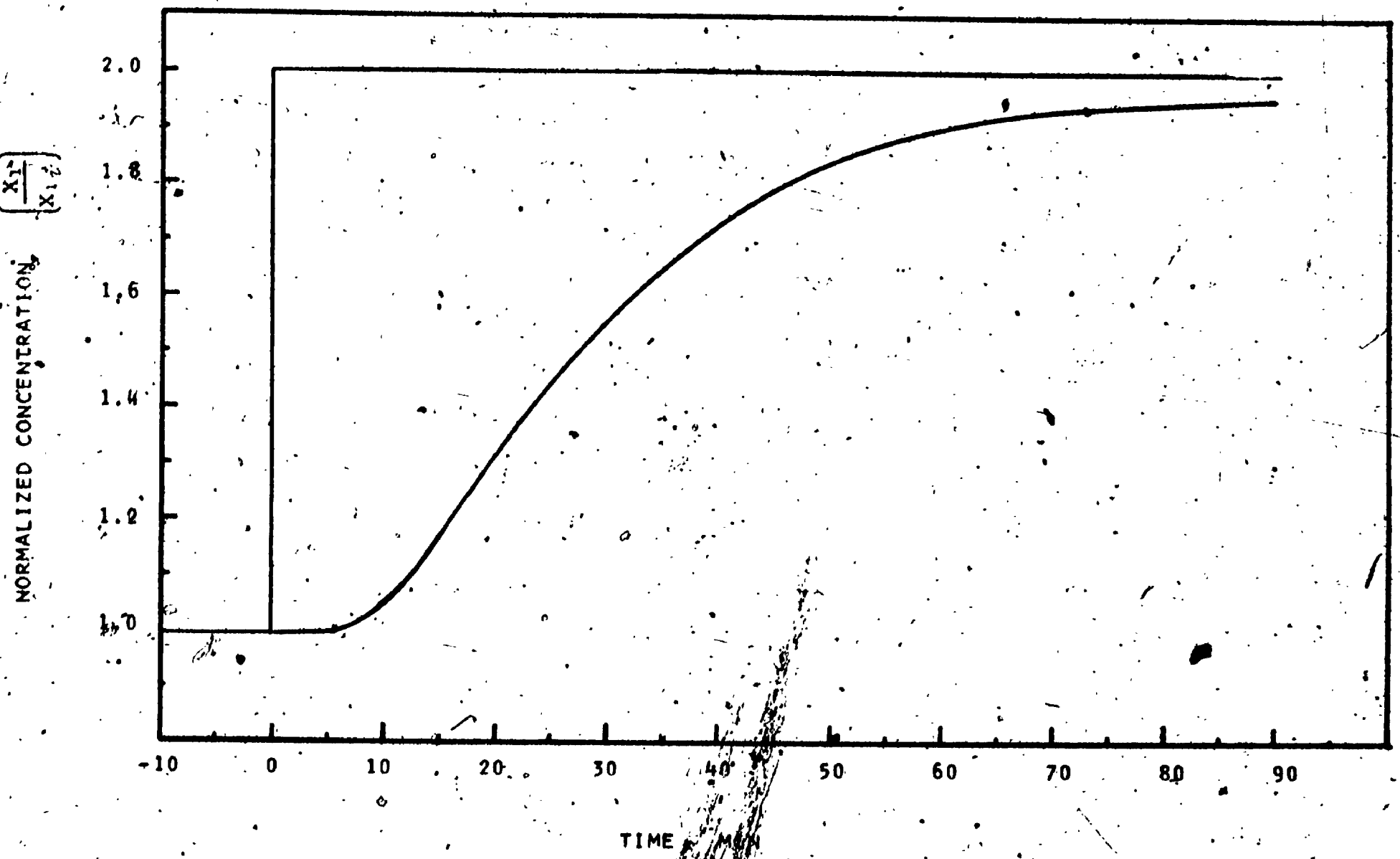

FIGURE 43. OPEN LOOP RESPONSE OF THE CS_2 OUTLET CONCENTRATION TO A STEP INPUT OF THE INLET CONCENTRATION FROM 0.1% TO 0.2%

is very slow and even after 90 minutes the steady state had not yet been reached. This slow response of the effluent composition to a disturbance of the inlet composition is actually beneficial from the control point of view. In fact, the sluggish behavior of the controlled variable will give the controller enough time to adjust the manipulating variable.

Figure 44 shows the open loop response of the CS_2 effluent concentration to a step decrease of the carbon flow-rate from 0.4 to 0.3 lb./min. The CS_2 inlet concentration was kept constant at 0.1% while the time constant τ of the solids holdup varied from 0 to 2.0 minutes. It is interesting to note that for values of the time constant between 0 and 0.5 minutes the response of the effluent composition is practically the same. It should be noted that a time constant range of 0.2 - 0.5 minutes corresponds to an increase of the downcomer weir height from 1 to 3 inches.

Figure 45 shows the closed loop response of the CS_2 effluent concentration to a step change of the inlet concentration from 0.1% to 0.25%. Using a proportional controller and a time constant for the solids holdup dynamics of 2 minutes resulted in a stable non-oscillatory response. The offset from the desired value decreased as the controller gain increased; at gain equal to 16.0 the offset was practically eliminated.

Figure 46 shows the closed loop response of the effluent composition from 0.1% to 0.2% when the solids holdup time

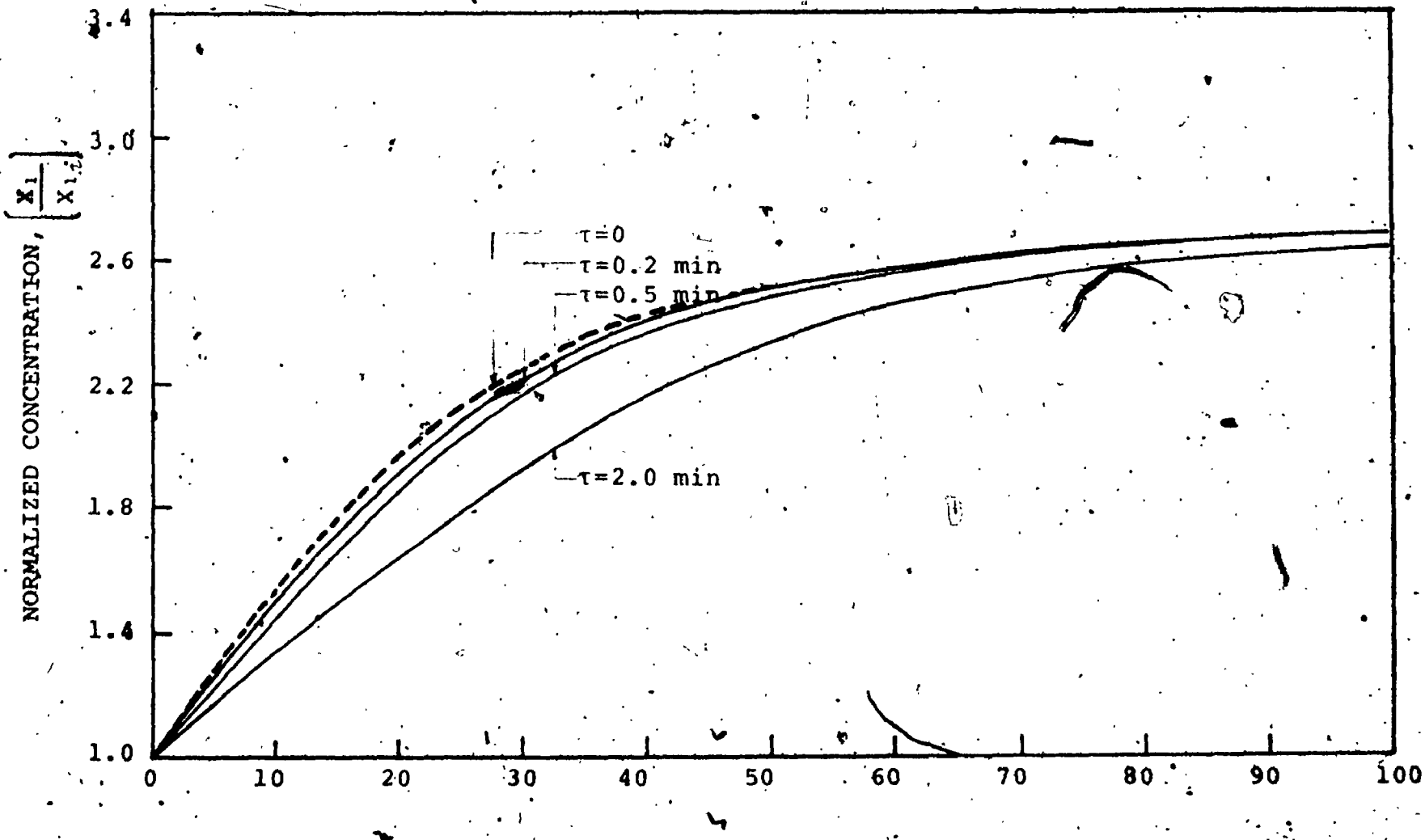

FIGURE 44. OBEN LOOP RESPONSE OF THE CS_2 OUTLET CONCENTRATION TO A STEP CHANGE OF THE CARBON FEED FROM 0.4 LB/MIN TO 0.3 LB/MIN (Δt=0.1 MIN)

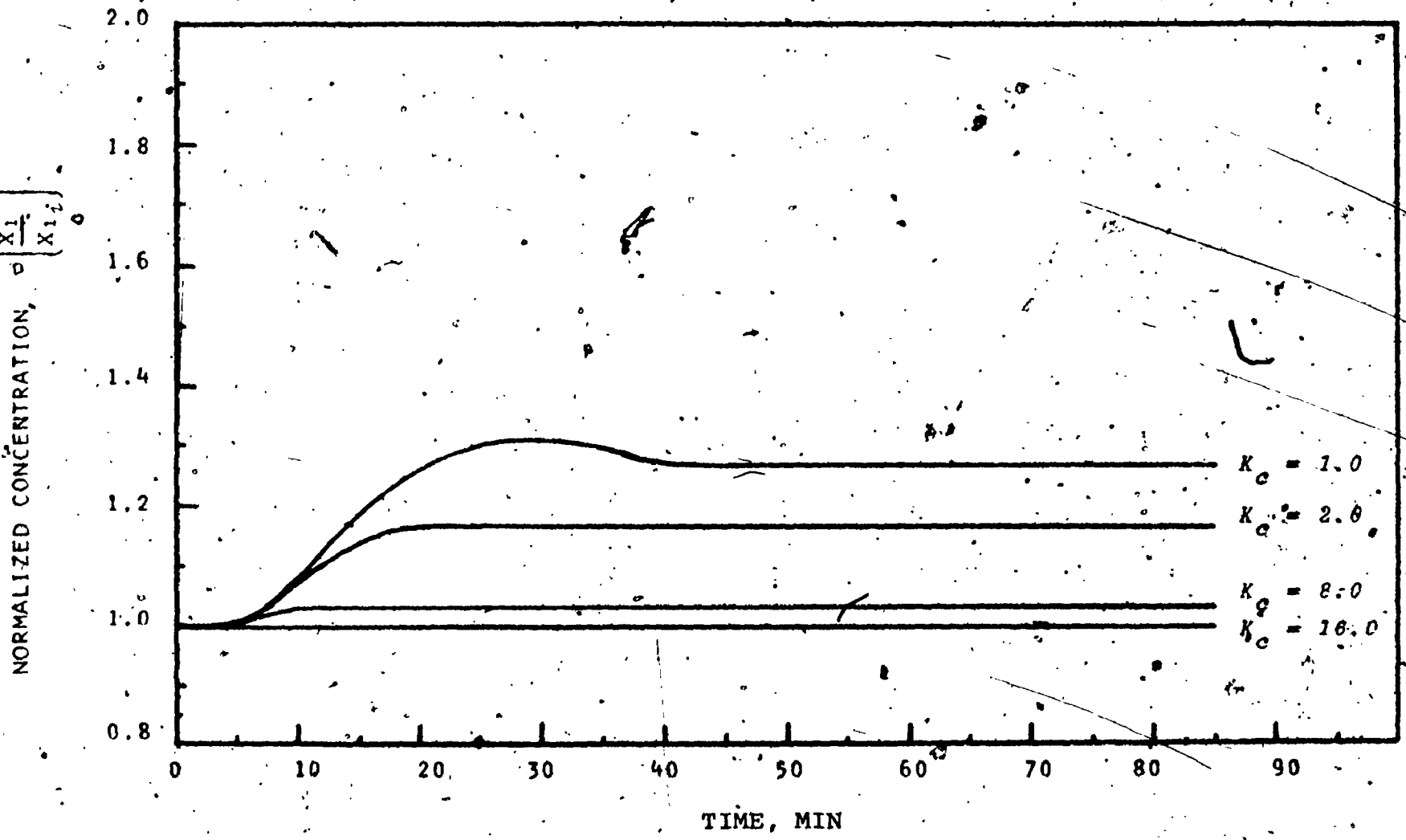

FIGURE 45. CLOSED LOOP RESPONSE OF THE OUTLET CONCENTRATION TO A STEP CHANGE OF THE INLET CONCENTRATION FROM 0.1% to 0.25% AND A TIME CONSTANT FOR THE SOLIDS 2.0 MINUTES

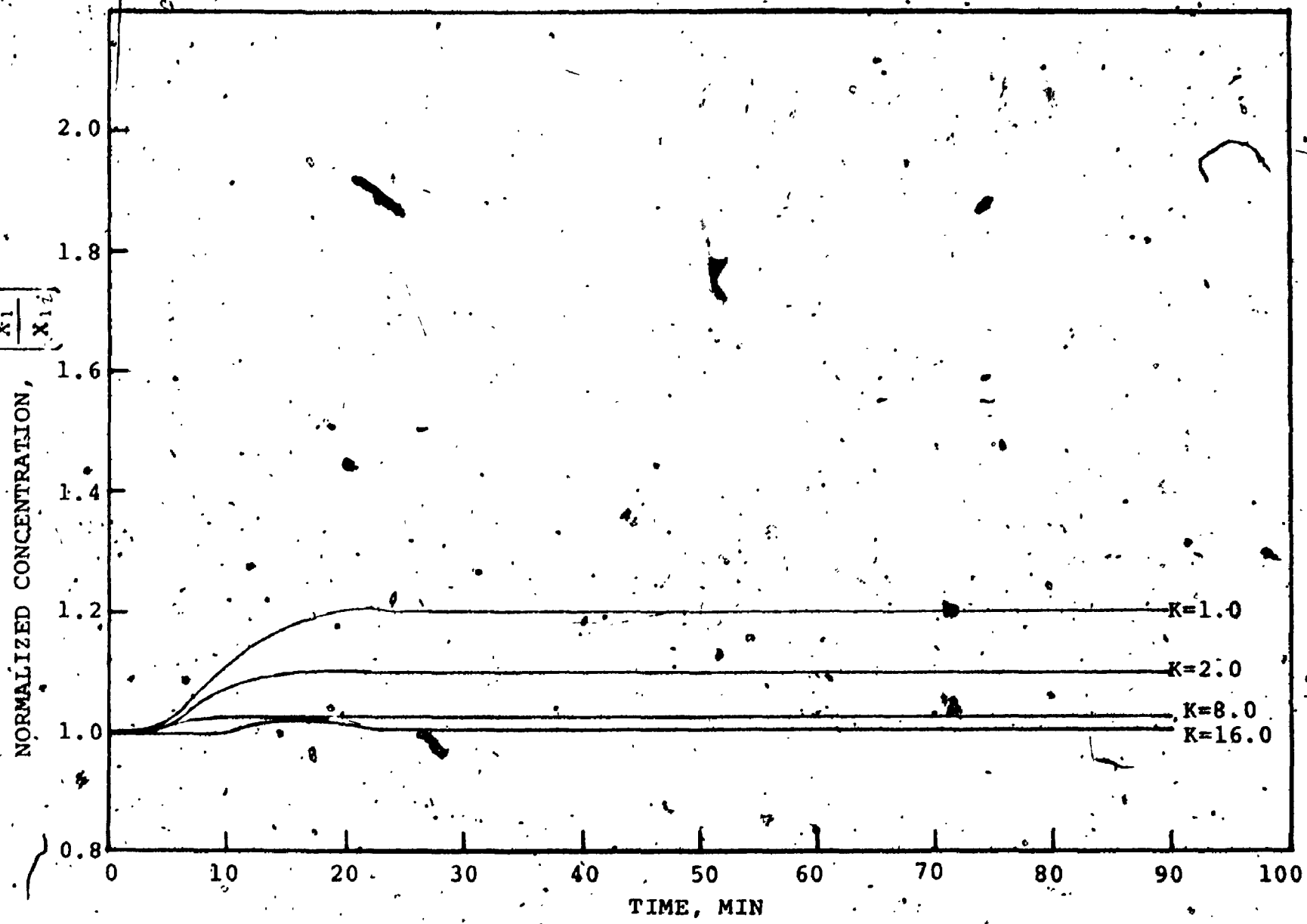

FIGURE 46. CLOSED LOOP RESPONSE OF THE OUTLET CONCENTRATION TO A STEP CHANGE OF THE INLET CONCENTRATION FROM 0.1% to 0.2% AND A TIME CONSTANT FOR THE SOLIDS 0.2 MINUTES

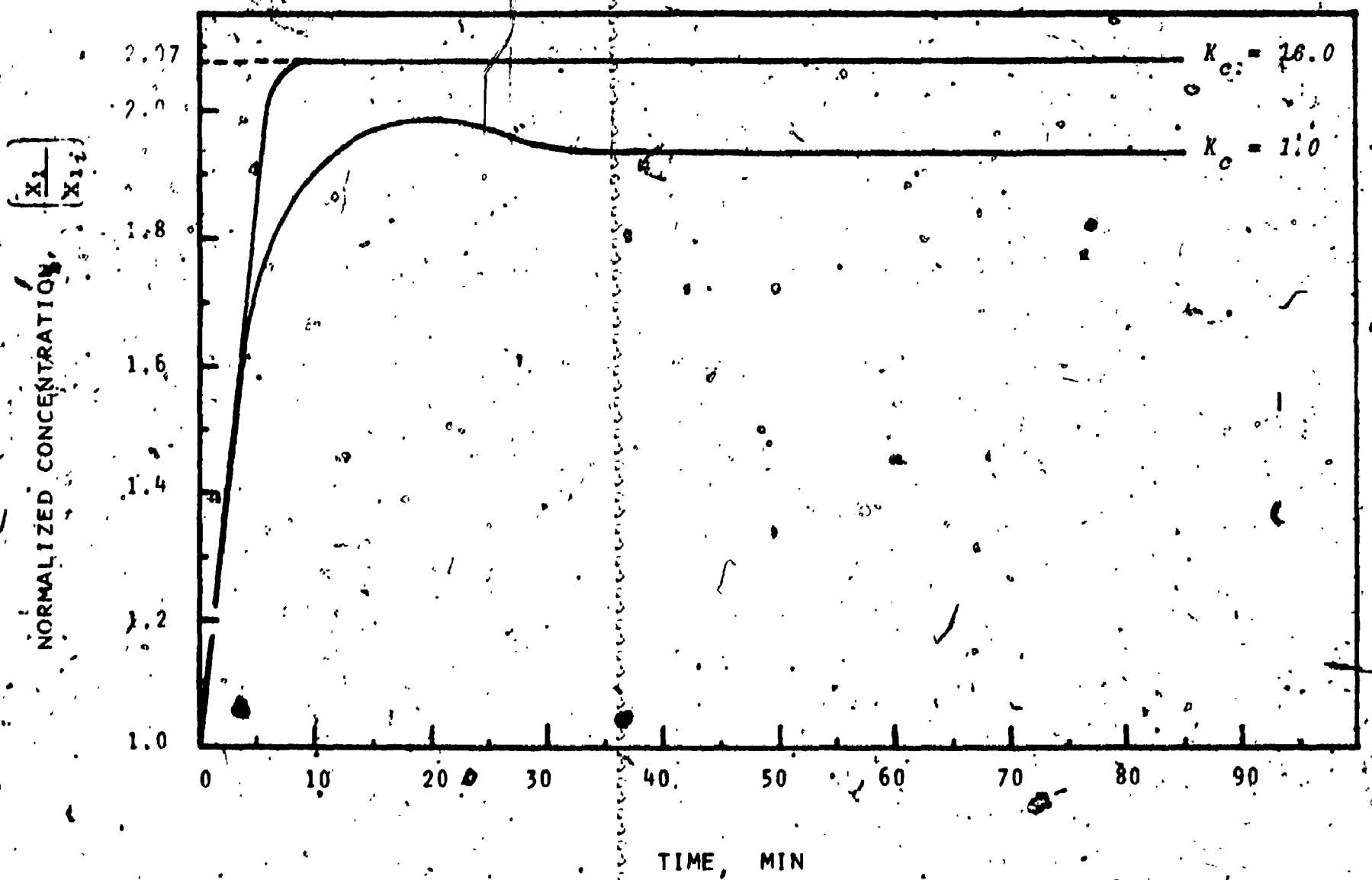

FIGURE 47. RESPONSE OF THE CS_2 OUTLET CONCENTRATION TO A STEP CHANGE OF THE CONTROLLER SET POINT BY 10% AND A TIME CONSTANT FOR THE SOLIDS 2 MINUTES

constant was 0.2 minutes. It can be seen that the response is almost identical to that when a time constant of 2 minutes was used. This behavior could be anticipated from the results of Figure 44 where it is shown that the time constant τ affects only slightly the response of the effluent composition.

Figure 47 shows the response of the CS_2 effluent concentration to a step change of the controller set point by 107%. The time constant for the solids holdup was set at 2.0 minutes. Here again the response was stable, non-oscillatory and the offset was practically eliminated when the controller gain was set equal to 16.0

The above results indicated that the effluent concentration from a multistage fluidized bed gas adsorber designed according to Molodov and Jshkin (7) can be easily regulated by a proportional controller. The effect of the time constant of the solids holdup is insignificant. The effluent composition is very sensitive to the solids flowrate when compared to the tray solids holdup. In fact, a 25% change in the carbon flowrate resulted in 170% change in the contaminant effluent composition and only a 7% change in the tray solids holdup. This means that the effluent composition can be efficiently controlled by slight variations in the carbon flowrate. Under these conditions the dynamics of the solids can be neglected and hence the solids flowrate L and the holdup H can be assumed constant. The mathematical model for the process then becomes:

$$\dot{\underset{\sim}{X}} = \underset{\sim}{A}\,\underset{\sim}{X} + \underset{\sim}{W} \qquad (5.19)$$

where

$$\underset{\sim}{A} = \begin{bmatrix} -\frac{L+Fm}{H} & \frac{Fm}{H} & 0 & 0 \\ \frac{L}{H} & -\frac{L+Fm}{H} & \frac{Fm}{H} & 0 \\ 0 & \frac{L}{H} & -\frac{L+Fm}{H} & \frac{Fm}{H} \\ 0 & 0 & \frac{L}{H} & -\frac{L+Fm}{H} \end{bmatrix} \quad (5.20)$$

and

$$\underset{\sim}{W} = \begin{bmatrix} 0 \\ 0 \\ 0 \\ FY_i \end{bmatrix} \quad (5.21)$$

The exact solution of equation (5.19) can be obtained if the eigenvalues of the matrix A can be found. For the four stage bed this solution is presented in Appendix D. This approximation seems justified in the light of the results of Figure 44 where for time constants between 0 and 0.5 minutes the influence on the response of the outlet composition was insignificant. Under these conditions, the effect of the small time constant changes due to the dynamics of the solids can be ignored and the integration interval can be made larger thus reducing the computing time. It should be noted that the time constant due to the dynamics of the composition for one plate is $\frac{H}{L+Fm} \simeq 5$ minutes. A numerical solution of equation (5.19) with integration intervals from 0.1 up to 5 minutes resulted in no detectable error. Thus by neglecting the relatively small time constant of the solids, computing time can be substantially reduced.

All the results of the CSMP simulation were obtained using an integration interval of 0.1 minutes. The reproducibility of these results was checked for integration intervals between 0.05 and 0.5 minutes. It was noticed that the accuracy of the results was related to the ratio of the integration interval to the smallest time constant $\Delta t/\tau$. In fact, when this ratio was greater than 1 a large error resulted. On the contrary, for values of this ratio less than 1 the results were reproducible. This is demonstrated in Figure 48.

Two sample programs, one for the open loop and another for the closed system can be found in Appendix E. Appendix E also contains printouts of all the results presented in this chapter.

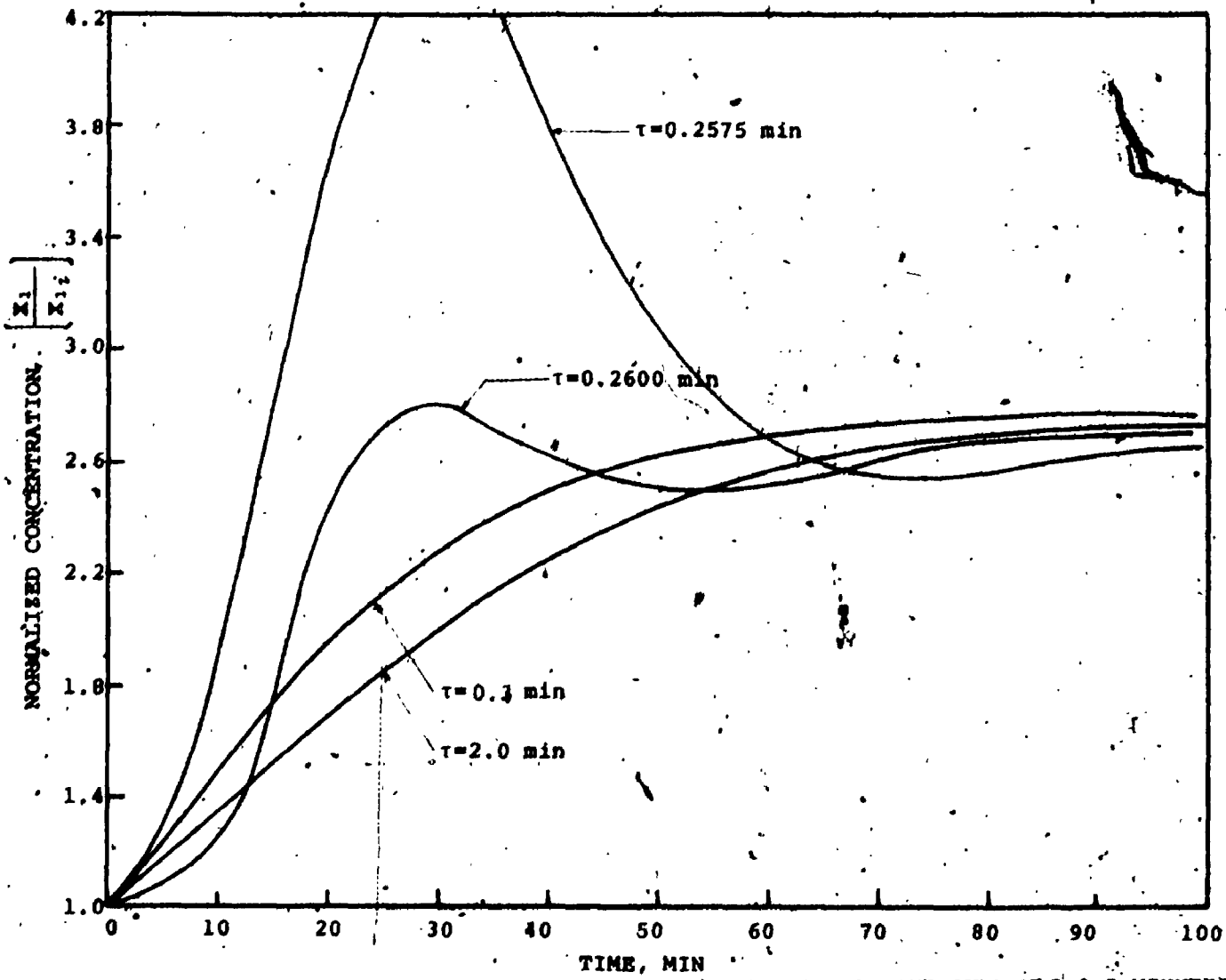

FIGURE 48. TREND OF INSTABILITY WHEN THE INTEGRATION INTERVAL WAS 0.5 MINUTES. THE PLOTS SHOW THE OPEN LOOP RESPONSE OF THE EFFLUENT CONCENTRATION TO A STEP DECREASE OF THE CARBON FLOWRATE FROM 0.4 LB/MIN TO 0.3 LB/MIN

CHAPTER 6

CONCLUSIONS AND RECOMMENDATIONS

The conclusions that can be drawn from the present work are as follows:

1. By using strain gages, a momentum dissipation type solids flowmeter was designed and constructed for as low a flowrate as 0.01 lb./min. This flowmeter was used successfully in a feedback loop to control solids feed to a fluidized bed.
2. Fluidized solids do not rest on the grid but they are totally suspended.
3. The relationship between the solids tray holdup H and the exiting solids flowrate L was found to be linear over the range of flowrates 0.25 to 2.0 lb./min. whereas for flowrates less than 0.25 lb./min. it was non-linear. The linear part of this relationship has the form $H = H_s + \tau L$ and demonstrates that the dynamics of the solids holdup for a shallow bed with downcomer are first order with time constant τ.
4. For activated carbon of 420 microns geometric mean diameter of the solids the time constant is independent of the gas flowrate over the range 50 to 70 cu.ft.

per minute and depends only on the height of the weir. When the weir height varied between 1 and 3 inches, the time constant varied between about 0.2 and 0.5 minutes. For sand of geometric mean 120 microns the time constant under the same conditions was 2.3 times that of carbon; the effect of the gas flowrate on the time constant was negligible.

5. In a multistage fluidized bed gas adsorber the effluent concentration can be easily regulated with a proportional controller. The effect of the time constant of the solids holdup on the effluent concentration is insignificant and in all the simulated cases resulted in a stable non-oscillatory response.

As a continuation of this work, further study is recommended. Some areas that should be investigated are as follows:

1. A better insight into the effect of the particle density and the size distribution on the time constant of the tray solids holdup.
2. Study of mixing of solids as a function of the weir height. This study would define an optimum weir height as there is a strong indication that either a low or a high weir does not promote good mixing.
3. The experimental proof of the results as obtained via simulation in Chapter 5.

APPENDIX A

DRAWINGS FOR THE COLUMN

TOP SECTION OF THE GOLUMN
(Material: acrylic)

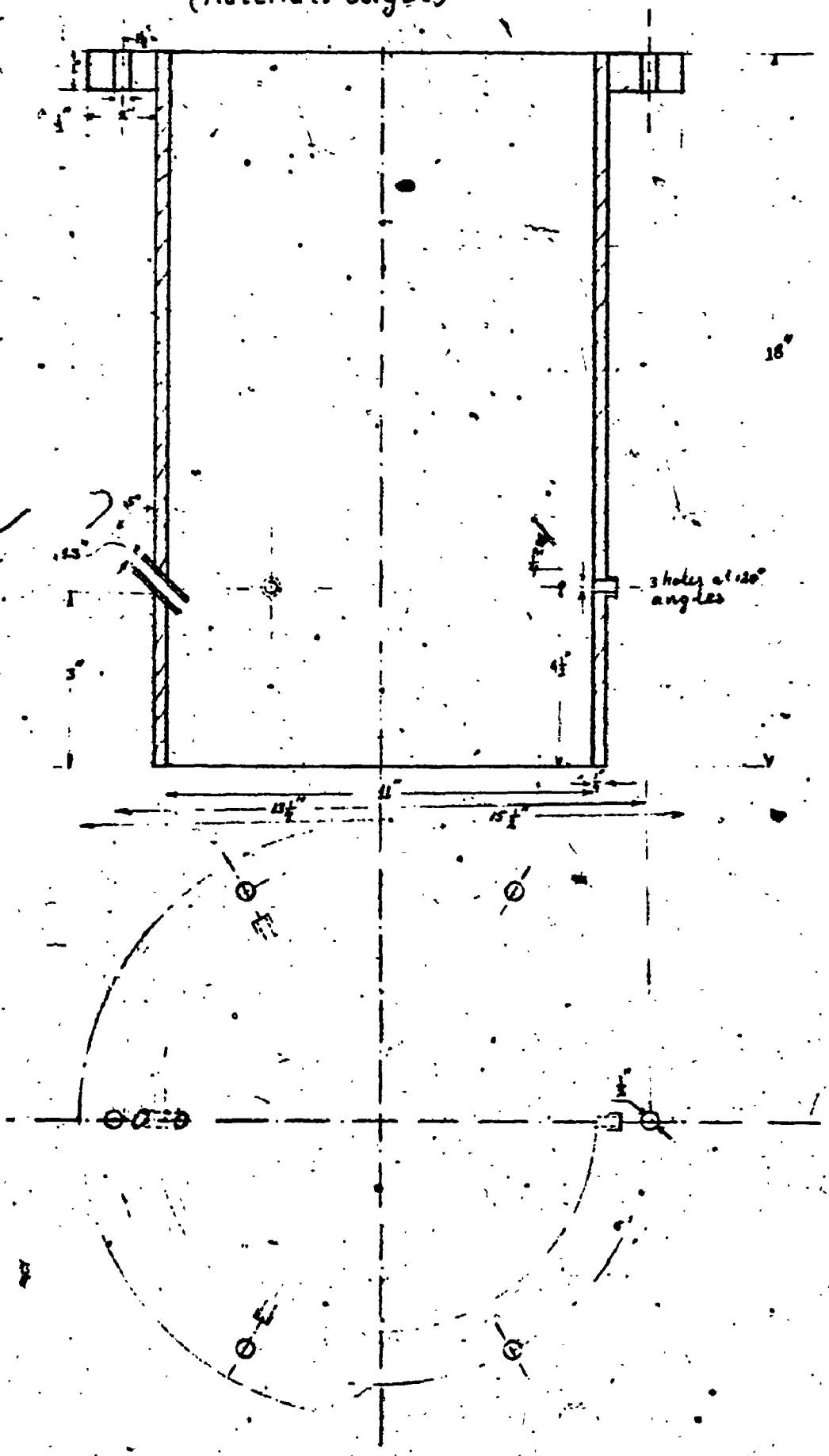

LOW SECTION OF THE COLUMN
(Material: acrylic)

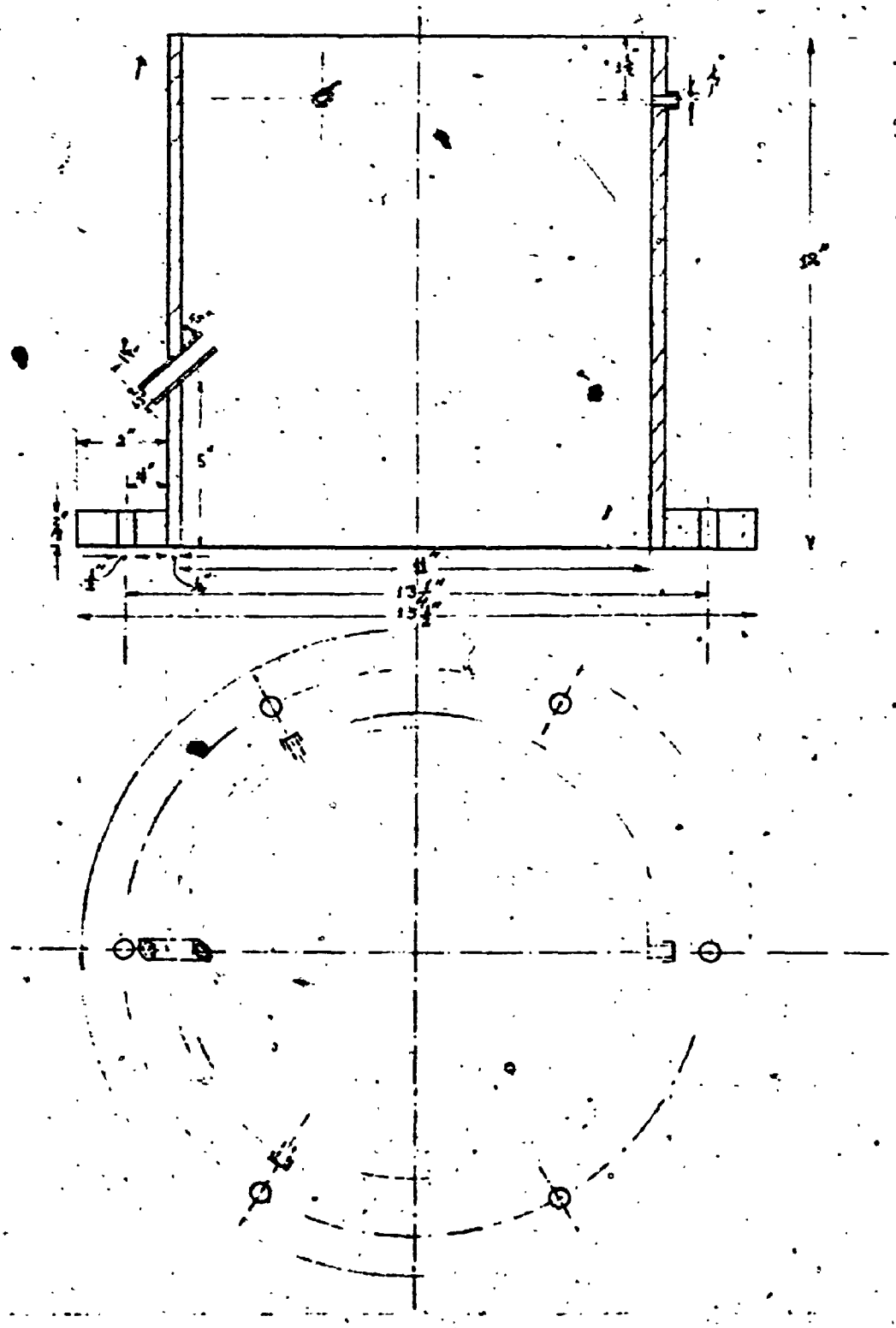

MIDDLE SECTIONS OF THE COLUMN
(Three pieces off: Material: acrylic)

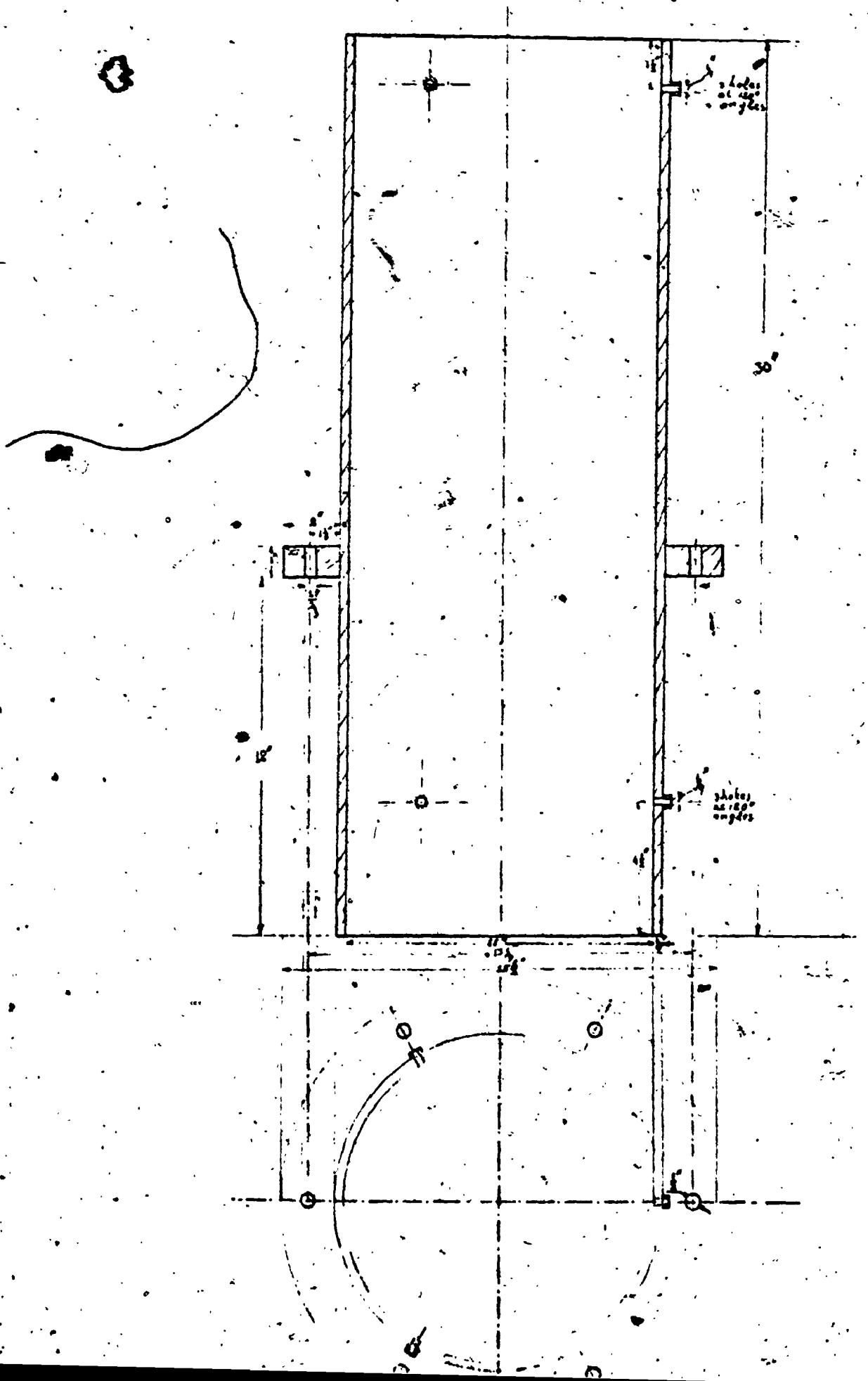

SUPPORT STRIPS
(12 pieces off: Material: aluminum)

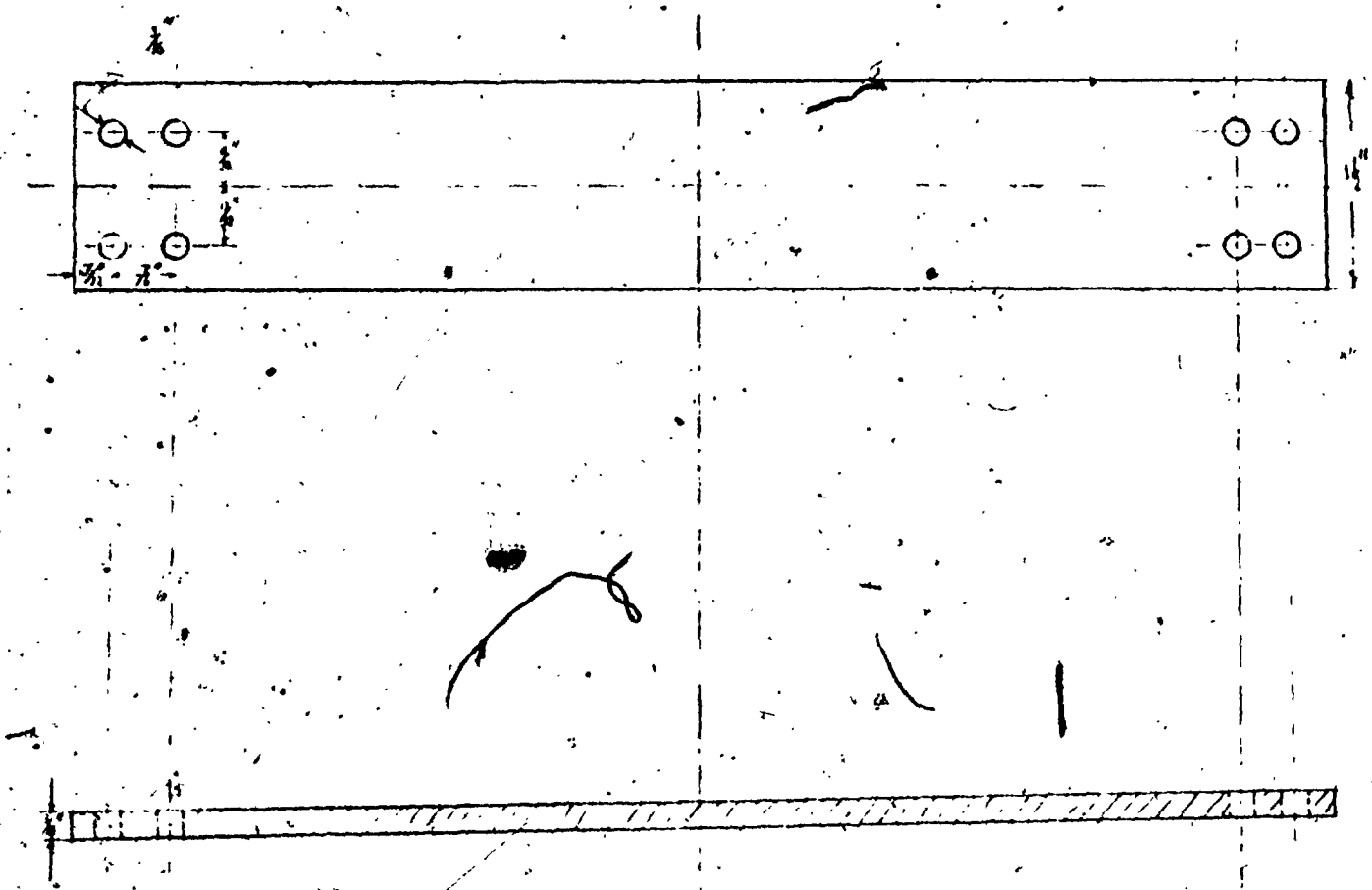

PLATE HOLDER
(4 pieces off: Material: aluminum)

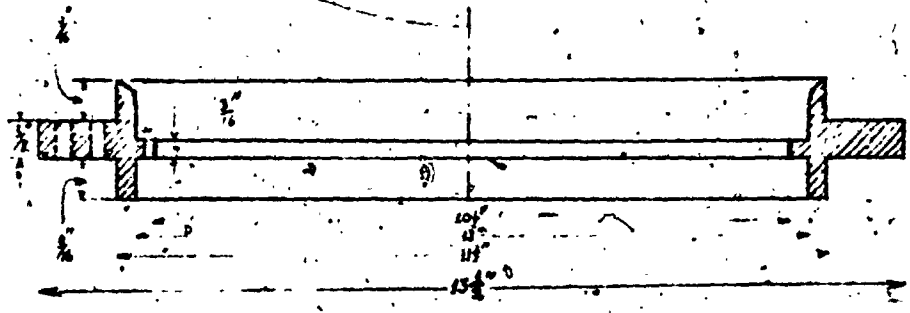

APPENDIX B

TABLES OF DATA

SAMPLE PROGRAM

FOR DETERMINING THE SLOPE, THE INTERCEPT AND THE CORRELATION COEFFICIENT OF A LINEAR RELATIONSHIP

```
// FOR
* IOCS (CARD,1403 PRINTER)
* LIST SOURCE PROGRAM
      DIMENSION X(40),Y(40)
C
C  LEAST SQUARES METHOD FOR DETERMINING THE SLOPE A AND THE INTERCEPT B
C                          OF A LINEAR RELATIONSHIP
C
      READ (2,10) N
10    FORMAT(I3)
      READ(2,11) (X(I),Y(I),I=1,N)
11    FORMAT(2F7.2)
      SUM=0
      S=0
      SU=0
      SS=0
      SSS=0
      DO 5 I=1,N
      S=S+X(I)
      SS=SS+Y(I)
      SSS=SSS+X(I)*Y(I)
      SU=SU+Y(I)**2
      SUM=SUM+X(I)**2
5     A=(N*SSS-S*SS)/(N*SUM-(S**2))
      B=(SUM*SS-S*SSS)/(N*SUM-(S**2))
      R=(SSS-(S*SS/N))/(((SUM-(S*S/N))*(SU-(SS*SS/N)))**0.5)
      A=A+0.005
      B=B+0.5
      R=R+0.0005
      WRITE(5,12) A,B,R
12    FORMAT(1X,'A=',F6.2,5X,'B=',F6.0,5X,'R=',F6.3)
      CALL EXIT
      END

FEATURES SUPPORTED
 IOCS

CORE REQUIREMENTS FOR
 COMMON      0  VARIABLES     190  PROGRAM     316

END OF COMPILATION

// XEQ
```

TABLE 81

DATA FOR CALIBRATION CURVE OF SOLIDS FLOWMETER

WITH 437 TYPE CARBON

NO	RECORDER OUTPUT,	SOLIDS FLOW, LB/MIN
1	26.5	0.64
2	37.0	0.85
3	48.5	1.14
4	63.0	1.51
5	17.5	0.44
6	6.8	0.18
7	77.0	1.78
8	70.0	1.54
9	74.5	1.72
10	89.0	2.04
11	71.0	1.63
12	43.0	0.94
13	14.0	0.36
14	43.0	0.92
15	41.5	0.84

TABLE 82

DATA FOR CARBON TRAY HOLDUP AT 50 CFM GAS FLOWRATE USING

3.0 INCH HIGH AND 1.25 INCH DIAMETER WEIR

NO	RECORDER OUTPUT,	SOLIDS FLOW, LB/MIN	HOLDUP, LB
1	87.0	1.99	2.90
2	36.5	0.85	2.53
3	87.5	2.00	2.90
4	37.5	0.87	2.36
5	72.0	1.65	2.74
6	38.5	0.89	2.40
7	72.0	1.65	2.73
8	40.0	0.93	2.45
9	55.0	1.27	2.53
10	88.5	2.03	2.88
11	55.0	1.27	2.57
12	89.0	2.04	2.90
13	41.0	0.95	2.39
14	50.5	1.16	2.51
15	41.0	0.95	2.44
16	51.5	1.18	2.50
17	12.0	0.29	1.95
18	9.0	0.22	1.97
19	14.0	0.33	1.99
20	11.0	0.26	2.04
21	30.5	0.71	2.28
22	11.0	0.26	2.09
23	30.0	0.69	2.29
24	4.5	0.11	2.01
25	4.5	0.11	2.07
26	25.0	0.58	2.31
27	27.0	0.63	2.37
28	64.0	1.47	2.65
29	65.5	1.50	2.63
30	73.5	1.69	2.71
31	76.0	1.73	2.70

TABLE B3

DATA FOR CARBON TRAY HOLDUP AT 60 CFM GAS FLOWRATE USING

3.0 INCH HIGH AND 1.25 INCH DIAMETER WEIR

NO.	RECORDER OUTPUT,	SOLIDS FLOW, LB/MIN	HOLDUP, LB
1	87.0	1.99	2.56
2	88.0	2.01	2.62
3	78.0	1.77	2.48
4	77.0	1.76	2.56
5	64.5	1.48	2.39
6	64.0	1.47	2.32
7	64.5	1.48	2.36
8	50.0	1.16	2.15
9	52.0	1.20	2.16
10	35.5	0.83	2.06
11	35.0	0.81	1.99
12	17.0	0.40	1.78
13	6.0	0.15	1.70
14	7.5	0.19	1.75
15	8.0	0.20	1.79

TABLE B3

DATA FOR CARBON TRAY HOLDUP AT 60 CFM GAS FLOWRATE USING

3.0 INCH HIGH AND 1.25 INCH DIAMETER WEIR

NO	RECORDER OUTPUT,	SOLIDS FLOW, LB/MIN	HOLDUP, LB
1	87.0	1.99	2.56
2	88.0	2.01	2.62
3	78.0	1.77	2.48
4	77.0	1.76	2.56
5	64.5	1.48	2.39
6	64.0	1.47	2.32
7	64.5	1.48	2.36
8	50.0	1.16	2.15
9	52.0	1.20	2.16
10	35.5	0.83	2.06
11	35.0	0.81	1.99
12	17.0	0.40	1.78
13	6.0	0.15	1.70
14	7.5	0.19	1.75
15	8.0	0.20	1.79

TABLE 84

DATA FOR CARBON TRAY HOLDUP AT 70 CFM GAS FLOWRATE USING

3.0 INCH HIGH AND 1.25 INCH DIAMETER WEIR

NO	RECORDER OUTPUT,	SOLIDS FLOW, LB/MIN	HOLDUP, LB
1	60.0	1.38	2.20
2	60.0	1.38	2.13
3	60.0	1.38	2.17
4	86.0	1.97	2.37
5	87.0	1.98	2.46
6	98.0	2.01	2.42
7	28.0	0.65	1.76
8	31.0	0.72	1.82
9	31.0	0.71	1.83
10	72.5	1.66	2.33
11	72.5	1.66	2.30
12	46.5	1.07	2.04
13	46.5	1.07	2.03
14	15.5	0.36	1.61
15	14.5	0.33	1.61
16	55.5	1.27	2.09
17	55.5	1.27	2.08

TABLE B5

DATA FOR CARBON TRAY HOLDUP AT 50 CFM GAS FLOWRATE USING

2.0 INCH HIGH AND 1.25 INCH DIAMETER WEIR

NO	RECORDER OUTPUT,	SOLIDS FLOW, LB/MIN	HOLDUP, LB
1	85.0	1.93	1.98
2	87.0	1.99	1.97
3	71.0	1.57	1.88
4	72.0	1.65	1.90
5	57.5	1.32	1.82
6	58.0	1.33	1.80
7	46.0	1.06	1.69
8	47.5	1.10	1.69
9	28.0	0.65	1.55
10	29.0	0.67	1.60
11	15.5	0.36	1.44
12	14.5	0.34	1.46
13	15.0	0.35	1.48
14	59.5	1.37	1.82

TABLE B6

DATA FOR CARBON TRAY HOLDUP AT 60 CFM GAS FLOWRATE USING

2.0 INCH HIGH AND 1.25 INCH DIAMETER WEIR

NO	RECORDER OUTPUT,	SOLIDS FLOW, LB/MIN	HOLDUP, LB
1	87.0	1.99	1.77
2	87.0	1.99	1.81
3	72.0	1.65	1.69
4	73.0	1.67	1.70
5	59.0	1.36	1.56
6	59.0	1.37	1.61
7	45.0	1.04	1.52
8	44.0	1.01	1.47
9	33.0	0.76	1.40
10	34.0	0.78	1.41

TABLE B7

DATA FOR CARBON TRAY HOLDUP AT 70 CFM GAS FLOWRATE USING

2.0 INCH HIGH AND 1.25 INCH DIAMETER WEIR

NO	RECORDER OUTPUT,	SOLIDS FLOW, LB/MIN	HOLDUP, LB
1	19.0	0.44	1.09
2	18.0	0.42	1.07
3	52.5	1.21	1.38
4	53.0	1.22	1.36
5	68.0	1.56	1.51
6	68.5	1.57	1.47
7	85.0	1.94	1.58
8	86.0	1.97	1.54
9	83.0	1.90	1.61
10	40.0	0.93	1.32
11	40.5	0.94	1.28
12	41.0	0.95	1.30
13	22.0	0.52	1.06
14	20.0	0.47	1.12
15	10.0	0.24	0.97
16	10.0	0.24	1.01

TABLE B8

DATA FOR CARBON TRAY HOLDUP AT 50 CFM GAS FLOWRATE USING

1.0 INCH HIGH AND 1.25 INCH DIAMETER WEIR

NO	RECORDER OUTPUT,	SOLIDS FLOW, LB/MIN	HOLDUP, LB
1	86.0	1.97	1.20
2	85.5	1.95	1.22
3	56.0	1.29	1.10
4	55.5	1.28	1.13
5	37.0	0.86	1.00
6	37.0	0.86	1.05
7	70.5	1.62	1.12
8	70.5	1.62	1.17
9	15.0	0.24	0.89
10	15.0	0.24	0.91

TABLE 89

DATA FOR CARBON TRAY HOLDUP AT 60 CFM GAS FLOWRATE USING

1.0 INCH HIGH AND 1.25 INCH DIAMETER WEIR

NO	RECORDER OUTPUT,	SOLIDS FLOW, LB/MIN	HOLDUP, LB
1	89.0	2.04	1.4
2	13.0	0.31	0.70
3	40.5	0.94	0.83
4	40.0	0.93	0.86
5	58.5	1.36	0.93
6	59.5	1.37	0.97
7	74.0	1.70	0.98
8	74.0	1.70	0.97
9	59.0	1.35	0.89
10	73.0	1.67	0.97
11	31.0	0.72	0.78
12	32.0	0.74	0.82

TABLE B10

DATA FOR CARBON TRAY HOLDUP AT 70 CFM GAS FLOWRATE USING

1.0 INCH HIGH AND 1.25 INCH DIAMETER WEIR

NC	RECORDER OUTPUT,	SOLIDS FLOW, LB/MIN	HOLDUP, LB
1	86.5	1.98	0.99
2	34.0	0.79	0.66
3	86.0	1.97	0.99
4	34.0	0.79	0.67
5	57.0	1.31	0.84
6	43.0	0.99	0.77
7	58.0	1.33	0.82
8	43.0	0.99	0.72
9	23.0	0.54	0.58
10	55.0	1.27	0.85
11	26.0	0.61	0.65
12	69.0	1.59	0.88
13	25.0	0.58	0.63
14	69.0	1.59	0.86
15	73.0	1.67	0.90
16	53.0	1.22	0.85
17	73.0	1.67	0.93
18	52.0	1.20	0.83
19	40.5	0.94	0.69
20	82.0	1.88	0.95
21	43.0	0.99	0.72
22	81.5	1.87	0.90
23	55.0	1.27	0.79
24	16.0	0.39	0.50

TABLE B11

DATA FOR CARBON TRAY HOLDUP AT 1.27 LB/MIN SOLIDS FLOWRATE

USING 1.0 INCH HIGH AND 1.25 INCH DIAMETER WEIR

NO	GAS FLOWRATE,CFM	HOLDUP,LB
1	50.0	1.11
2	50.0	1.08
3	60.0	0.93
4	60.0	0.96
5	70.0	0.79
6	70.0	0.84

TABLE B12

DATA FOR CARBON TRAY HOLDUP AT 1.27 LB/MIN SOLIDS FLOWRATE

USING 2.0 INCH HIGH AND 1.25 INCH DIAMETER WEIR

NO	GAS FLOWRATE,CFM	HOLDUP,LB
1	50.0	1.76
2	50.0	1.78
3	60.0	1.52
4	60.0	1.62
5	70.0	1.34

TABLE B13

DATA FOR CARBON TRAY HOLDUP AT 1.27 LB/MIN SOLIDS FLOWRATE

USING 3.0 INCH HIGH AND 1.25 INCH DIAMETER WEIR

NO	GAS FLOWRATE,CFM	HOLDUP,LB
1	50.0	2.58
2	50.0	2.53
3	60.0	2.25
4	70.0	2.07
5	70.0	2.08

TABLE B14

DATA FOR RECALIBRATION OF FLOWMETER USING 437 CARBON AS FLOWING SOLIDS AND MORE VISCOUS OIL IN THE DASHPOT

NO	RECORDER OUTPUT,	SOLIDS FLOW, LB/MIN
1	8.5	0.25
2	10.0	0.31
3	28.0	0.78
4	32.5	0.84
5	37.5	1.03
6	43.0	1.12
7	45.0	1.26
8	54.0	1.45
9	55.0	1.51
10	60.0	1.67
11	61.0	1.67
12	69.0	1.92
13	70.0	1.92
14	69.0	1.95
15	84.0	2.30

TABLE B15

DATA FOR RECALIBRATION OF FLOWMETER USING SILICA SAND #5005 AS FLOWING SOLIDS

NO	RECORDER OUTPUT,	SOLIDS FLOW, LB/MIN
1	15.0	0.39
2	15.0	0.30
3	20.0	0.53
4	23.0	0.58
5	27.5	0.61
6	30.0	0.71
7	38.0	0.82
8	45.0	1.00
9	47.5	1.02
10	56.5	1.20
11	65.0	1.37
12	70.0	1.54
13	88.0	1.90

TABLE B16

DATA FOR CARBON TRAY HOLDUP AT 50 CFM GAS FFLOWRATE USING

1.0 INCH HIGH AND 2.5 INCH DIAMETER WEIR

NO	RECORDER OUTPUT,	SOLIDS FLOW,LB/MIN	HOLDUP,LB
1	52.0	1.42	0.85
2	52.0	1.42	0.86
3	61.0	1.68	0.88
4	29.0	0.80	0.75
5	29.0	0.80	0.74
6	88.0	2.40	0.92
7	11.0	0.30	0.69
8	10.0	0.27	0.62
9	10.0	0.27	0.61
10	75.0	1.98	0.89
11	78.0	2.12	0.87
12	61.0	1.67	0.81
13	6.5	0.17	0.60
14	6.5	0.17	0.59
15	11.5	0.31	0.65
16	11.5	0.31	0.64
17	67.0	1.83	0.86
18	65.0	1.78	0.86
19	49.0	1.35	0.81
20	49.0	1.35	0.82
21	5.0	0.13	0.55
22	23.5	0.64	0.69
23	35.0	0.96	0.75

TABLE B17

DATA FOR CARBON TRAY HOLDUP AT 60 CFM GAS FFLOWRATE USING

1.0 INCH HIGH AND 2.5 INCH DIAMETER WEIR

NO	RECORDER OUTPUT,	SOLIDS FLOW, LB/MIN	HOLDUP, LB
1	36.0	0.98	0.74
2	36.5	1.00	0.71
3	45.0	1.23	0.79
4	45.0	1.23	0.75
5	62.0	1.70	0.83
6	62.0	1.70	0.80
7	76.0	2.08	0.83
8	77.0	2.10	0.86

TABLE B18

DATA FOR CARBON TRAY HOLDUP AT 50 CFM GAS FFLOWRATE USING

2.0 INCH HIGH AND 2.5 INCH DIAMETER WEIR

NO	RECORDER OUTPUT,	SOLIDS FLOW, LB/MIN	HOLDUP, LB
1	7.0	0.18	1.15
2	8.0	0.21	1.22
3	14.5	0.40	1.27
4	24.0	0.65	1.34
5	41.0	1.12	1.46
6	41.5	1.13	1.48
7	60.0	1.64	1.57
8	60.0	1.64	1.59
9	82.0	2.24	1.70
10	87.0	2.38	1.74
11	82.0	2.24	1.68
12	66.5	1.82	1.60
13	29.0.	0.80	1.37

TABLE B19

DATA FOR CARBON TRAY HOLDUP AT 60 CFM GAS FFLOWRATE USING

2.0 INCH HIGH AND 2.5 INCH DIAMETER WEIR

NO	RECORDER OUTPUT,	SOLIDS FLOW,LB/MIN	HOLDUP,LB
1	64.0	1.25	1.37
2	12.0	0.32	1.11
3	12.0	0.32	1.04
4	64.0	1.76	1.44
5	41.0	1.13	1.30
6	28.5	0.79	1.26
7	28.5	0.78	1.19
8	42.5	1.16	1.30
9	73.0	2.00	1.46
10	21.0	0.57	1.21
11	22.5	0.61	1.15
12	75.0	2.05	1.47

TABLE B20

DATA FOR CARBON TRAY HOLDUP AT 70 CFM GAS FFLOWRATE USING

2.0 INCH HIGH AND 2.5 INCH DIAMETER WEIR

NO	RECORDER OUTPUT,	SOLIDS FLOW,LB/MIN	HOLDUP,LB
1	50.0	1.37	1.08
2	18.5	0.50	0.89
3	17.5	0.47	0.88
4	52.0	1.42	1.12
5	75.0	2.05	1.23
6	31.0	0.85	1.05
7	31.0	0.85	1.01
8	76.5	2.09	1.26
9	61.0	1.67	1.21
10	39.0	1.07	1.09
11	39.5	1.08	1.06
12	63.0	1.72	1.19

TABLE B21

DATA FOR CARBON TRAY HOLDUP AT 60 CFM GAS FFLOWRATE USING

3.0 INCH HIGH AND 2.5 INCH DIAMETER WEIR

NO	RECORDER OUTPUT,	SOLIDS FLOW, LB/MIN	HOLDUP, LB
1	58.0	1.59	2.09
2	7.0	0.19	1.57
3	8.0	0.21	1.47
4	51.0	1.39	2.01
5	65.5	1.80	2.12
6	14.0	0.38	1.70
7	17.0	0.46	1.62
8	67.0	1.84	2.12
9	36.0	0.98	1.84
10	28.0	0.76	1.75
11	36.0	0.98	1.88
12	28.0	0.76	1.83
13	76.0	2.08	2.18
14	80.0	2.18	2.23

TABLE B22

DATA FOR CARBON TRAY HOLDUP AT 70 CFM GAS FFLOWRATE USING

3.0 INCH HIGH AND 2.5 INCH DIAMETER WEIR

NO	RECORDER OUTPUT,	SOLIDS FLOW, LB/MIN	HOLDUP, LB
1	72.5	1.99	1.81
2	18.5	0.50	1.40
3	17.5	0.48	1.30
4	73.5	2.01	1.77
5	62.0	1.70	1.69
6	29.0	0.80	1.48
7	31.0	0.85	1.47
8	62.5	1.71	1.71
9	55.0	1.50	1.67
10	55.0	1.50	1.66
11	41.5	1.14	1.53
12	42.0	1.19	1.57

TABLE B23

DATA FOR CARBON TRAY HOLDUP AT 60 CFM GAS FFLOWRATE USING

1.0 INCH HIGH AND 0.81 INCH DIAMETER WEIR

NO	RECORDER OUTPUT,	SOLIDS FLOW, LB/MIN	HOLDUP, LB
1	7.0	0.19	0.88
2	7.0	0.19	1.00
3	14.0	0.38	0.99
4	14.0	0.38	1.08
5	33.0	0.90	1.13
6	33.0	0.90	1.24
7	49.5	1.35	1.25
8	49.5	1.35	1.29
9	60.5	1.65	1.32
10	60.5	1.65	1.27
11	71.0	1.94	1.32
12	71.0	1.94	1.38

TABLE B24

DATA FOR CARBON TRAY HOLDUP AT 60 CFM GAS FFLOWRATE USING

2.0 INCH HIGH AND 0.81 INCH DIAMETER WEIR

NO	RECORDER OUTPUT,	SOLIDS FLOW, LB/MIN	HOLDUP, LB
1	3.0	0.07	1.33
2	3.0	0.07	1.41
3	10.0	0.27	1.63
4	11.0	0.30	1.58
5	26.0	0.71	1.89
6	28.0	0.76	1.95
7	50.0	1.37	2.14
8	51.0	1.40	2.20
9	72.5	1.99	2.36
10	72.5	1.99	2.39
11	81.0	2.21	2.46
12	81.0	2.21	2.45
13	38.0	1.04	2.07
14	38.0	1.04	2.04
15	5.5	0.15	1.49

TABLE B23

DATA FOR CARBON TRAY HOLDUP AT 60 CFM GAS FFLOWRATE USING

1.0 INCH HIGH AND 0.81 INCH DIAMETER WEIR

NO	RECORDER OUTPUT,	SOLIDS FLOW,LB/MIN	HOLDUP,LB
1	7.0	0.19	0.88
2	7.0	0.19	1.00
3	14.0	0.38	0.99
4	14.0	0.38	1.08
5	33.0	0.90	1.13
6	33.0	0.90	1.24
7	49.5	1.35	1.25
8	49.5	1.35	1.29
9	60.5	1.65	1.32
10	60.5	1.65	1.27
11	71.0	1.94	1.32
12	71.0	1.94	1.38

TABLE B24

DATA FOR CARBON TRAY HOLDUP AT 60 CFM GAS FFLOWRATE USING

2.0 INCH HIGH AND 0.81 INCH DIAMETER WEIR

NO	RECORDER OUTPUT,	SOLIDS FLOW,LB/MIN	HOLDUP,LB
1	3.0	0.07	1.33
2	3.0	0.07	1.41
3	10.0	0.27	1.63
4	11.0	0.30	1.58
5	26.0	0.71	1.89
6	28.0	0.76	1.95
7	50.0	1.37	2.14
8	51.0	1.40	2.20
9	72.5	1.99	2.36
10	72.5	1.99	2.39
11	81.0	2.21	2.46
12	81.0	2.21	2.45
13	38.0	1.04	2.07
14	38.0	1.04	2.04
15	5.5	0.15	1.49

TABLE B25

DATA FOR CARBON TRAY HOLDUP AT 60 CFM GAS FFLOWRATE USING

3.0 INCH HIGH AND 0.81 INCH DIAMETER WEIR

NO	RECORDER OUTPUT,	SOLIDS FLOW,LB/MIN	HOLDUP,LB
1	47.0	1.29	3.38
2	48.0	1.31	3.34
3	9.0	0.30	2.31
4	9.0	0.30	2.24
5	35.0	0.96	2.96
6	35.0	0.96	2.95
7	66.5	1.82	4.26
8	19.0	0.51	2.52
9	69.0	1.69	4.35

TABLE B26

DATA FOR SAND TRAY HOLDUP AT 70 CFM GAS FLOWRATE USING

2.0 INCH HIGH AND 1.25 INCH DIAMETER WEIR

NO	RECORDER OUTPUT,	SOLIDS FLOW,LB/MIN	HOLDUP,LB
1	15.0	0.37	4.12
2	25.0	0.58	4.47
3	72.0	1.57	5.15
4	14.5	0.36	4.13
5	26.0	0.60	4.50
6	47.0	1.04	4.80
7	82.0	1.78	5.31
8	69.0	1.50	5.11
9	34.5	0.78	4.48
10	55.0	1.21	4.76
11	69.0	1.50	5.02
12	21.0	0.49	4.16

TABLE B27

DATA FOR SAND TRAY HOLDUP AT 80 CFM GAS FLOWRATE USING

2.0 INCH HIGH AND 1.25 INCH DIAMETER WEIR

NO	RECORDER OUTPUT,	SOLIDS FLOW, LB/MIN	HOLDUP, LB
1	40.5	0.90	4.34
2	59.0	1.30	4.60
3	71.0	1.55	4.79
4	88.0	1.90	5.00
5	16.0	0.40	3.87
6	38.0	0.85	4.30
7	62.5	1.37	4.68
8	74.5	1.62	4.88

TABLE B28

DATA FOR SAND TRAY HOLDUP AT 90 CFM GAS FLOWRATE USING

2.0 INCH HIGH AND 1.25 INCH DIAMETER WEIR

NO	RECORDER OUTPUT,	SOLIDS FLOW, LB/MIN	HOLDUP, LB
1	73.0	1.59	4.55
2	88.0	1.90	4.80
3	55.0	1.21	4.38
4	39.0	0.87	4.10
5	16.0	0.39	3.78
6	26.0	0.60	3.95
7	46.0	1.02	4.12
8	45.0	1.00	4.15
9	21.0	0.50	3.74
10	21.0	0.50	3.71
11	32.0	0.73	3.91
12	42.5	0.95	4.03
13	40.0	0.90	3.91

APPENDIX C

DIMENSIONAL ANALYSIS FOR TRAY SOLIDS HOLDUP

The tray solids holdup H can be considered to depend on the solids flowrate L, the weir height h_ω, the superficial gas velocity u_f, the weir diameter d_ω, the particle density ρ_p, and the column diameter d_b. The quantities with the dimensions in which they are measured are given below. Over the range considered it will be assumed that the relation between the holdup H and the variables can be expressed as a product of powers of the variables, i.e.

$$H \propto [L^{n_1} . h_\omega^{n_2} . u_f^{n_3} . d_\omega^{n_4} . \rho_p^{n_5} . d_b^{n_6}] \quad (1)$$

Dimensions of the various terms in length L, mass M, and time T are as follows:

H	Holdup	M (lb.)
L	Solids flowrate	MT^{-1} (lb./min.)
h_ω	Weir height	L (ft.)
u_f	Superficial gas velocity	LT^{-1} (ft./min.)
d_ω	Diameter of the weir	L (ft)
ρ_p	Particle density	ML^{-3} (lb./ft^3)
d_b	Diameter of the column	L (ft.)

Equating the indices on each side of equation (1) with respect to the dimensions of length L, mass M, and time T, the following equations are obtained.

in length,	$n_2 + n_3 + n_4 - 3n_5 + n_6 = 0$	(2)
in mass,	$n_1 + n_5 = 1$	(3)
in time,	$-n_1 - n_3 = 0$	(4)

These equations may be solved in terms of n_1, n_2, and n_3 to obtain groups of which each will contain only one of the

The tray solids holdup H can be considered to depend on the solids flowrate L, the weir height h_ω, the superficial gas velocity u_f, the weir diameter d_ω, the particle density ρ_p, and the column diameter d_b. The quantities with the dimensions in which they are measured are given below. Over the range considered it will be assumed that the relation between the holdup H and the variables can be expressed as a product of powers of the variables, i.e.

$$H \propto [L^{n_1} . h_\omega^{n_2} . u_f^{n_3} . d_\omega^{n_4} . \rho_p^{n_5} . d_b^{n_6}] \qquad (1)$$

Dimensions of the various terms in length L, mass M, and time T are as follows:

H	Holdup	M	(lb.)
L	Solids flowrate	MT^{-1}	(lb./min.)
h_ω	Weir height	L	(ft.)
u_f	Superficial gas velocity	LT^{-1}	(ft./min.)
d_ω	Diameter of the weir	L	(ft)
ρ_p	Particle density	ML^{-3}	($lb./ft^3$
d_b	Diameter of the column	L	(ft.)

Equating the indices on each side of equation (1) with respect to the dimensions of length L, mass M, and time T, the following equations are obtained.

$$\text{in length,} \quad n_2 + n_3 + n_4 - 3n_5 + n_6 = 0 \qquad (2)$$

$$\text{in mass,} \quad n_5 = 1 \qquad (3)$$

$$\text{in time,} \quad -n_1 - n_3 = 0 \qquad (4)$$

These equations may be solved in terms of n_1, n_2, and n_3 to obtain groups of which each will contain only one of the

variables L, h_ω, and d_ω.

Solving the system of equations (2), (3), and (4) the following solution is obtained:

$$n_3 = -n_1$$

$$n_5 = 1-n_1$$

$$n_6 = 3-2n_1-n_2-n_4$$

Hence,

$$H \propto [L^{n_1} . h_\omega^{n_2} . u_f^{-n_1} . d_\omega^{n_4} . \rho_p^{1-n_1} . d_b^{3-2n_1-n_2-n_4}] \qquad (5)$$

or

$$H \propto \left(\frac{L}{d_b^2 \rho_p u_f}\right)^{n_1} \cdot \left(\frac{h_\omega}{d_b}\right)^{n_2} \cdot \left(\frac{d_\omega}{d_b}\right)^{n_4} \cdot d_b^3 \cdot \rho_p \qquad (6)$$

or

$$\left(\frac{H}{d_b^3 \rho_p}\right) = C\left(\frac{L}{d_b^2 \rho_p u_f}\right)^{n_1} \cdot \left(\frac{h_\omega}{d_b}\right)^{n_2} \cdot \left(\frac{d_\omega}{d_b}\right)^{n_4} \qquad (7)$$

To determine the coefficients n_1, n_2, n_4, and C a least squares fit was applied after taking logarithms on both sides of equation (7). This resulted in a linear equation of the following form:

$$\omega = n_1 x + n_2 y + n_4 z + C' \qquad (8)$$

where, $\omega = \log \frac{H}{d_b^3 \rho_p}$, $x = \log \frac{L}{d_b^2 \rho_p u_f}$, $y = \log \frac{h_\omega}{d_b}$,

$z = \log \frac{d_\omega}{d_b}$ and $C' = \log C$

By applying the least squares theory, the constants n_1, n_2, n_4, and C' are determined by solving the following system of equation:

$$
\begin{aligned}
(\Sigma x).n_1 + (\Sigma y).n_2 + (\Sigma z).n_4 + N.C' &= \Sigma\omega \\
(\Sigma x^2).n_1 + (\Sigma xy).n_2 + (\Sigma xz).n_4 + (\Sigma x).C' &= \Sigma\omega x \\
(\Sigma xy).n_1 + (\Sigma y^2).n_2 + (\Sigma yz).n_4 + (\Sigma y).C' &= \Sigma\omega y \\
(\Sigma xz).n_1 + (\Sigma yz).n_2 + (\Sigma z^2).n_4 + (\Sigma z).C' &= \Sigma\omega z
\end{aligned} \qquad (9)
$$

where Σ indicates summation over N values. A computer program to solve the system (9) and apply the solution, that is the values for n_1, n_2, n_4, and C', to equation (7) is given below. The computer outputs are also presented.

```
      PROGRAM TST(INPUT,OUTPUT,TAPE5=INPUT,TAPE6=OUTPUT)
      REAL L
      DIMENSION KM(313),H(313),L(313),HW(312),UF(313),DW(313),RP(313),
     1HA(313),HI(313),D(313),GH(313),GL(313),GHW(313),GDW(313),B(5,5),Y
     2(4)
C
C     THIS PROGRAM COMPUTES THE HOLDUP H AS A FUNCTION OF THE FOLLOWING
C                          PARAMETERS
C
C          L          THE SOLIDS FLOWRATE
C          HW         THE WEIR HEIGHT
C          UF         THE SUPERFICIAL GAS VELOCITY
C          DW         THE WEIR DIAMETER
C          RP         THE PARTICLE DENSITY
C          D          THE DIAMETER OF THE COLUMN
C
      READ(5,1) N
    1 FORMAT(I3)
      READ(5,2) (KM(I),H(I),L(I),HW(I),UF(I),DW(I),RP(I),D(I),I=1,N)
    2 FORMAT(I3,/F7.3)
C
      WRITE(6,13)
   13 FORMAT(1H1,54X,"DATA")
      WRITE(6,14)
   14 FORMAT(//,7X,"NO",13X,"H",14X,"L",13X,"HW",11X,"DW",13X,"UF",11X,
     1"D",13X,"RP")
      WRITE(6,15)(KM(I),H(I),L(I),HW(I),DW(I),UF(I),D(I),RP(I),I=1,N)
   15 FORMAT(6X,I3,8X,F7.3,8X,F7.3,7X,F7.3,8X,F7.3,8X,F7.3,8X,F7.3,8X,
     1F7.3)
      DO 3 J=1,N
      GH(J)=ALOG(H(J)/(D(J)**3*RP(J)))
      GL(J)=ALOG(L(J)/(D(J)**2*RP(J)*UF(J)))
      GHW(J)=ALOG(HW(J)/D(J))
      GDW(J)=ALOG(DW(J)/D(J))
    3 CONTINUE
C
C  CALCULATION OF COEFFICIENTS N1,N2,N3,AND C OF THE EQUATION
C        W=N1X+N2Y+N3Z+C BY THE LEASTS SQUARES METHOD.
C
      S1=0
      S2=0
      S3=0
      S4=0
      S5=0
      S6=0
      S7=0
      S8=0
      S9=0
      S10=0
      S11=0
      S12=0
      S13=0
      DO 4 J=1,N
      S1=S1+GL(J)
      S2=S2+GHW(J)
      S3=S3+GDW(J)
      S4=S4+GH(J)
```

```
      S5=S5+GL(J)*GL(J)
      S6=S6+GHW(J)*GHW(J)
      S7=S7+GDW(J)*GDW(J)
      S8=S8+GL(J)*GHW(J)
      S9=S9+GL(J)*GDW(J)
      S10=S10+GH(J)*GL(J)
      S11=S11+GHW(J)*GDW(J)
      S12=S12+GH(J)*GHW(J)
      S13=S13+GH(J)*GDW(J)
    4 CONTINUE
      B(1,1)=S1
      B(1,2)=S2
      B(1,3)=S3
      B(1,4)=N
      B(1,5)=S4
      B(2,1)=S5
      B(2,2)=S8
      B(2,3)=S9
      B(2,4)=S1
      B(2,5)=S10
      B(3,1)=S8
      B(3,2)=S6
      B(3,3)=S11
      B(3,4)=S2
      B(3,5)=S12
      B(4,1)=S9
      B(4,2)=S11
      B(4,3)=S7
      B(4,4)=S3
      B(4,5)=S13
C
C     SOLUTION OF A SYSTEM WITH FOUR LINEAR EQUATIONS
C
      CALL SYST(B,Y)
C
      C=EXP(Y(4))
      DO 7 I=1,N
      HA(I)=H(I)/(D(I)**3*RP(I))
      HT(I)=C*((L(I)/(D(I)**2*RP(I)*UP(I)))**Y(1))*((HW(I)/D(I))**Y(2))*
     1((DW(I)/D(I))**Y(3))
    7 CONTINUE
C
      WRITE(6,11)
   11 FORMAT(///,5X,"NO",5X,"ACTUAL HOLDUP",3X,"THEORETICAL HOLDUP")
      WRITE(6,12)(NN(I),HA(I),HT(I),I=1,N)
   12 FORMAT(I8,F12.4,5X,F12.4)
      CALL EXIT
      END
```

```
      SUBROUTINE SYST(A,X)
      DIMENSION A(5,5),AU(5,5),AL(5,5),R(5,5),EX(5),X(5)
      M=4
      N=5
      WRITE(6,166)
  166 FORMAT(///,15X,"BASIC MATRIX")
      WRITE(6,155) ((A(I,J),J=1,N),I=1,M)
  155 FORMAT (///,5F15.4)
      DO 2 KA=1,N
    1 DO 5 I=1,M
      J=1
      AU(I,J)=A(I,J)
    5 CONTINUE
      DO 6 J=2,M
      IF(A(1,1)) 6,8,6
    6 AU(1,J)=A(1,J)/A(1,1)
      GO TO 7
    8 DO 9 K=2,M
      IF(A(K,1)) 11,9,11
   11 DO 10 L=1,N
      AB=A(K,L)
      AC=A(1,L)
      A(1,L)=AB
      A(K,L)=AC
   10 CONTINUE
      GO TO 1
    9 CONTINUE
    7 DO 30 II=2,M
      JA=II
      DO 12 J=JA,M
      JJ=J-1
      IA=II
      DO 13 I=IA,M
      IL=I-1
      IF(I-J) 15,16,16
   16 S=0
      DO 14 K=1,JJ
   14 S=S+AU(I,K)*AU(K,J)
      AU(I,J)=A(I,J)-S
      GO TO 13
   15 IF (AU(II,II)) 17,21,17
   17 S=0
      DO 20 K=1,IL
   20 S=S+AU(I,K)*AU(K,J)
      AU(I,J)=(A(I,J)-S)/AU(II,II)
      GO TO 12
   13 CONTINUE
   12 CONTINUE
      IF(I-M) 30,40,40
   30 CONTINUE
   21 DO 25 KK=1,N
      BC=A(JJ,KK)
      BD=A(KA,KK)
      A(KA,KK)=BC
      A(JJ,KK)=BD
   25 CONTINUE
    2 CONTINUE
```

```
   40 DO 33 I=1,M
      DO 34 J=1,M
      IF(I-J) 36,37,38
   36 AL(I,J)=0
      R(I,J)=AU(I,J)
      GO TO 34
   37 AL(I,J)=AU(I,J)
      R(I,J)=1.0
      GO TO 34
   38 AL(I,J)=AU(I,J)
      R(I,J)=0
   34 CONTINUE
   33 CONTINUE
      EX(1)=A(1,N)/AU(1,1)
      DO 53 I=2,M
      LL=I-1
      S=0
      DO 55 K=1,LL
   55 S=S+AL(I,K)*EX(K)
      EX(I)=(A(I,N)-S)/AL(I,I)
   53 CONTINUE
      X(M)=EX(M)
      I=M-1
   82 K=I+1
      S=0
      DO 44 KI=K,M
   44 S=S+R(I,KI)*X(KI)
      X(I)=EX(I)-S
      I=I-1
      IF(I-1) 81,82,82
   81 DO 19 I=1,M
      IF(X(I)) 91,92,92
   91 X(I)=X(I)-0.00005
      GO TO 19
   92 X(I)=X(I)+0.00005
   19 WRITE(6,122) I,X(I)
  122 FORMAT(///,10X,"X(",I1,")=",F10.5)
      RETURN
      END
```

RESULTS FOR CARBON HOLDUP CORRELATION

X(1)= ...18192

X(2)= .82907

X(3)= -.38375

X(4)= -1.49039

NO	ACTUAL HOLDUP	THEORETICAL HOLDUP
1	.0458	.0423
2	.0368	.0362
3	.0458	.0423
4	.0372	.0364
5	.0432	.0409
6	.0379	.0365
7	.0431	.0409
8	.0387	.0368
9	.0399	.0390
10	.0454	.0424
11	.0405	.0390
12	.0458	.0425
13	.0377	.0370
14	.0396	.0363
15	.0385	.0370
16	.0394	.0364
17	.0308	.0298
18	.0311	.0283
19	.0314	.0305
20	.0322	.0292
21	.0360	.0351
22	.0330	.0292
23	.0361	.0349
24	.0317	.0259
25	.0327	.0258
26	.0364	.0338
27	.0374	.0343
28	.0418	.0400
29	.0415	.0402
30	.0428	.0410
31	.0426	.0412
32	.0404	.0409
33	.0413	.0410
34	.0391	.0400
35	.0404	.0400
36	.0377	.0388
37	.0366	.0387
38	.0372	.0388
39	.0339	.0371
40	.0341	.0373

41	.0325	.0349
42	.0314	.0347
43	.0281	.0305
44	.0268	.0256
45	.0276	.0267
46	.0282	.0269
47	.0347	.0372
48	.0336	.0312
49	.0342	.0312
50	.0374	.0391
51	.0388	.0397
52	.0382	.0398
53	.0278	.0324
54	.0287	.0331
55	.0289	.0330
56	.0368	.0385
57	.0363	.0385
58	.0322	.0355
59	.0320	.0355
60	.0254	.0291
61	.0254	.0287
62	.0330	.0361
63	.0328	.0361
64	.0312	.0301
65	.0311	.0303
66	.0297	.0290
67	.0300	.0292
68	.0287	.0281
69	.0284	.0281
70	.0267	.0270
71	.0267	.0272
72	.0245	.0247
73	.0252	.0248
74	.0227	.0222
75	.0230	.0219
76	.0233	.0221
77	.0287	.0283
78	.0279	.0293
79	.0286	.0293
80	.0267	.0283
81	.0268	.0284
82	.0246	.0273
83	.0254	.0274
84	.0240	.0260
85	.0232	.0259
86	.0221	.0246
87	.0222	.0247
88	.0172	.0215
89	.0169	.0214
90	.0218	.0260
91	.0215	.0260
92	.0238	.0272
93	.0232	.0273
94	.0249	.0283
95	.0243	.0284
96	.0254	.0282
97	.0208	.0249
98	.0202	.0248
99	.0205	.0249
100	.0167	.0223

101	.0177	.0219
102	.0153	.0194
103	.0159	.0194
104	.0189	.0169
105	.0192	.0169
106	.0174	.0157
107	.0178	.0156
108	.0158	.0146
109	.0166	.0146
110	.0177	.0163
111	.0185	.0164
112	.0140	.0115
113	.0144	.0115
114	.0221	.0165
115	.0110	.0117
116	.0131	.0143
117	.0136	.0143
118	.0147	.0153
119	.0153	.0153
120	.0155	.0159
121	.0153	.0159
122	.0140	.0153
123	.0153	.0159
124	.0123	.0136
125	.0129	.0137
126	.0156	.0159
127	.0104	.0135
128	.0156	.0159
129	.0106	.0135
130	.0133	.0145
131	.0121	.0140
132	.0129	.0148
133	.0114	.0140
134	.0092	.0126
135	.0134	.0147
136	.0103	.0129
137	.0139	.0153
138	.0099	.0127
139	.0136	.0153
140	.0142	.0154
141	.0134	.0146
142	.0147	.0154
143	.0131	.0145
144	.0109	.0139
145	.0150	.0158
146	.0114	.0140
147	.0142	.0158
148	.0125	.0147
149	.0079	.0119
150	.0134	.0122
151	.0136	.0122
152	.0139	.0126
153	.0118	.0110
154	.0117	.0110
155	.0145	.0134
156	.0109	.0092
157	.0098	.0090
158	.0096	.0090
159	.0140	.0130
160	.0137	.0131

161	.0128	.0126
162	.0095	.0083
163	.0093	.0083
164	.0103	.0093
165	.0101	.0093
166	.0136	.0124
167	.0136	.0127
168	.0128	.0121
169	.0129	.0121
170	.0087	.0079
171	.0109	.0106
172	.0118	.0114
173	.0117	.0110
174	.0112	.0111
175	.0125	.0115
176	.0118	.0115
177	.0131	.0122
178	.0126	.0122
179	.0131	.0127
180	.0136	.0127
181	.0170	.0204
182	.0140	.0140
183	.0139	.0138
184	.0177	.0205
185	.0194	.0214
186	.0166	.0187
187	.0159	.0187
188	.0199	.0220
189	.0191	.0211
190	.0172	.0195
191	.0167	.0195
192	.0188	.0212
193	.0216	.0219
194	.0175	.0161
195	.0164	.0161
196	.0227	.0219
197	.0205	.0202
198	.0199	.0189
199	.0188	.0189
200	.0205	.0203
201	.0230	.0225
202	.0191	.0179
203	.0181	.0181
204	.0232	.0225
205	.0181	.0154
206	.0192	.0154
207	.0200	.0173
208	.0211	.0189
209	.0230	.0209
210	.0233	.0209
211	.0248	.0224
212	.0251	.0224
213	.0268	.0231
214	.0275	.0240
215	.0265	.0231
216	.0252	.0224
217	.0216	.0197
218	.0286	.0305
219	.0221	.0237
220	.0205	.0235

221	.0279	.0305
222	.0267	.0296
223	.0233	.0258
224	.0232	.0261
225	.0270	.0297
226	.0263	.0290
227	.0262	.0290
228	.0241	.0275
229	.0248	.0276
230	.0330	.0301
231	.0248	.0204
232	.0232	.0208
233	.0317	.0294
234	.0334	.0308
235	.0268	.0232
236	.0256	.0240
237	.0334	.0309
238	.0290	.0276
239	.0276	.0263
240	.0297	.0276
241	.0289	.0263
242	.0344	.0316
243	.0352	.0314
244	.0139	.0125
245	.0158	.0126
246	.0156	.0143
247	.0170	.0143
248	.0178	.0167
249	.0196	.0167
250	.0197	.0180
251	.0204	.0180
252	.0200	.0167
253	.0208	.0187
254	.0208	.0192
255	.0218	.0192
256	.0210	.0187
257	.0222	.0187
258	.0257	.0240
259	.0249	.0244
260	.0298	.0286
261	.0308	.0289
262	.0338	.0322
263	.0347	.0323
264	.0317	.0345
265	.0372	.0345
266	.0388	.0351
267	.0387	.0351
268	.0321	.0308
269	.0322	.0306
270	.0235	.0215
271	.0533	.0445
272	.0527	.0445
273	.0364	.0341
274	.0353	.0341
275	.0467	.0422
276	.0465	.0422
277	.0472	.0474
278	.0398	.0376
279	.0686	.0477

RESULTS FOR SAND HOLDUP CORRELATION

X(1)= .17257

X(2)= .23132

X(3)= -1.12505

X(4)= -2.00005

NO	ACTUAL HOLDUP	THEORETICAL HOLDUP
280	.0369	.0384
281	.0389	.0395
282	.0355	.0366
283	.0332	.0345
284	.0306	.0301
285	.0320	.0324
286	.0334	.0355
287	.0336	.0354
288	.0303	.0314
289	.0301	.0314
290	.0317	.0335
291	.0327	.0351
292	.0317	.0348
293	.0334	.0312
294	.0362	.0337
295	.0417	.0400
296	.0335	.0310
297	.0365	.0334
298	.0389	.0372
299	.0430	.0409
300	.0414	.0397
301	.0363	.0354
302	.0386	.0382
303	.0407	.0397
304	.0337	.0327
305	.0352	.0355
306	.0373	.0378
307	.0388	.0390
308	.0405	.0404
309	.0314	.0309
310	.0349	.0351
311	.0379	.0382
312	.0396	.0393

RESULTS FOR BOTH CARBON AND SAND HOLDUP CORRELATION

X(1)= .10730

X(2)= .83998

X(3)= -.42506

X(4)= -2.16417

NO	ACTUAL HOLDUP	THEORETICAL HOLDUP
1	.0456	.0418
2	.0368	.0382
3	.0456	.0418
4	.0372	.0383
5	.0432	.0410
6	.0379	.0384
7	.0431	.0410
8	.0387	.0385
9	.0399	.0398
10	.0454	.0419
11	.0405	.0394
12	.0456	.0419
13	.0377	.0386
14	.0396	.0395
15	.0385	.0386
16	.0394	.0395
17	.0308	.0340
18	.0311	.0330
19	.0314	.0345
20	.0322	.0336
21	.0360	.0374
22	.0330	.0336
23	.0361	.0373
24	.0317	.0306
25	.0321	.0306
26	.0364	.0366
27	.0374	.0370
28	.0418	.0405
29	.0415	.0406
30	.0428	.0411
31	.0426	.0412
32	.0404	.0410
33	.0413	.0410
34	.0391	.0405
35	.0404	.0405
36	.0377	.0397
37	.0366	.0397
38	.0372	.0397
39	.0339	.0367

40	.0341	.0388
41	.0325	.0373
42	.0314	.0372
43	.0281	.0345
44	.0288	.0311
45	.0276	.0319
46	.0282	.0320
47	.0347	.0388
48	.0336	.0388
49	.0342	.0388
50	.0374	.0403
51	.0388	.0403
52	.0382	.0404
53	.0278	.0358
54	.0287	.0362
55	.0269	.0361
56	.0368	.0396
57	.0363	.0396
58	.0322	.0377
59	.0320	.0377
60	.0254	.0336
61	.0254	.0333
62	.0330	.0384
63	.0328	.0384
64	.0312	.0297
65	.0311	.0298
66	.0297	.0290
67	.0300	.0292
68	.0287	.0285
69	.0284	.0285
70	.0267	.0278
71	.0267	.0280
72	.0245	.0264
73	.0252	.0265
74	.0227	.0248
75	.0230	.0246
76	.0233	.0247
77	.0287	.0286
78	.0279	.0292
79	.0286	.0292
80	.0267	.0286
81	.0268	.0287
82	.0246	.0280
83	.0254	.0281
84	.0240	.0274
85	.0232	.0272
86	.0221	.0263
87	.0222	.0264
88	.0172	.0244
89	.0169	.0243
90	.0218	.0272
91	.0215	.0273
92	.0238	.0280
93	.0232	.0280
94	.0249	.0281
95	.0243	.0281
96	.0254	.0286
97	.0208	.0265
98	.0202	.0265
99	.0205	.0265
100	.0161	.0244

101	.0177	.0206
102	.0153	.0229
103	.0159	.0229
104	.0189	.0165
105	.0192	.0165
106	.0174	.0158
107	.0178	.0158
108	.0158	.0151
109	.0166	.0151
110	.0177	.0162
111	.0185	.0162
112	.0140	.0132
113	.0144	.0132
114	.0221	.0153
115	.0110	.0134
116	.0131	.0150
117	.0136	.0150
118	.0147	.0156
119	.0153	.0156
120	.0155	.0160
121	.0153	.0160
122	.0140	.0156
123	.0153	.0159
124	.0123	.0146
125	.0129	.0146
126	.0156	.0160
127	.0104	.0145
128	.0156	.0160
129	.0106	.0145
130	.0133	.0153
131	.0121	.0158
132	.0129	.0153
133	.0114	.0146
134	.0092	.0139
135	.0134	.0152
136	.0103	.0141
137	.0139	.0156
138	.0099	.0140
139	.0136	.0156
140	.0142	.0157
141	.0134	.0157
142	.0147	.0157
143	.0131	.0151
144	.0109	.0147
145	.0150	.0159
146	.0114	.0146
147	.0142	.0159
148	.0125	.0152
149	.0079	.0134
150	.0134	.0119
151	.0136	.0119
152	.0139	.0121
153	.0118	.0112
154	.0117	.0112
155	.0145	.0126
156	.0109	.0101
157	.0098	.0100
158	.0096	.0100
159	.0140	.0123
160	.0137	.0124

101	.0177	.0266
102	.0153	.0229
103	.0159	.0229
104	.0189	.0165
105	.0192	.0165
106	.0174	.0154
107	.0178	.0154
108	.0158	.0151
109	.0166	.0151
110	.0177	.0162
111	.0185	.0162
112	.0140	.0132
113	.0144	.0132
114	.0221	.0163
115	.0110	.0133
116	.0131	.0150
117	.0136	.0150
118	.0147	.0156
119	.0153	.0156
120	.0155	.0160
121	.0153	.0160
122	.0140	.0156
123	.0153	.0159
124	.0123	.0146
125	.0129	.0146
126	.0156	.0160
127	.0104	.0145
128	.0156	.0160
129	.0106	.0145
130	.0133	.0153
131	.0121	.0148
132	.0129	.0153
133	.0114	.0148
134	.0092	.0139
135	.0134	.0152
136	.0103	.0141
137	.0139	.0156
138	.0099	.0140
139	.0136	.0156
140	.0142	.0157
141	.0134	.0152
142	.0147	.0157
143	.0131	.0151
144	.0109	.0147
145	.0150	.0159
146	.0114	.0146
147	.0142	.0159
148	.0125	.0152
149	.0079	.0134
150	.0134	.0119
151	.0136	.0119
152	.0139	.0121
153	.0118	.0112
154	.0117	.0112
155	.0145	.0126
156	.0109	.0101
157	.0098	.0100
158	.0096	.0100
159	.0140	.0123
160	.0137	.0124

161	.0128	.0121
162	.0095	.0095
163	.0093	.0095
164	.0103	.0101
165	.0101	.0101
166	.0136	.0122
167	.0136	.0122
168	.0128	.0118
169	.0129	.0118
170	.0087	.0092
171	.0109	.0109
172	.0118	.0114
173	.0117	.0112
174	.0112	.0112
175	.0125	.0115
176	.0118	.0115
177	.0131	.0119
178	.0126	.0119
179	.0131	.0122
180	.0136	.0122
181	.0170	.0206
182	.0140	.0185
183	.0139	.0183
184	.0177	.0206
185	.0194	.0215
186	.0166	.0195
187	.0159	.0195
188	.0199	.0215
189	.0191	.0210
190	.0172	.0200
191	.0167	.0200
192	.0188	.0211
193	.0216	.0215
194	.0175	.0174
195	.0164	.0174
196	.0221	.0215
197	.0205	.0205
198	.0199	.0197
199	.0188	.0197
200	.0205	.0205
201	.0230	.0218
202	.0191	.0190
203	.0181	.0192
204	.0232	.0218
205	.0181	.0171
206	.0192	.0174
207	.0200	.0187
208	.0211	.0197
209	.0230	.0209
210	.0233	.0209
211	.0248	.0217
212	.0251	.0217
213	.0268	.0225
214	.0275	.0226
215	.0265	.0225
216	.0252	.0220
217	.0216	.0201
218	.0286	.0300
219	.0221	.0259
220	.0205	.0258

221	.0279	.0301
222	.0267	.0295
223	.0233	.0272
224	.0232	.0274
225	.0270	.0296
226	.0263	.0291
227	.0262	.0291
228	.0241	.0283
229	.0248	.0283
230	.0330	.0298
231	.0248	.0287
232	.0232	.0280
233	.0317	.0294
234	.0334	.0302
235	.0268	.0256
236	.0256	.0261
237	.0334	.0304
238	.0290	.0283
239	.0276	.0275
240	.0297	.0283
241	.0289	.0275
242	.0344	.0307
243	.0352	.0308
244	.0139	.0151
245	.0158	.0151
246	.0156	.0163
247	.0170	.0163
248	.0178	.0179
249	.0196	.0179
250	.0197	.0187
251	.0204	.0187
252	.0200	.0191
253	.0208	.0191
254	.0208	.0194
255	.0218	.0194
256	.0210	.0244
257	.0222	.0244
258	.0257	.0282
259	.0249	.0286
260	.0298	.0313
261	.0308	.0315
262	.0338	.0336
263	.0347	.0337
264	.0377	.0350
265	.0372	.0350
266	.0388	.0354
267	.0387	.0354
268	.0327	.0326
269	.0322	.0326
270	.0235	.0265
271	.0533	.0469
272	.0527	.0470
273	.0364	.0401
274	.0353	.0401
275	.0467	.0454
276	.0465	.0454
277	.0672	.0486
278	.0398	.0424
279	.0666	.0488
280	.0369	.0254

281	.0389	.0259
282	.0355	.0247
283	.0332	.0236
284	.0306	.0219
285	.0320	.0229
286	.0334	.0242
287	.0336	.0242
288	.0303	.0225
289	.0301	.0225
290	.0317	.0234
291	.0327	.0241
292	.0317	.0239
293	.0334	.0223
294	.0362	.0234
295	.0417	.0261
296	.0335	.0223
297	.0365	.0235
298	.0389	.0250
299	.0430	.0264
300	.0414	.0260
301	.0363	.0242
302	.0386	.0254
303	.0407	.0260
304	.0337	.0230
305	.0352	.0242
306	.0373	.0252
307	.0388	.0257
308	.0405	.0262
309	.0314	.0222
310	.0349	.0241
311	.0379	.0253
312	.0396	.0259

APPENDIX D

EXACT SOLUTION OF THE EQUATION

$$\underset{\sim}{X} = \underset{\sim}{A}\underset{\sim}{X} + \underset{\sim}{W}$$

Find eigenvalues of the homogeneous equation:

$$\dot{\underset{\sim}{X}} = \underset{\sim}{A}\,\underset{\sim}{X} \qquad (1)$$

General solution of equation (1)

$$\underset{\sim}{X} = \underset{\sim}{X}_0\, e^{\lambda t} \qquad (2)$$

where $\underset{\sim}{X}_0$ is the mode

Differentiating (2) results in

$$\dot{\underset{\sim}{X}} = \lambda\, \underset{\sim}{X} \qquad (3)$$

Combining (1) and (3) results in

$$\underset{\sim}{A}\,\underset{\sim}{X} = \lambda\, \underset{\sim}{X} \qquad (4)$$

which says that λ is the eigenvalue of $\underset{\sim}{A}$. The eigenvalues can be found from the characteristic equation of $\underset{\sim}{A}$, that is

$$\begin{vmatrix} (a-\lambda) & c & 0 & 0 \\ b & (a-\lambda) & c & 0 \\ 0 & b & (a-\lambda) & c \\ 0 & 0 & b & (a-\lambda) \end{vmatrix} = 0 \qquad (5)$$

where $a = \frac{L + Fm}{H}$, $b = \frac{L}{H}$, and $c = \frac{Fm}{H}$.

Expanding the determinant (5) results in the following equation:

$$(a-\lambda)^4 - 3bc\,(a-\lambda)^2 + b^2c^2 = 0 \qquad (6)$$

which can be solved for λ.

For L = 0.4 lb/min

F = 60 cu. ft/min

m = .002 lb/cu.ft., and

H = 2.7 lb.

the values for a, b, and c become:

$a = -.1926$

$b = .1481$

$c = .0444$

Solving equation (6) for λ and substituting the values of a, b, and c, the eigenvalues are found to be as follows:

$\lambda_1 = -0.0614$

$\lambda_2 = -0.1425$

$\lambda_3 = -0.2427$

$\lambda_4 = -0.3238$

or the corresponding time constants

$\tau_1 = 16.29$ min

$\tau_2 = 7.02$ "

$\tau_3 = 4.12$ "

$\tau_4 = 3.09$ "

Solution of equation

$$\dot{\underset{\sim}{X}} = \underset{\sim}{A}\,\underset{\sim}{X} + \underset{\sim}{W} \tag{7}$$

In general,

$$\underset{\sim}{X} = \Sigma C_i\, \underset{\sim}{X}_0^{(i)}\, e^{\lambda i t} + \underset{\sim}{\alpha},\quad i = 1, 2, 3, 4 \tag{8}$$

where $\underset{\sim}{X}_0^{(i)}$ is the mode and C_i a constant

Differentiating (8) results in

$$\dot{\underset{\sim}{X}} = \sum_{(i)} C_i\, \lambda_i\, \underset{\sim}{X}_0^{(i)}\, e^{\lambda i t} \tag{9}$$

Multiplying (8) by A results in

$$\underset{\sim}{A}\,\underset{\sim}{X} = \sum_{(i)} C_i\, \lambda_i\, \underset{\sim}{X}_0^{(i)}\, e^{\lambda i t} + \underset{\sim}{A}\,\underset{\sim}{\alpha} \tag{10}$$

Combining (7), (9), and (10) results in

$$\underset{\sim}{\alpha} = -\underset{\sim}{A}^{-1}\,\underset{\sim}{W} \tag{11}$$

Therefore

$$\underset{\sim}{X} = \sum_{(i)} C_i \, \underset{\sim}{X}_o^{(i)} \, e^{\lambda_i t} - \underset{\sim}{A}^{-1} \, \underset{\sim}{W} \qquad (12)$$

To determine the coefficients $C_i \underset{\sim}{X}_o^{(i)}$ in (12) the time t is set equal to zero: Therefore

$$\underset{\sim}{X}(0) = \sum_{(i)} C_i \, \underset{\sim}{X}_o^{(i)} - \underset{\sim}{A}^{-1} \, \underset{\sim}{W} \qquad (13)$$

or

$$\sum_{(i)} C_i \, \underset{\sim}{X}_o^{(i)} = \underset{\sim}{X}(0) + \underset{\sim}{A}^{-1} \, \underset{\sim}{W} \qquad (14)$$

and solve for

$$\underset{\sim}{C}^{(i)} = C_i \, \underset{\sim}{X}_o^{(i)}$$

where

$$\underset{\sim}{X}_o = \left[\frac{C_1}{b} \; \frac{C_2}{b} \; \frac{C_3}{b} \; \ldots\right]^T \quad \text{and} \quad b^2 = C_1^2 + C_2^2 + C_3^2 + \ldots \qquad (15)$$

APPENDIX E

CSMP SAMPLE PROGRAMS AND OUTPUTS

a) OPEN LOOP RESPONSE OF THE OUTLET CONTAMINANT CONCENTRATION TO A STEP INCREASE OF THE CONTAMINANT INLET CONCENTRATION FROM 0.1% TO 0.2%.

CONTINUOUS SYSTEM MODELING PROGRAM
A DIGITAL ANALOG SIMULATOR PROGRAM FOR THE IBM 1130

CONFIGURATION SPECIFICATION

OUTPUT NAME	BLOCK	TYPE	INPUT 1	INPUT 2	INPUT 3
H1	1	I	9	0	0
H2	2	I	10	0	0
H3	3	I	11	0	0
H4	4	I	12	0	0
L1	5	/	51	13	0
L2	6	/	52	13	0
L3	7	/	53	13	0
L4	8	/	54	13	0
DH1	9	+	15	-5	0
DH2	10	+	5	-6	0
DH3	11	+	6	-7	0
DH4	12	+	7	-8	0
T	13	K	0	0	0
HS	14	K	0	0	0
LO	15	K	0	0	0
X1	16	I	20	21	0
X2	17	I	22	23	24
X3	18	I	25	26	27
X4	19	I	28	29	30
MUL20	20	X	16	31	0
MUL21	21	X	17	32	0
MUL22	22	X	17	33	0
MUL23	23	X	16	34	0
MUL24	24	X	18	35	0
MUL25	25	X	18	36	0
MUL26	26	X	17	37	0
MUL27	27	X	19	38	0
MUL28	28	X	19	39	0
MUL29	29	X	18	40	0
MUL30	30	X	41	50	0
DIV31	31	/	42	1	0
DIV32	32	/	48	1	0
DIV33	33	/	43	2	0

DIV34	34	/	5	2	0
DIV35	35	/	48	2	0
DIV36	36	/	44	3	0
DIV37	37	/	6	3	0
DIV38	38	/	48	3	0
DIV39	39	/	45	4	0
DIV40	40	/	7	4	0
DIV41	41	/	46	4	0
AD42	42	+	-15	-48	0
AD43	43	+	-5	-48	0
AD44	44	+	-6	-48	0
AD45	45	+	-7	-48	0
F	46	K	0	0	0
M	47	K	0	0	0
FM	48	X	46	47	0
YF	49	X	-16	47	0
YI	50	X	0	0	0
AD51	51	+	1	-14	0
AD52	52	+	2	-14	0
AD53	53	+	3	-14	0
AD54	54	+	4	-14	0

INITIAL CONDITIONS AND PARAMETERS

IC/PAR NAME	BLOCK	IC/PAR1	PAR2	PAR3
H1	1	2.7000	0.0000	0.0000
H2	2	2.7000	0.0000	0.0000
H3	3	2.7000	0.0000	0.0000
H4	4	2.7000	0.0000	0.0000
T	13	2.0000	0.0000	0.0000
L0	15	0.4000	0.0000	0.0000
F	46	60.0000	0.0000	0.0000
M	47	0.0020	0.0000	0.0000
X1	16	0.0029	1.0000	0.0000
X2	17	0.0123	1.0000	1.0000
X3	18	0.0439	1.0000	1.0000
X4	19	0.1492	1.0000	1.0000
HS	14	1.9000	0.0000	0.0000
YI	50	0.0020	0.0000	0.0000

(0.1000) INTEGRATION INTERVAL

(100.0000) TOTAL TIME

(1.0000) PRINT INTERVAL

TIME	OUTPUT 19	OUTPUT 18	OUTPUT 17	OUTPUT 16
0.000	0.1492	0.0439	0.0123	0.0029
1.000	0.1694	0.0443	0.0123	0.0029
2.000	0.1862	0.0454	0.0124	0.0029
3.000	0.2002	0.0470	0.0125	0.0029
4.000	0.2120	0.0488	0.0126	0.0029
5.000	0.2220	0.0507	0.0128	0.0029
6.000	0.2305	0.0527	0.0130	0.0029
7.000	0.2378	0.0548	0.0133	0.0029
8.000	0.2441	0.0567	0.0136	0.0030
9.000	0.2495	0.0586	0.0140	0.0030
10.000	0.2543	0.0605	0.0143	0.0030
11.000	0.2584	0.0622	0.0147	0.0031
12.000	0.2621	0.0638	0.0151	0.0032
13.000	0.2653	0.0654	0.0155	0.0032
14.000	0.2682	0.0668	0.0159	0.0033
15.000	0.2707	0.0682	0.0163	0.0034
16.000	0.2730	0.0695	0.0167	0.0034
17.000	0.2750	0.0707	0.0171	0.0035
18.000	0.2769	0.0718	0.0174	0.0036
19.000	0.2786	0.0728	0.0178	0.0037
20.000	0.2801	0.0738	0.0181	0.0038
21.000	0.2814	0.0747	0.0185	0.0038
22.000	0.2827	0.0755	0.0188	0.0039
23.000	0.2838	0.0763	0.0191	0.0040
24.000	0.2848	0.0770	0.0194	0.0041
25.000	0.2858	0.0777	0.0197	0.0042
26.000	0.2867	0.0783	0.0200	0.0042
27.000	0.2875	0.0789	0.0202	0.0043
28.000	0.2882	0.0795	0.0205	0.0044
29.000	0.2889	0.0800	0.0207	0.0044
30.000	0.2895	0.0805	0.0209	0.0045
31.000	0.2901	0.0809	0.0211	0.0046
32.000	0.2906	0.0813	0.0213	0.0046
33.000	0.2911	0.0817	0.0215	0.0047
34.000	0.2916	0.0821	0.0217	0.0047
35.000	0.2920	0.0825	0.0219	0.0048
36.000	0.2924	0.0828	0.0220	0.0048
37.000	0.2928	0.0831	0.0222	0.0049
38.000	0.2932	0.0834	0.0223	0.0049
39.000	0.2935	0.0836	0.0224	0.0050
40.000	0.2938	0.0839	0.0226	0.0050
41.000	0.2941	0.0841	0.0227	0.0050
42.000	0.2943	0.0844	0.0228	0.0051
43.000	0.2946	0.0846	0.0229	0.0051
44.000	0.2948	0.0848	0.0230	0.0051
45.000	0.2950	0.0849	0.0231	0.0052
46.000	0.2952	0.0851	0.0232	0.0052
47.000	0.2954	0.0853	0.0233	0.0052
48.000	0.2956	0.0854	0.0234	0.0053
49.000	0.2958	0.0856	0.0234	0.0053
50.000	0.2959	0.0857	0.0235	0.0053
51.000	0.2961	0.0858	0.0236	0.0053
52.000	0.2962	0.0859	0.0236	0.0053
53.000	0.2963	0.0861	0.0237	0.0054

5) CLOSED LOOP RESPONSE OF THE OUTLET CONTAMINANT CONCENTRATION TO A STEP INCREASE OF THE CONTAMINANT INLET CONCENTRATION FROM 0.1% TO 0.25% AND CONTROLLER GAIN K_c = 2.0.

CONTINUOUS SYSTEM MODELING PROGRAM
A DIGITAL ANALOG SIMULATOR PROGRAM FOR THE IBM 1130

CONFIGURATION SPECIFICATION

OUTPUT NAME	BLOCK	TYPE	INPUT 1	INPUT 2	INPUT 3
H1	1	I	9	0	0
H2	2	I	10	0	0
H3	3	I	11	0	0
H4	4	I	12	0	0
L1	5	/	51	13	0
L2	6	/	52	13	0
L3	7	/	53	13	0
L4	8	/	54	13	0
DH1	9	+	15	-5	0
DH2	10	+	5	-6	0
DH3	11	+	6	-7	0
DH4	12	+	7	-8	0
T	13	K	0	0	0
HS	14	K	0	0	0
LO	15	+	63	64	0
X1	16	I	20	21	0
X2	17	I	22	23	24
X3	18	I	25	26	27
X4	19	I	28	29	30
MUL20	20	X	16	31	0
MUL21	21	X	17	32	0
MUL22	22	X	17	33	0
MUL23	23	X	16	34	0
MUL24	24	X	18	35	0
MUL25	25	X	18	36	0
MUL26	26	X	17	37	0
MUL27	27	X	19	38	0
MUL28	28	X	19	39	0
MUL29	29	X	18	40	0
MUL30	30	X	41	50	0
DIV31	31	/	42	1	0
DIV32	32	/	48	1	0
DIV33	33	/	43	2	0

DIV34	34	/	5	2	0
DIV35	35	/	48	2	0
DIV36	36	/	44	3	0
DIV37	37	/	6	3	0
DIV38	38	/	48	3	0
DIV39	39	/	45	4	0
DIV40	40	/	7	4	0
DIV41	41	/	46	4	0
AD42	42	+	-15	-48	0
AD43	43	+	-5	-48	0
AD44	44	+	-6	-48	0
AD45	45	+	-7	-48	0
F	46	K	0	0	0
M	47	K	0	0	0
FM	48	X	46	47	0
YI	49	X	16	47	0
YI	50	K	0	0	0
AD51	51	+	1	-14	0
AD52	52	+	2	-14	0
AD53	53	+	3	-14	0
AD54	54	+	4	-14	0
SP	55	K	0	0	0
COMP	56	+	-55	16	0
TRANS	57	G	56	0	0
LIM1	58	L	57	0	0
CONTR	59	G	58	0	0
LIM2	60	L	59	0	0
PSI	61	K	0	0	0
FEED	62	+	60	61	0
CAR	63	G	62	0	0
CARH	64	K	0	0	0

INITIAL CONDITIONS AND PARAMETERS

IC/PAR NAME	BLOCK	IC/PAR1	PAR2	PAR3
H1	1	2.7000	0.0000	0.0000
H2	2	2.7000	0.0000	0.0000
H3	3	2.7000	0.0000	0.0000
H4	4	2.7000	0.0000	0.0000
T	13	2.0000	0.0000	0.0000
F	46	60.0000	0.0000	0.0000
M	47	0.0020	0.0000	0.0000
X1	16	0.0029	1.0000	0.0000
X2	17	0.0125	1.0000	1.0000
X3	18	0.0443	1.0000	1.0000
X4	19	0.1498	1.0000	1.0000
HS	14	1.9000	0.0000	0.0000
YI	50	0.0025	0.0000	0.0000
SP	55	0.0029	0.0000	0.0000
TRANS	57	3000.0004	0.0000	0.0000
LIM1	58	6.0000	-6.0000	0.0000
CONTR	59	2.0000	0.0000	0.0000
LIM2	60	6.0000	-6.0000	0.0000
PSI	61	9.0000	0.0000	0.0000
CAR	63	0.0333	0.0000	0.0000
CARH	64	0.1000	0.0000	0.0000

.1 0.1000) INTEGRATION INTERVAL

(100.0000) TOTAL TIME

(1.0000) PRINT INTERVAL

TIME	OUTPUT 19	OUTPUT 18	OUTPUT 17	OUTPUT 16
0.000	0.1498	0.0443	0.0125	0.0029
1.000	0.1801	0.0449	0.0125	0.0029
2.000	0.2052	0.0466	0.0126	0.0029
3.000	0.2262	0.0489	0.0127	0.0029
4.000	0.2439	0.0516	0.0129	0.0029
5.000	0.2589	0.0545	0.0132	0.0029
6.000	0.2716	0.0575	0.0135	0.0029
7.000	0.2825	0.0604	0.0139	0.0030
8.000	0.2918	0.0633	0.0143	0.0030
9.000	0.2997	0.0660	0.0148	0.0030
10.000	0.3064	0.0686	0.0153	0.0031
11.000	0.3120	0.0709	0.0157	0.0031
12.000	0.3166	0.0729	0.0161	0.0032
13.000	0.3202	0.0746	0.0165	0.0032
14.000	0.3228	0.0761	0.0169	0.0033
15.000	0.3247	0.0773	0.0172	0.0033
16.000	0.3258	0.0782	0.0175	0.0033
17.000	0.3262	0.0788	0.0177	0.0034
18.000	0.3261	0.0792	0.0178	0.0034
19.000	0.3254	0.0794	0.0179	0.0034
20.000	0.3243	0.0794	0.0180	0.0034
21.000	0.3229	0.0793	0.0181	0.0034
22.000	0.3212	0.0790	0.0181	0.0034
23.000	0.3194	0.0787	0.0181	0.0034
24.000	0.3175	0.0782	0.0180	0.0034
25.000	0.3156	0.0778	0.0180	0.0034
26.000	0.3138	0.0773	0.0179	0.0034
27.000	0.3120	0.0767	0.0178	0.0034
28.000	0.3103	0.0762	0.0177	0.0034
29.000	0.3087	0.0757	0.0177	0.0034
30.000	0.3073	0.0753	0.0176	0.0034
31.000	0.3060	0.0748	0.0175	0.0034
32.000	0.3049	0.0744	0.0174	0.0034
33.000	0.3040	0.0741	0.0173	0.0034
34.000	0.3032	0.0738	0.0173	0.0034
35.000	0.3026	0.0735	0.0172	0.0034
36.000	0.3022	0.0733	0.0172	0.0034
37.000	0.3018	0.0731	0.0171	0.0034
38.000	0.3016	0.0730	0.0171	0.0034
39.000	0.3015	0.0728	0.0171	0.0034
40.000	0.3014	0.0728	0.0170	0.0034
41.000	0.3015	0.0727	0.0170	0.0034
42.000	0.3016	0.0727	0.0170	0.0034
43.000	0.3017	0.0727	0.0170	0.0034
44.000	0.3019	0.0727	0.0170	0.0034
45.000	0.3021	0.0728	0.0170	0.0033
46.000	0.3024	0.0728	0.0170	0.0033
47.000	0.3026	0.0729	0.0170	0.0033
48.000	0.3029	0.0729	0.0170	0.0033
49.000	0.3031	0.0730	0.0170	0.0033
50.000	0.3034	0.0731	0.0170	0.0033
51.000	0.3036	0.0731	0.0170	0.0034

COMPUTER OUTPUTS FOR

FIGURE 44

(PLOTS REFER TO OUTPUT 16)

TIME CONSTANT.0 MIN

TIME	OUTPUT 17	OUTPUT 18	OUTPUT 19	OUTPUT 1
0.000	0.0123	0.0439	0.1492	0.0029
5.000	0.0150	0.0522	0.1677	0.0036
10.000	0.0176	0.0593	0.1777	0.0044
15.000	0.0197	0.0651	0.1836	0.0051
20.000	0.0214	0.0699	0.1874	0.0057
25.000	0.0228	0.0738	0.1901	0.0062
30.000	0.0240	0.0770	0.1919	0.0065
35.000	0.0249	0.0797	0.1932	0.0069
40.000	0.0256	0.0819	0.1942	0.0071
45.000	0.0262	0.0838	0.1949	0.0073
50.000	0.0267	0.0853	0.1954	0.0074
55.000	0.0271	0.0865	0.1958	0.0075
60.000	0.0274	0.0875	0.1961	0.0075
65.000	0.0276	0.0883	0.1963	0.0076
70.000	0.0278	0.0889	0.1964	0.0076
75.000	0.0280	0.0893	0.1966	0.0077
80.000	0.0270	0.0896	0.1966	0.0077
85.000	0.0270	0.0898	0.1967	0.0077
90.000	0.0271	0.0899	0.1968	0.0077
95.000	0.0271	0.0899	0.1968	0.0077
100.000	0.0271	0.0900	0.1968	0.0077
105.000	0.0271	0.0900	0.1968	0.0077
110.000	0.0271	0.0900	0.1969	0.0077
115.000	0.0271	0.0900	0.1969	0.0077
120.000	0.0271	0.0900	0.1969	0.0078
125.000	0.0271	0.0900	0.1969	0.0078
130.000	0.0271	0.0900	0.1969	0.0078
135.000	0.0271	0.0900	0.1969	0.0078
140.000	0.0271	0.0900	0.1969	0.0078
145.000	0.0271	0.0900	0.1969	0.0078
150.000	0.0271	0.0900	0.1969	0.0078
155.000	0.0272	0.0900	0.1969	0.0078
160.000	0.0272	0.0900	0.1969	0.0078
165.000	0.0272	0.0900	0.1969	0.0078
170.000	0.0272	0.0900	0.1969	0.0078
175.000	0.0272	0.0900	0.1969	0.0078
180.000	0.0272	0.0900	0.1969	0.0078
185.000	0.0272	0.0900	0.1969	0.0078
190.000	0.0272	0.0900	0.1969	0.0078
195.000	0.0272	0.0900	0.1969	0.0078

TIME CONSTANT 0.2 MIN

TIME	OUTPUT 19	OUTPUT 18	OUTPUT 17	OUTPUT 16
0.000	.1495	0.0443	0.0125	0.0029
2.000	.1564	0.0468	0.0134	0.0032
4.000	.1637	0.0489	0.0144	0.0035
6.000	.1694	0.0529	0.0154	0.0037
8.000	.1736	0.0555	0.0164	0.0040
10.000	.1770	0.0578	0.0174	0.0043
12.000	.1794	0.0599	0.0183	0.0046
14.000	.1821	0.0617	0.0192	0.0049
16.000	.1840	0.0633	0.0200	0.0051
18.000	.1856	0.0647	0.0207	0.0054
20.000	.1870	0.0660	0.0214	0.0056
22.000	.1882	0.0671	0.0220	0.0058
24.000	.1892	0.0680	0.0225	0.0060
26.000	.1901	0.0689	0.0230	0.0062
28.000	.1909	0.0696	0.0234	0.0063
30.000	.1915	0.0703	0.0238	0.0065
32.000	.1922	0.0709	0.0242	0.0066
34.000	.1927	0.0714	0.0245	0.0067
36.000	.1932	0.0719	0.0248	0.0068
38.000	.1936	0.0723	0.0251	0.0069
40.000	.1940	0.0727	0.0253	0.0070
42.000	.1943	0.0730	0.0255	0.0071
44.000	.1946	0.0733	0.0257	0.0072
46.000	.1948	0.0735	0.0258	0.0072
48.000	.1951	0.0738	0.0260	0.0073
50.000	.1953	0.0740	0.0261	0.0073
52.000	.1954	0.0742	0.0262	0.0074
54.000	.1956	0.0743	0.0263	0.0074
56.000	.1957	0.0745	0.0264	0.0075
58.000	.1959	0.0746	0.0265	0.0075
60.000	.1960	0.0747	0.0266	0.0075
62.000	.1961	0.0748	0.0266	0.0076
64.000	.1962	0.0749	0.0267	0.0076
66.000	.1962	0.0750	0.0267	0.0076
68.000	.1963	0.0751	0.0268	0.0076
70.000	.1964	0.0751	0.0268	0.0076
72.000	.1964	0.0752	0.0269	0.0076
74.000	.1965	0.0752	0.0269	0.0077
76.000	.1965	0.0753	0.0269	0.0077
78.000	.1965	0.0753	0.0269	0.0077
80.000	.1965	0.0754	0.0270	0.0077
82.000	.1966	0.0754	0.0270	0.0077
84.000	.1967	0.0754	0.0270	0.0077
86.000	.1967	0.0754	0.0270	0.0077
88.000	.1967	0.0755	0.0270	0.0077
90.000	.1967	0.0755	0.0271	0.0077
92.000	.1967	0.0755	0.0271	0.0077
94.000	.1968	0.0755	0.0271	0.0077
96.000	.1968	0.0755	0.0271	0.0077
98.000	.1968	0.0755	0.0271	0.0077
100.000	.1968	0.0756	0.0271	0.0077

TIME CONSTANT 0.5 MIN

TIME	OUTPUT 13	OUTPUT 14	OUTPUT 17	OUTPUT 15
0.000	0.1434	0.0443	0.0125	0.0029
2.000	.1522	0.0454	0.0132	0.0032
4.000	0.1602	0.0467	0.0141	0.0034
6.000	0.1664	0.0515	0.0150	0.0037
8.000	.1712	0.0542	0.0160	0.0039
10.000	.1751	0.0566	0.0169	0.0042
12.000	.1783	0.0587	0.0178	0.0044
14.000	.1809	0.0606	0.0187	0.0047
16.000	.1831	0.0622	0.0195	0.0050
18.000	.1849	0.0637	0.0202	0.0052
20.000	.1865	0.0650	0.0209	0.0054
22.000	.1878	0.0662	0.0215	0.0056
24.000	.1888	0.0672	0.0221	0.0058
26.000	.1898	0.0681	0.0226	0.0060
28.000	.1906	0.0689	0.0230	0.0062
30.000	.1913	0.0696	0.0235	0.0063
32.000	.1919	0.0703	0.0238	0.0065
34.000	.1924	0.0708	0.0242	0.0066
36.000	.1929	0.0714	0.0245	0.0067
38.000	0.1931	0.0718	0.0248	0.0068
40.000	0.1935	0.0722	0.0250	0.0069
42.000	0.1939	0.0726	0.0252	0.0070
44.000	0.1942	0.0729	0.0254	0.0071
46.000	0.1945	0.0732	0.0256	0.0072
48.000	0.1947	0.0734	0.0258	0.0072
50.000	.1950	0.0737	0.0259	0.0073
52.000	.1952	0.0739	0.0260	0.0073
54.000	0.1953	0.0741	0.0262	0.0074
56.000	0.1955	0.0742	0.0263	0.0074
58.000	0.1956	0.0744	0.0264	0.0074
60.000	0.1958	0.0745	0.0264	0.0075
62.000	0.1959	0.0746	0.0265	0.0075
64.000	0.1960	0.0747	0.0266	0.0075
66.000	0.1961	0.0748	0.0266	0.0076
68.000	0.1962	0.0749	0.0267	0.0076
70.000	0.1963	0.0750	0.0267	0.0075
72.000	0.1963	0.0751	0.0268	0.0076
74.000	0.1964	0.0751	0.0268	0.0076
76.000	0.1964	0.0752	0.0269	0.0076
78.000	0.1965	0.0752	0.0269	0.0077
80.000	0.1965	0.0753	0.0269	0.0077
82.000	0.1966	0.0753	0.0269	0.0077
84.000	0.1966	0.0754	0.0270	0.0077
86.000	0.1966	0.0754	0.0270	0.0077
88.000	0.1967	0.0754	0.0270	0.0077
90.000	0.1967	0.0754	0.0270	0.0077
92.000	0.1967	0.0755	0.0270	0.0077
94.000	0.1967	0.0755	0.0270	0.0077
96.000	0.1967	0.0755	0.0271	0.0077
98.000	0.1968	0.0755	0.0271	0.0077
100.000	0.1968	0.0755	0.0271	0.0077

TIME CONSTANT 2.0 MIN

TIME	OUTPUT 19	OUTPUT 18	OUTPUT 17	OUTPUT 16
0.000	0.1438	0.0443	0.0125	0.0029
2.000	0.1493	0.0445	0.0127	0.0031
4.000	0.1512	0.0455	0.0133	0.0033
6.000	0.1542	0.0470	0.0139	0.0034
8.000	0.1553	0.0469	0.0145	0.0036
10.000	0.1625	0.0509	0.0152	0.0038
12.000	0.1663	0.0529	0.0159	0.0040
14.000	0.1706	0.0549	0.0166	0.0042
16.000	0.1733	0.0563	0.0173	0.0044
18.000	0.1767	0.0584	0.0179	0.0046
20.000	0.1791	0.0596	0.0186	0.0047
22.000	0.1811	0.0614	0.0192	0.0049
24.000	0.1829	0.0627	0.0198	0.0051
26.000	0.1844	0.0639	0.0204	0.0053
28.000	0.1857	0.0650	0.0209	0.0055
30.000	0.1868	0.0659	0.0214	0.0056
32.000	0.1878	0.0668	0.0219	0.0058
34.000	0.1887	0.0676	0.0223	0.0059
36.000	0.1895	0.0683	0.0227	0.0061
38.000	0.1902	0.0690	0.0231	0.0062
40.000	0.1908	0.0696	0.0234	0.0063
42.000	0.1913	0.0701	0.0238	0.0065
44.000	0.1919	0.0705	0.0240	0.0066
46.000	0.1923	0.0710	0.0243	0.0067
48.000	0.1927	0.0714	0.0245	0.0068
50.000	0.1931	0.0718	0.0248	0.0068
52.000	0.1934	0.0722	0.0250	0.0069
54.000	0.1937	0.0725	0.0252	0.0070
56.000	0.1940	0.0727	0.0253	0.0071
58.000	0.1943	0.0730	0.0255	0.0071
60.000	0.1945	0.0732	0.0256	0.0072
62.000	0.1947	0.0734	0.0258	0.0072
64.000	0.1949	0.0736	0.0259	0.0073
66.000	0.1951	0.0738	0.0260	0.0073
68.000	0.1952	0.0740	0.0261	0.0073
70.000	0.1954	0.0741	0.0262	0.0074
72.000	0.1955	0.0742	0.0263	0.0074
74.000	0.1956	0.0744	0.0263	0.0074
76.000	0.1957	0.0745	0.0264	0.0075
78.000	0.1958	0.0746	0.0265	0.0075
80.000	0.1959	0.0747	0.0265	0.0075
82.000	0.1960	0.0748	0.0266	0.0075
84.000	0.1961	0.0748	0.0266	0.0076
86.000	0.1962	0.0749	0.0267	0.0076
88.000	0.1962	0.0750	0.0267	0.0076
90.000	0.1963	0.0750	0.0268	0.0076
92.000	0.1963	0.0751	0.0268	0.0076
94.000	0.1964	0.0751	0.0268	0.0077
96.000	0.1964	0.0752	0.0269	0.0076
98.000	0.1965	0.0752	0.0269	0.0077
100.000	0.1965	0.0753	0.0269	0.0077

COMPUTER OUTPUTS FOR

FIGURE 45

(PLOTS REFER TO OUTPUT 16)

TIME	OUTPUT 19	OUTPUT 18	OUTPUT 17	OUTPUT 16
0.000	0.1498	0.0443	0.0125	0.0029
1.000	0.1801	0.0449	0.0125	0.0029
2.000	0.2052	0.0466	0.0126	0.0029
3.000	0.2262	0.0489	0.0127	0.0029
4.000	0.2437	0.0516	0.0129	0.0029
5.000	0.2589	0.0545	0.0132	0.0029
6.000	0.2716	0.0575	0.0135	0.0029
7.000	0.2825	0.0604	0.0139	0.0030
8.000	0.2919	0.0634	0.0144	0.0030
9.000	0.2999	0.0661	0.0149	0.0031
10.000	0.3068	0.0687	0.0153	0.0031
11.000	0.3126	0.0712	0.0158	0.0032
12.000	0.3176	0.0734	0.0163	0.0032
13.000	0.3217	0.0753	0.0168	0.0033
14.000	0.3250	0.0771	0.0172	0.0034
15.000	0.3276	0.0786	0.0176	0.0034
16.000	0.3295	0.0798	0.0180	0.0035
17.000	0.3308	0.0808	0.0183	0.0035
18.000	0.3316	0.0816	0.0186	0.0036
19.000	0.3319	0.0822	0.0188	0.0036
20.000	0.3318	0.0826	0.0190	0.0036
21.000	0.3313	0.0829	0.0192	0.0037
22.000	0.3305	0.0829	0.0193	0.0037
23.000	0.3294	0.0829	0.0193	0.0037
24.000	0.3282	0.0827	0.0194	0.0038
25.000	0.3269	0.0825	0.0194	0.0038
26.000	0.3255	0.0822	0.0194	0.0038
27.000	0.3240	0.0818	0.0194	0.0038
28.000	0.3225	0.0815	0.0193	0.0038
29.000	0.3211	0.0810	0.0193	0.0038
30.000	0.3197	0.0806	0.0192	0.0038
31.000	0.3183	0.0802	0.0192	0.0038
32.000	0.3171	0.0798	0.0191	0.0038
33.000	0.3160	0.0794	0.0190	0.0038
34.000	0.3149	0.0790	0.0190	0.0038
35.000	0.3140	0.0787	0.0189	0.0038
36.000	0.3132	0.0784	0.0188	0.0038
37.000	0.3125	0.0781	0.0188	0.0038
38.000	0.3119	0.0778	0.0187	0.0037
39.000	0.3114	0.0776	0.0186	0.0037
40.000	0.3110	0.0774	0.0186	0.0037
41.000	0.3107	0.0772	0.0185	0.0037
42.000	0.3104	0.0771	0.0185	0.0037
43.000	0.3103	0.0770	0.0185	0.0037
44.000	0.3102	0.0769	0.0184	0.0037
45.000	0.3101	0.0768	0.0184	0.0037
46.000	0.3101	0.0768	0.0184	0.0037
47.000	0.3102	0.0767	0.0184	0.0037
48.000	0.3102	0.0767	0.0184	0.0037
49.000	0.3103	0.0767	0.0183	0.0037
50.000	0.3105	0.0767	0.0183	0.0037
51.000	0.3106	0.0767	0.0183	0.0037

52.000	0.3107	0.0768	0.0183	0.0037
53.000	0.3109	0.0768	0.0183	0.0037
54.000	0.3111	0.0768	0.0183	0.0037
55.000	0.3112	0.0769	0.0183	0.0037
56.000	0.3114	0.0769	0.0184	0.0037
57.000	0.3115	0.0770	0.0184	0.0037
58.000	0.3116	0.0770	0.0184	0.0037
59.000	0.3117	0.0770	0.0184	0.0037
60.000	0.3119	0.0771	0.0184	0.0037
61.000	0.3120	0.0771	0.0184	0.0037
62.000	0.3121	0.0772	0.0184	0.0037
63.000	0.3122	0.0772	0.0184	0.0037
64.000	0.3122	0.0772	0.0184	0.0037
65.000	0.3123	0.0772	0.0184	0.0037
66.000	0.3123	0.0773	0.0184	0.0037
67.000	0.3124	0.0773	0.0184	0.0037
68.000	0.3124	0.0773	0.0184	0.0037
69.000	0.3124	0.0773	0.0184	0.0037
70.000	0.3124	0.0773	0.0184	0.0037
71.000	0.3125	0.0773	0.0184	0.0037
72.000	0.3125	0.0774	0.0184	0.0037
73.000	0.3125	0.0774	0.0184	0.0037
74.000	0.3124	0.0774	0.0184	0.0037
75.000	0.3124	0.0774	0.0184	0.0037
76.000	0.3124	0.0774	0.0184	0.0037
77.000	0.3124	0.0774	0.0184	0.0037
78.000	0.3124	0.0774	0.0184	0.0037
79.000	0.3124	0.0774	0.0184	0.0037
80.000	0.3124	0.0773	0.0184	0.0037
81.000	0.3123	0.0773	0.0184	0.0037
82.000	0.3123	0.0773	0.0184	0.0037
83.000	0.3123	0.0773	0.0184	0.0037
84.000	0.3123	0.0773	0.0184	0.0037
85.000	0.3123	0.0773	0.0184	0.0037
86.000	0.3123	0.0773	0.0184	0.0037
87.000	0.3123	0.0773	0.0184	0.0037
88.000	0.3122	0.0773	0.0184	0.0037
89.000	0.3122	0.0773	0.0184	0.0037
90.000	0.3122	0.0773	0.0184	0.0037
91.000	0.3122	0.0773	0.0184	0.0037
92.000	0.3122	0.0773	0.0184	0.0037
93.000	0.3122	0.0773	0.0184	0.0037
94.000	0.3122	0.0773	0.0184	0.0037
95.000	0.3122	0.0773	0.0184	0.0037
96.000	0.3122	0.0773	0.0184	0.0037
97.000	0.3122	0.0773	0.0184	0.0037
98.000	0.3122	0.0773	0.0184	0.0037
99.000	0.3122	0.0773	0.0184	0.0037
100.000	0.3122	0.0773	0.0184	0.0037

CONTROLLER GAIN 8.0

TIME	OUTPUT 19	OUTPUT 18	OUTPUT 17	OUTPUT 16
0.000	0.1494	0.0443	0.0125	0.0029
1.000	0.1801	0.0449	0.0125	0.0029
2.000	0.2052	0.0466	0.0126	0.0029
3.000	0.2263	0.0489	0.0129	0.0029
4.000	0.2439	0.0516	0.0133	0.0029
5.000	0.2589	0.0545	0.0137	0.0029
6.000	0.2716	0.0574	0.0141	0.0029
7.000	0.2824	0.0604	0.0145	0.0029
8.000	0.2915	0.0631	0.0149	0.0030
9.000	0.2991	0.0657	0.0153	0.0030
10.000	0.3053	0.0680	0.0156	0.0030
11.000	0.3101	0.0699	0.0159	0.0030
12.000	0.3137	0.0716	0.0161	0.0030
13.000	0.3161	0.0729	0.0163	0.0030
14.000	0.3175	0.0735	0.0164	0.0030
15.000	0.3179	0.0744	0.0165	0.0030
16.000	0.3175	0.0746	0.0165	0.0031
17.000	0.3166	0.0749	0.0165	0.0031
18.000	0.3151	0.0748	0.0165	0.0031
19.000	0.3132	0.0745	0.0165	0.0031
20.000	0.3111	0.0741	0.0165	0.0031
21.000	0.3089	0.0737	0.0164	0.0031
22.000	0.3066	0.0732	0.0164	0.0031
23.000	0.3045	0.0726	0.0163	0.0031
24.000	0.3024	0.0721	0.0162	0.0031
25.000	0.3005	0.0716	0.0162	0.0030
26.000	0.2989	0.0711	0.0161	0.0030
27.000	0.2974	0.0706	0.0160	0.0030
28.000	0.2962	0.0702	0.0160	0.0030
29.000	0.2952	0.0699	0.0159	0.0030
30.000	0.2944	0.0696	0.0159	0.0030
31.000	0.2938	0.0694	0.0158	0.0030
32.000	0.2934	0.0692	0.0158	0.0030
33.000	0.2932	0.0690	0.0158	0.0030
34.000	0.2931	0.0690	0.0157	0.0030
35.000	0.2931	0.0689	0.0157	0.0030
36.000	0.2932	0.0689	0.0157	0.0030
37.000	0.2934	0.0689	0.0157	0.0030
38.000	0.2936	0.0689	0.0157	0.0030
39.000	0.2939	0.0689	0.0157	0.0030
40.000	0.2942	0.0690	0.0157	0.0030
41.000	0.2945	0.0691	0.0157	0.0030
42.000	0.2948	0.0691	0.0157	0.0030
43.000	0.2951	0.0692	0.0157	0.0030
44.000	0.2954	0.0693	0.0157	0.0030
45.000	0.2956	0.0694	0.0158	0.0030
46.000	0.2958	0.0694	0.0158	0.0030
47.000	0.2960	0.0695	0.0158	0.0030
48.000	0.2962	0.0695	0.0158	0.0030
49.000	0.2963	0.0696	0.0158	0.0030
50.000	0.2964	0.0696	0.0158	0.0030
51.000	0.2964	0.0696	0.0158	0.0030

52.000	0.2965	0.0697	0.0158	0.0030
53.000	0.2965	0.0697	0.0158	0.0030
54.000	0.2965	0.0697	0.0158	0.0030
55.000	0.2965	0.0697	0.0158	0.0030
56.000	0.2965	0.0697	0.0158	0.0030
57.000	0.2964	0.0697	0.0158	0.0030
58.000	0.2964	0.0697	0.0158	0.0030
59.000	0.2964	0.0697	0.0158	0.0030
60.000	0.2963	0.0697	0.0158	0.0030
61.000	0.2963	0.0697	0.0158	0.0030
62.000	0.2962	0.0698	0.0158	0.0030
63.000	0.2962	0.0696	0.0158	0.0030
64.000	0.2962	0.0696	0.0158	0.0030
65.000	0.2961	0.0696	0.0158	0.0030
66.000	0.2961	0.0696	0.0158	0.0030
67.000	0.2961	0.0696	0.0158	0.0030
68.000	0.2961	0.0696	0.0158	0.0030
69.000	0.2961	0.0696	0.0158	0.0030
70.000	0.2961	0.0696	0.0158	0.0030
71.000	0.2961	0.0696	0.0158	0.0030
72.000	0.2961	0.0696	0.0158	0.0030
73.000	0.2961	0.0696	0.0158	0.0030
74.000	0.2960	0.0696	0.0158	0.0030
75.000	0.2960	0.0696	0.0158	0.0030
76.000	0.2960	0.0696	0.0158	0.0030
77.000	0.2960	0.0696	0.0158	0.0030
78.000	0.2960	0.0696	0.0158	0.0030
79.000	0.2961	0.0696	0.0158	0.0030
80.000	0.2961	0.0696	0.0158	0.0030
81.000	0.2961	0.0696	0.0158	0.0030
82.000	0.2961	0.0696	0.0158	0.0030
83.000	0.2961	0.0696	0.0158	0.0030
84.000	0.2961	0.0696	0.0158	0.0030
85.000	0.2961	0.0696	0.0158	0.0030
86.000	0.2961	0.0696	0.0158	0.0030
87.000	0.2961	0.0696	0.0158	0.0030
88.000	0.2961	0.0696	0.0158	0.0030
89.000	0.2961	0.0696	0.0158	0.0030
90.000	0.2961	0.0696	0.0158	0.0030
91.000	0.2961	0.0696	0.0158	0.0030
92.000	0.2961	0.0696	0.0158	0.0030
93.000	0.2961	0.0696	0.0158	0.0030
94.000	0.2961	0.0696	0.0158	0.0030
95.000	0.2961	0.0696	0.0158	0.0030
96.000	0.2961	0.0696	0.0158	0.0030
97.000	0.2961	0.0696	0.0158	0.0030
98.000	0.2961	0.0696	0.0158	0.0030
99.000	0.2961	0.0696	0.0158	0.0030
100.000	0.2961	0.0696	0.0158	0.0030

TIME	OUTPUT 19	OUTPUT 18	OUTPUT 17	OUTPUT 16
0.000	0.1495	0.0443	0.0125	0.0029
1.000	0.1801	0.0449	0.0125	0.0029
2.000	0.2052	0.0466	0.0126	0.0029
3.000	0.2263	0.0489	0.0127	0.0029
4.000	0.2439	0.0516	0.0129	0.0029
5.000	0.2589	0.0545	0.0131	0.0029
6.000	0.2716	0.0574	0.0135	0.0029
7.000	0.2823	0.0603	0.0138	0.0029
8.000	0.2913	0.0630	0.0142	0.0029
9.000	0.2988	0.0655	0.0146	0.0029
10.000	0.3047	0.0677	0.0149	0.0029
11.000	0.3092	0.0695	0.0152	0.0030
12.000	0.3124	0.0710	0.0155	0.0030
13.000	0.3145	0.0722	0.0157	0.0030
14.000	0.3155	0.0730	0.0159	0.0030
15.000	0.3155	0.0735	0.0160	0.0030
16.000	0.3148	0.0737	0.0161	0.0030
17.000	0.3136	0.0737	0.0161	0.0030
18.000	0.3118	0.0735	0.0161	0.0030
19.000	0.3098	0.0732	0.0161	0.0030
20.000	0.3076	0.0728	0.0161	0.0030
21.000	0.3054	0.0723	0.0161	0.0030
22.000	0.3032	0.0718	0.0160	0.0030
23.000	0.3011	0.0713	0.0159	0.0030
24.000	0.2992	0.0708	0.0159	0.0030
25.000	0.2975	0.0703	0.0158	0.0030
26.000	0.2961	0.0699	0.0158	0.0030
27.000	0.2949	0.0695	0.0157	0.0030
28.000	0.2939	0.0692	0.0157	0.0030
29.000	0.2930	0.0689	0.0156	0.0030
30.000	0.2924	0.0687	0.0156	0.0030
31.000	0.2920	0.0685	0.0155	0.0030
32.000	0.2917	0.0683	0.0155	0.0030
33.000	0.2916	0.0682	0.0155	0.0030
34.000	0.2916	0.0682	0.0155	0.0030
35.000	0.2917	0.0682	0.0155	0.0030
36.000	0.2919	0.0682	0.0156	0.0030
37.000	0.2922	0.0682	0.0155	0.0030
38.000	0.2924	0.0682	0.0155	0.0030
39.000	0.2927	0.0683	0.0155	0.0030
40.000	0.2930	0.0683	0.0155	0.0030
41.000	0.2933	0.0684	0.0155	0.0030
42.000	0.2936	0.0685	0.0155	0.0030
43.000	0.2938	0.0685	0.0155	0.0030
44.000	0.2940	0.0686	0.0155	0.0030
45.000	0.2942	0.0687	0.0155	0.0030
46.000	0.2944	0.0687	0.0155	0.0030
47.000	0.2945	0.0688	0.0155	0.0030
48.000	0.2946	0.0688	0.0155	0.0030
49.000	0.2947	0.0688	0.0155	0.0030
50.000	0.2947	0.0688	0.0155	0.0030
51.000	0.2947	0.0689	0.0155	0.0030

52.000	0.2945	0.0689	0.0155	0.0030
53.000	0.2945	0.0689	0.0155	0.0030
54.000	0.2947	0.0689	0.0155	0.0030
55.000	0.2947	0.0689	0.0156	0.0030
56.000	0.2947	0.0689	0.0156	0.0030
57.000	0.2946	0.0689	0.0155	0.0030
58.000	0.2946	0.0689	0.0155	0.0030
59.000	0.2946	0.0689	0.0155	0.0030
60.000	0.2945	0.0689	0.0155	0.0030
61.000	0.2945	0.0688	0.0155	0.0030
62.000	0.2945	0.0688	0.0155	0.0030
63.000	0.2944	0.0688	0.0155	0.0030
64.000	0.2944	0.0688	0.0155	0.0030
65.000	0.2944	0.0688	0.0155	0.0030
66.000	0.2944	0.0688	0.0155	0.0030
67.000	0.2944	0.0688	0.0155	0.0030
68.000	0.2944	0.0688	0.0155	0.0030
69.000	0.2943	0.0688	0.0155	0.0030
70.000	0.2943	0.0688	0.0155	0.0030
71.000	0.2943	0.0688	0.0155	0.0030
72.000	0.2943	0.0688	0.0155	0.0030
73.000	0.2943	0.0688	0.0155	0.0030
74.000	0.2943	0.0688	0.0155	0.0030
75.000	0.2944	0.0688	0.0155	0.0030
76.000	0.2944	0.0688	0.0155	0.0030
77.000	0.2944	0.0688	0.0155	0.0030
78.000	0.2944	0.0688	0.0155	0.0030
79.000	0.2944	0.0688	0.0155	0.0030
80.000	0.2944	0.0688	0.0155	0.0030
81.000	0.2944	0.0688	0.0155	0.0030
82.000	0.2944	0.0688	0.0155	0.0030
83.000	0.2944	0.0688	0.0155	0.0030
84.000	0.2944	0.0688	0.0155	0.0030
85.000	0.2944	0.0688	0.0155	0.0030
86.000	0.2944	0.0688	0.0155	0.0030
87.000	0.2944	0.0688	0.0155	0.0030
88.000	0.2944	0.0688	0.0155	0.0030
89.000	0.2944	0.0688	0.0155	0.0030
90.000	0.2944	0.0688	0.0155	0.0030
91.000	0.2944	0.0688	0.0155	0.0030
92.000	0.2944	0.0688	0.0155	0.0030
93.000	0.2944	0.0688	0.0155	0.0030
94.000	0.2944	0.0688	0.0155	0.0030
95.000	0.2944	0.0688	0.0155	0.0030
96.000	0.2944	0.0688	0.0155	0.0030
97.000	0.2944	0.0688	0.0155	0.0030
98.000	0.2944	0.0688	0.0155	0.0030
99.000	0.2944	0.0688	0.0155	0.0030
100.000	0.2944	0.0688	0.0155	0.0030

COMPUTER OUTPUTS FOR

FIGURE 46

(PLOTS REFER TO OUTPUT 16)

CONTROLLER GAIN 1.0

TIME	OUTPUT 19	OUTPUT 18	OUTPUT 17	OUTPUT 16
0.000	.1[illegible]	0.0443	0.0125	0.0029
2.000	.1972	0.0469	0.0126	0.0029
4.000	.2255	0.0520	0.0130	0.0029
6.000	.2451	0.0572	0.0138	0.0030
8.000	0.2565	0.0616	0.0146	0.0031
10.000	0.2624	0.0649	0.0154	0.0032
12.000	0.2655	0.0671	0.0161	0.0033
14.000	0.2665	0.0682	0.0165	0.0034
16.000	0.2665	0.0687	0.0168	0.0034
18.000	0.2663	0.0688	0.0169	0.0035
20.000	.2658	0.0686	0.0170	0.0035
22.000	.2652	0.0683	0.0170	0.0035
24.000	.2645	0.0681	0.0169	0.0035
26.000	.2638	0.0678	0.0169	0.0035
28.000	.2632	0.0677	0.0168	0.0035
30.000	.2627	0.0676	0.0168	0.0035
32.000	0.2623	0.0675	0.0168	0.0035
34.000	0.2620	0.0675	0.0168	0.0035
36.000	0.2619	0.0675	0.0168	0.0035
38.000	.2618	0.0675	0.0168	0.0035
40.000	.2618	0.0675	0.0168	0.0035
42.000	0.2611	0.0675	0.0168	0.0035
44.000	0.2611	0.0675	0.0168	0.0035
46.000	0.2611	0.0675	0.0168	0.0035
48.000	0.2611	0.0675	0.0168	0.0035
50.000	0.2611	0.0675	0.0168	0.0035
52.000	0.2611	0.0675	0.0168	0.0035
54.000	0.2611	0.0675	0.0168	0.0035
56.000	0.2611	0.0675	0.0168	0.0035
58.000	0.2611	0.0675	0.0168	0.0035
60.000	0.2611	0.0675	0.0168	0.0035
62.000	0.2611	0.0675	0.0168	0.0035
64.000	0.2611	0.0675	0.0168	0.0035
66.000	0.2611	0.0675	0.0168	0.0035
68.000	0.2611	0.0675	0.0168	0.0035
70.000	0.2611	0.0675	0.0168	0.0035
72.000	0.2611	0.0675	0.0168	0.0035
74.000	0.2611	0.0675	0.0168	0.0035
76.000	0.2611	0.0675	0.0168	0.0035
78.000	0.2611	0.0675	0.0168	0.0035
80.000	0.2611	0.0675	0.0168	0.0035
82.000	0.2611	0.0675	0.0168	0.0035
84.000	0.2611	0.0675	0.0168	0.0035
86.000	0.2611	0.0675	0.0168	0.0035
88.000	0.2611	0.0675	0.0168	0.0035
90.000	0.2611	0.0675	0.0168	0.0035
92.000	0.2611	0.0675	0.0168	0.0035
94.000	0.2611	0.0675	0.0168	0.0035
96.000	0.2611	0.0675	0.0168	0.0035
98.000	0.2611	0.0675	0.0168	0.0035
100.000	0.2611	0.0675	0.0168	0.0035
102.000	0.2611	0.0675	0.0168	0.0035

CONTROLLER GAIN 1.0

$\Delta t = 0.05$

TIME	OUTPUT 14	OUTPUT 15	OUTPUT 17	OUTPUT 16
0.000	.1438	0.0443	0.0125	0.0029
2.000	.1972	0.0469	0.0126	0.0029
4.000	.2245	0.0520	0.0130	0.0029
6.000	.2401	0.0572	0.0138	0.0030
8.000	.2565	0.0616	0.0146	0.0031
10.000	.2629	0.0649	0.0154	0.0032
12.000	.2658	0.0671	0.0161	0.0033
14.000	.2665	0.0682	0.0165	0.0034
16.000	.2660	0.0687	0.0168	0.0034
18.000	.2649	0.0688	0.0169	0.0035
20.000	.2638	0.0686	0.0170	0.0035
22.000	.2627	0.0683	0.0170	0.0035
24.000	.2621	0.0681	0.0169	0.0035
26.000	.2615	0.0678	0.0169	0.0035
28.000	.2612	0.0677	0.0168	0.0035
30.000	.2611	0.0676	0.0168	0.0035
32.000	.2611	0.0675	0.0168	0.0035
34.000	.2611	0.0675	0.0168	0.0035
36.000	.2611	0.0675	0.0168	0.0035
38.000	.2611	0.0675	0.0168	0.0035
40.000	.2611	0.0675	0.0168	0.0035
42.000	.2611	0.0675	0.0168	0.0035
44.000	.2611	0.0675	0.0168	0.0035
46.000	.2611	0.0675	0.0168	0.0035
48.000	.2611	0.0675	0.0168	0.0035
50.000	.2611	0.0675	0.0168	0.0035
52.000	.2611	0.0675	0.0168	0.0035
54.000	.2611	0.0675	0.0168	0.0035
56.000	.2611	0.0675	0.0168	0.0035
58.000	.2611	0.0675	0.0168	0.0035
60.000	.2611	0.0675	0.0168	0.0035
62.000	.2611	0.0675	0.0168	0.0035
64.000	.2611	0.0675	0.0168	0.0035
66.000	.2611	0.0675	0.0168	0.0035
68.000	.2611	0.0675	0.0168	0.0035
70.000	.2611	0.0675	0.0168	0.0035
72.000	.2611	0.0675	0.0168	0.0035
74.000	.2611	0.0675	0.0168	0.0035
76.000	.2611	0.0675	0.0168	0.0035
78.000	.2611	0.0675	0.0168	0.0035
80.000	.2611	0.0675	0.0168	0.0035
82.000	.2611	0.0675	0.0168	0.0035
84.000	.2611	0.0675	0.0168	0.0035
86.000	.2611	0.0675	0.0168	0.0035
88.000	.2611	0.0675	0.0168	0.0035
90.000	.2611	0.0675	0.0168	0.0035
92.000	.2611	0.0675	0.0168	0.0035
94.000	.2611	0.0675	0.0168	0.0035
96.000	.2611	0.0675	0.0168	0.0035
98.000	.2611	0.0675	0.0168	0.0035
100.000	.2611	0.0675	0.0168	0.0035
102.000	.2611	0.0675	0.0168	0.0035

CONTROLLER GAIN 2.0

TIME	OUTPUT 19	OUTPUT 18	OUTPUT 17	OUTPUT 16
0.000	.1498	0.0443	0.0125	0.0029
2.000	.1972	0.0469	0.0126	0.0029
4.000	.2203	0.0519	0.0130	0.0029
6.000	.2449	0.0571	0.0137	0.0030
8.000	.2551	0.0612	0.0145	0.0030
10.000	.2561	0.0640	0.0151	0.0031
12.000	.2515	0.0655	0.0156	0.0032
14.000	.2561	0.0661	0.0159	0.0032
16.000	.2537	0.0661	0.0160	0.0032
18.000	.2553	0.0659	0.0160	0.0032
20.000	.2572	0.0656	0.0160	0.0033
22.000	.2565	0.0653	0.0159	0.0032
24.000	.2563	0.0651	0.0159	0.0032
26.000	.2561	0.0650	0.0159	0.0032
28.000	.2561	0.0649	0.0159	0.0032
30.000	.2561	0.0649	0.0158	0.0032
32.000	.2561	0.0649	0.0158	0.0032
34.000	.2561	0.0649	0.0158	0.0032
36.000	.2561	0.0649	0.0158	0.0032
38.000	.2561	0.0649	0.0158	0.0032
40.000	.2561	0.0649	0.0158	0.0032
42.000	.2561	0.0649	0.0158	0.0032
44.000	.2561	0.0649	0.0158	0.0032
46.000	.2561	0.0649	0.0158	0.0032
48.000	.2561	0.0649	0.0158	0.0032
50.000	.2561	0.0649	0.0158	0.0032
52.000	.2561	0.0649	0.0158	0.0032
54.000	.2561	0.0649	0.0158	0.0032
56.000	.2561	0.0649	0.0158	0.0032
58.000	.2561	0.0649	0.0158	0.0032
60.000	.2561	0.0649	0.0158	0.0032
62.000	.2561	0.0649	0.0158	0.0032
64.000	.2561	0.0649	0.0158	0.0032
66.000	.2561	0.0649	0.0158	0.0032
68.000	.2561	0.0649	0.0158	0.0032
70.000	.2561	0.0649	0.0158	0.0032
72.000	.2561	0.0649	0.0158	0.0032
74.000	.2561	0.0649	0.0158	0.0032
76.000	.2561	0.0649	0.0158	0.0032
78.000	.2561	0.0649	0.0158	0.0032
80.000	.2561	0.0649	0.0158	0.0032
82.000	.2561	0.0649	0.0158	0.0032
84.000	.2561	0.0649	0.0158	0.0032
86.000	.2561	0.0649	0.0158	0.0032
88.000	.2561	0.0649	0.0158	0.0032
90.000	.2561	0.0649	0.0158	0.0032
92.000	.2561	0.0649	0.0158	0.0032
94.000	.2561	0.0649	0.0158	0.0032
96.000	.2561	0.0649	0.0158	0.0032
98.000	.2561	0.0649	0.0158	0.0032
100.000	.2561	0.0649	0.0158	0.0032
102.000	.2561	0.0649	0.0158	0.0032

CONTROLLER GAIN 8.0

TIME	OUTPUT 19	OUTPUT 18	OUTPUT 17	OUTPUT 16
0.000	.1494	0.0443	0.0125	0.0029
2.000	.1973	0.0464	0.0126	0.0029
4.000	.2284	0.0519	0.0130	0.0029
6.000	.2433	0.0567	0.0136	0.0029
8.000	.2517	0.0601	0.0142	0.0030
10.000	.2546	0.0620	0.0146	0.0030
12.000	.2546	0.0628	0.0148	0.0030
14.000	.2536	0.0630	0.0150	0.0030
16.000	.2527	0.0629	0.0150	0.0030
18.000	.2519	0.0627	0.0150	0.0030
20.000	.2513	0.0625	0.0150	0.0030
22.000	.2507	0.0624	0.0149	0.0030
24.000	.2506	0.0623	0.0149	0.0030
26.000	.2505	0.0623	0.0149	0.0030
28.000	.2505	0.0623	0.0149	0.0030
30.000	.2507	0.0623	0.0149	0.0030
32.000	.2507	0.0623	0.0149	0.0030
34.000	.2507	0.0623	0.0149	0.0030
36.000	.2507	0.0623	0.0149	0.0030
38.000	.2507	0.0623	0.0149	0.0030
40.000	.2507	0.0623	0.0149	0.0030
42.000	.2507	0.0623	0.0149	0.0030
44.000	.2507	0.0623	0.0149	0.0030
46.000	.2507	0.0623	0.0149	0.0030
48.000	.2507	0.0623	0.0149	0.0030
50.000	.2507	0.0623	0.0149	0.0030
52.000	.2507	0.0623	0.0149	0.0030
54.000	.2507	0.0623	0.0149	0.0030
56.000	.2507	0.0623	0.0149	0.0030
58.000	.2507	0.0623	0.0149	0.0030
60.000	.2507	0.0623	0.0149	0.0030
62.000	.2507	0.0623	0.0149	0.0030
64.000	.2507	0.0623	0.0149	0.0030
66.000	.2507	0.0623	0.0149	0.0030
68.000	.2507	0.0623	0.0149	0.0030
70.000	.2507	0.0623	0.0149	0.0030
72.000	.2507	0.0623	0.0149	0.0030
74.000	.2507	0.0623	0.0149	0.0030
76.000	.2507	0.0623	0.0149	0.0030
78.000	.2507	0.0623	0.0149	0.0030
80.000	.2507	0.0623	0.0149	0.0030
82.000	.2507	0.0623	0.0149	0.0030
84.000	.2507	0.0623	0.0149	0.0030
86.000	.2507	0.0623	0.0149	0.0030
88.000	.2507	0.0623	0.0149	0.0030
90.000	.2507	0.0623	0.0149	0.0030
92.000	.2507	0.0623	0.0149	0.0030
94.000	.2507	0.0623	0.0149	0.0030
96.000	.2507	0.0623	0.0149	0.0030
98.000	.2507	0.0623	0.0149	0.0030
100.000	.2507	0.0623	0.0149	0.0030
102.000	.2507	0.0624	0.0149	0.0030

3 3

OF/DE

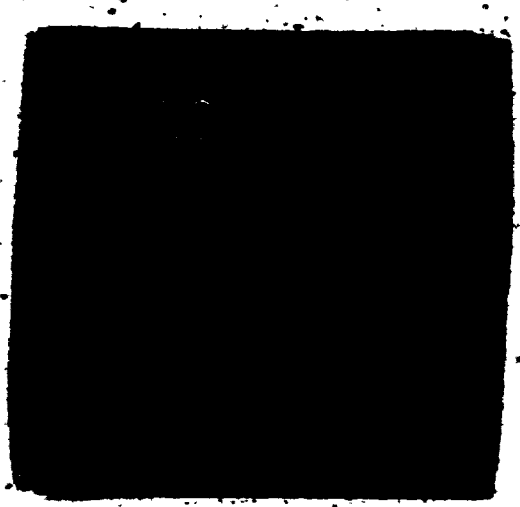

CONTROLLER GAIN 16.0

TIME	OUTPUT 19	OUTPUT 18	OUTPUT 17	OUTPUT 16
0.000	0.1498	0.0443	0.0125	0.0029
2.000	0.1973	0.0469	0.0126	0.0029
4.000	0.2262	0.0519	0.0130	0.0029
6.000	0.2427	0.0565	0.0136	0.0029
8.000	0.2505	0.0597	0.0141	0.0029
10.000	0.2531	0.0615	0.0144	0.0029
12.000	0.2530	0.0622	0.0147	0.0029
14.000	0.2521	0.0623	0.0148	0.0029
16.000	0.2511	0.0622	0.0148	0.0030
18.000	0.2503	0.0621	0.0148	0.0030
20.000	0.2499	0.0619	0.0148	0.0030
22.000	0.2497	0.0618	0.0147	0.0030
24.000	0.2496	0.0618	0.0147	0.0029
26.000	0.2496	0.0618	0.0147	0.0029
28.000	0.2496	0.0618	0.0147	0.0029
30.000	0.2496	0.0618	0.0147	0.0029
32.000	0.2496	0.0618	0.0147	0.0029
34.000	0.2497	0.0618	0.0147	0.0029
36.000	0.2497	0.0618	0.0147	0.0029
38.000	0.2497	0.0618	0.0147	0.0029
40.000	0.2497	0.0618	0.0147	0.0029
42.000	0.2497	0.0618	0.0147	0.0029
44.000	0.2497	0.0618	0.0147	0.0029
46.000	0.2497	0.0618	0.0147	0.0029
48.000	0.2497	0.0618	0.0147	0.0029
50.000	0.2497	0.0618	0.0147	0.0029
52.000	0.2497	0.0618	0.0147	0.0029
54.000	0.2497	0.0618	0.0147	0.0029
56.000	0.2497	0.0618	0.0147	0.0029
58.000	0.2497	0.0618	0.0147	0.0029
60.000	0.2497	0.0618	0.0147	0.0029
62.000	0.2497	0.0618	0.0147	0.0029
64.000	0.2497	0.0618	0.0147	0.0029
66.000	0.2497	0.0618	0.0147	0.0029
68.000	0.2497	0.0618	0.0147	0.0029
70.000	0.2497	0.0618	0.0147	0.0029
72.000	0.2497	0.0618	0.0147	0.0029
74.000	0.2497	0.0618	0.0147	0.0029
76.000	0.2497	0.0618	0.0147	0.0029
78.000	0.2497	0.0618	0.0147	0.0029
80.000	0.2497	0.0618	0.0147	0.0029
82.000	0.2497	0.0618	0.0147	0.0029
84.000	0.2497	0.0618	0.0147	0.0029
86.000	0.2497	0.0618	0.0147	0.0029
88.000	0.2497	0.0618	0.0147	0.0029
90.000	0.2497	0.0618	0.0147	0.0029
92.000	0.2497	0.0618	0.0147	0.0029
94.000	0.2497	0.0618	0.0147	0.0029
96.000	0.2497	0.0618	0.0147	0.0029
98.000	0.2497	0.0618	0.0147	0.0029
100.000	0.2497	0.0618	0.0147	0.0029
102.000	0.2497	0.0618	0.0147	0.0029

COMPUTER OUTPUTS FOR

FIGURE 47

(PLOTS REFER TO OUTPUT 16)

CONTROLLER GAIN 1.0

TIME	OUTPUT 19	OUTPUT 18	OUTPUT 17	OUTPUT 16
0.000	0.1498	0.0443	0.0125	0.0029
1.000	0.1498	0.0444	0.0128	0.0034
2.000	0.1504	0.0453	0.0136	0.0039
3.000	0.1524	0.0470	0.0147	0.0044
4.000	0.1562	0.0495	0.0159	0.0047
5.000	0.1617	0.0525	0.0171	0.0050
6.000	0.1684	0.0558	0.0183	0.0052
7.000	0.1757	0.0592	0.0192	0.0053
8.000	0.1829	0.0623	0.0201	0.0054
9.000	0.1895	0.0650	0.0207	0.0055
10.000	0.1949	0.0673	0.0213	0.0056
11.000	0.1990	0.0691	0.0218	0.0056
12.000	0.2018	0.0704	0.0221	0.0057
13.000	0.2033	0.0713	0.0224	0.0057
14.000	0.2037	0.0719	0.0226	0.0057
15.000	0.2033	0.0721	0.0227	0.0057
16.000	0.2023	0.0721	0.0228	0.0057
17.000	0.2008	0.0719	0.0228	0.0058
18.000	0.1991	0.0715	0.0228	0.0058
19.000	0.1971	0.0710	0.0227	0.0058
20.000	0.1952	0.0704	0.0227	0.0058
21.000	0.1932	0.0698	0.0226	0.0058
22.000	0.1917	0.0692	0.0225	0.0058
23.000	0.1894	0.0685	0.0224	0.0057
24.000	0.1878	0.0679	0.0223	0.0057
25.000	0.1862	0.0673	0.0221	0.0057
26.000	0.1848	0.0667	0.0220	0.0057
27.000	0.1836	0.0662	0.0219	0.0057
28.000	0.1825	0.0657	0.0218	0.0057
29.000	0.1815	0.0652	0.0217	0.0057
30.000	0.1807	0.0648	0.0216	0.0057
31.000	0.1801	0.0645	0.0215	0.0057
32.000	0.1795	0.0641	0.0214	0.0057
33.000	0.1791	0.0639	0.0213	0.0057
34.000	0.1787	0.0636	0.0213	0.0057
35.000	0.1785	0.0634	0.0212	0.0057
36.000	0.1783	0.0633	0.0212	0.0057
37.000	0.1782	0.0632	0.0211	0.0057
38.000	0.1781	0.0631	0.0211	0.0056
39.000	0.1781	0.0630	0.0211	0.0056
40.000	0.1782	0.0630	0.0210	0.0056
41.000	0.1783	0.0630	0.0210	0.0056
42.000	0.1784	0.0629	0.0210	0.0056
43.000	0.1785	0.0630	0.0210	0.0056
44.000	0.1786	0.0630	0.0210	0.0056
45.000	0.1788	0.0630	0.0210	0.0056
46.000	0.1789	0.0631	0.0210	0.0056
47.000	0.1791	0.0631	0.0210	0.0056
48.000	0.1792	0.0631	0.0210	0.0056
49.000	0.1794	0.0632	0.0210	0.0056
50.000	0.1795	0.0632	0.0210	0.0056
51.000	0.1796	0.0633	0.0210	0.0056

52.000	0.1797	0.0633	C.0211	0.0056
53.000	0.1799	0.0634	0.0211	0.0056
54.000	0.1799	0.0634	0.0211	0.0056
55.000	0.1800	0.0635	0.0211	0.0056
56.000	0.1801	0.0635	0.0211	0.0056
57.000	0.1802	0.0635	0.0211	0.0056
58.000	0.1802	0.0636	0.0211	0.0056
59.000	0.1803	0.0636	0.0211	0.0056
60.000	0.1803	0.0636	0.0211	0.0056
61.000	0.1803	0.0636	0.0211	0.0056
62.000	0.1803	0.0636	0.0211	0.0056
63.000	0.1804	0.0637	0.0211	0.0056
64.000	0.1804	0.0637	0.0211	0.0056
65.000	0.1804	0.0637	0.0211	0.0056
66.000	0.1804	0.0637	0.0211	0.0056
67.000	0.1804	0.0637	0.0211	0.0056
68.000	0.1804	0.0637	0.0211	0.0056
69.000	0.1803	0.0637	0.0211	0.0056
70.000	0.1803	0.0637	0.0211	0.0056
71.000	0.1803	0.0637	0.0211	0.0056
72.000	0.1803	0.0637	0.0211	0.0056
73.000	0.1803	0.0637	0.0211	0.0056
74.000	0.1803	0.0637	0.0211	0.0056
75.000	0.1803	0.0637	0.0211	0.0056
76.000	0.1803	0.0637	0.0211	0.0056
77.000	0.1802	0.0637	0.0211	0.0056
78.000	0.1802	0.0636	0.0211	0.0056
79.000	0.1802	0.0636	0.0211	0.0056
80.000	0.1802	0.0636	0.0211	0.0056
81.000	0.1802	0.0636	0.0211	0.0056
82.000	0.1802	0.0636	0.0211	0.0056
83.000	0.1802	0.0636	0.0211	0.0056
84.000	0.1802	0.0636	0.0211	0.0056
85.000	0.1802	0.0636	0.0211	0.0056
86.000	0.1802	0.0636	0.0211	0.0056
87.000	0.1802	0.0636	0.0211	0.0056
88.000	0.1802	0.0636	0.0211	0.0056
89.000	0.1802	0.0636	0.0211	0.0056
90.000	0.1802	0.0636	0.0211	0.0056
91.000	0.1802	0.0636	0.0211	0.0056
92.000	0.1802	0.0636	0.0211	0.0056
93.000	0.1802	0.0636	0.0211	0.0056
94.000	0.1802	0.0636	0.0211	0.0056
95.000	0.1802	0.0636	0.0211	0.0056
96.000	0.1802	0.0636	0.0211	0.0056
97.000	0.1802	0.0636	0.0211	0.0056
98.000	0.1802	0.0636	0.0211	0.0056
99.000	0.1802	0.0636	0.0211	0.0056
100.000	0.1802	0.0636	0.0211	0.0056

CONTROLLER GAIN 16.0

TIME	OUTPUT 19	OUTPUT 18	OUTPUT 17	OUTPUT 16
0.000	0.1498	0.0443	0.0125	0.0029
1.000	0.1495	0.0444	0.0128	0.0034
2.000	0.1504	0.0453	0.0136	0.0039
3.000	0.1524	0.0470	0.0147	0.0044
4.000	0.1562	0.0495	0.0161	0.0050
5.000	0.1620	0.0530	0.0178	0.0057
6.000	0.1696	0.0572	0.0195	0.0060
7.000	0.1786	0.0617	0.0208	0.0060
8.000	0.1879	0.0658	0.0218	0.0060
9.000	0.1964	0.0692	0.0224	0.0060
10.000	0.2033	0.0717	0.0229	0.0060
11.000	0.2080	0.0736	0.0232	0.0060
12.000	0.2107	0.0747	0.0235	0.0060
13.000	0.2116	0.0753	0.0236	0.0060
14.000	0.2111	0.0754	0.0237	0.0060
15.000	0.2096	0.0753	0.0237	0.0060
16.000	0.2074	0.0748	0.0237	0.0060
17.000	0.2049	0.0743	0.0237	0.0060
18.000	0.2022	0.0736	0.0236	0.0060
19.000	0.1995	0.0728	0.0235	0.0060
20.000	0.1970	0.0720	0.0234	0.0060
21.000	0.1945	0.0712	0.0233	0.0060
22.000	0.1923	0.0705	0.0232	0.0060
23.000	0.1903	0.0697	0.0230	0.0060
24.000	0.1886	0.0691	0.0229	0.0060
25.000	0.1870	0.0684	0.0228	0.0060
26.000	0.1857	0.0679	0.0227	0.0060
27.000	0.1846	0.0674	0.0226	0.0060
28.000	0.1837	0.0669	0.0225	0.0060
29.000	0.1829	0.0665	0.0224	0.0060
30.000	0.1823	0.0662	0.0224	0.0060
31.000	0.1819	0.0659	0.0223	0.0060
32.000	0.1815	0.0657	0.0222	0.0060
33.000	0.1813	0.0655	0.0222	0.0060
34.000	0.1812	0.0653	0.0221	0.0060
35.000	0.1811	0.0652	0.0221	0.0060
36.000	0.1811	0.0651	0.0221	0.0060
37.000	0.1811	0.0651	0.0221	0.0060
38.000	0.1812	0.0651	0.0220	0.0060
39.000	0.1813	0.0650	0.0220	0.0060
40.000	0.1814	0.0650	0.0220	0.0060
41.000	0.1816	0.0651	0.0220	0.0060
42.000	0.1817	0.0651	0.0220	0.0060
43.000	0.1819	0.0651	0.0220	0.0060
44.000	0.1820	0.0652	0.0220	0.0060
45.000	0.1822	0.0652	0.0220	0.0060
46.000	0.1823	0.0653	0.0220	0.0060
47.000	0.1825	0.0653	0.0220	0.0060
48.000	0.1826	0.0653	0.0220	0.0060
49.000	0.1827	0.0654	0.0220	0.0060
50.000	0.1828	0.0654	0.0221	0.0060
51.000	0.1829	0.0655	0.0221	0.0060

52.COC	0.1829	0.0655	0.0221	0.0060
53.COC	0.1830	0.0655	0.0221	0.0060
54.000	0.1831	0.0656	0.0221	0.0060
55.COC	0.1831	0.0656	0.0221	0.0060
56.COC	0.1831	0.0656	0.0221	0.0060
57.COC	0.1832	0.0656	0.0221	0.0060
58.000	0.1832	0.0656	0.0221	0.0060
59.000	0.1832	0.0656	0.0221	0.0060
60.COC	0.1832	0.0656	0.0221	0.0060
61.COC	0.1832	0.0657	0.0221	0.0060
62.COC	0.1832	0.0657	0.0221	0.0060
63.COC	0.1832	0.0657	0.0221	0.0060
64.000	0.1832	0.0657	0.0221	0.0060
65.COC	0.1832	0.0657	0.0221	0.0060
66.COC	0.1832	0.0657	0.0221	0.0060
67.COC	0.1832	0.0657	0.0221	0.0060
68.COC	0.1832	0.0657	0.0221	0.0060
69.COC	0.1831	0.0657	0.0221	0.0060
70.COC	0.1831	0.0657	0.0221	0.0060
71.COC	0.1831	0.0656	0.0221	0.0060
72.COC	0.1831	0.0656	0.0221	0.0060
73.COC	0.1831	0.0656	0.0221	0.0060
74.COC	0.1831	0.0656	0.0221	0.0060
75.COC	0.1831	0.0656	0.0221	0.0060
76.COC	0.1831	0.0656	0.0221	0.0060
77.COC	0.1831	0.0656	0.0221	0.0060
78.000	0.1831	0.0656	0.0221	0.0060
79.COC	0.1831	0.0656	0.0221	0.0060
80.COC	0.1831	0.0656	0.0221	0.0060
81.000	0.1831	0.0656	0.0221	0.0060
82.COC	0.1831	0.0656	0.0221	0.0060
83.000	0.1831	0.0656	0.0221	0.0060
84.COC	0.1831	0.0656	0.0221	0.0060
85.COC	0.1831	0.0656	0.0221	0.0060
86.COC	0.1831	0.0656	0.0221	0.0060
87.COC	0.1831	0.0656	0.0221	0.0060
88.COC	0.1831	0.0656	0.0221	0.0060
89.000	0.1831	0.0656	0.0221	0.0060
90.COC	0.1831	0.0656	0.0221	0.0060
91.COC	0.1831	0.0656	0.0221	0.0060
92.COC	0.1831	0.0656	0.0221	0.0060
93.000	0.1831	0.0656	0.0221	0.0060
94.COC	0.1831	0.0656	0.0221	0.0060
95.COC	0.1831	0.0656	0.0221	0.0060
96.COC	0.1831	0.0656	0.0221	0.0060
97.COC	0.1831	0.0656	0.0221	0.0060
98.COC	0.1831	0.0656	0.0221	0.0060
99.COC	0.1831	0.0656	0.0221	0.0060
100.COC	0.1831	0.0656	0.0221	0.0060

COMPUTER OUTPUTS FOR

FIGURE 48

(PLOTS REFER TO OUTPUT 16)

TIME CONSTANT 2.0 MIN

TIME	OUTPUT 19	OUTPUT 18	OUTPUT 17	OUTPUT 16
0.000	0.1498	0.0443	0.0125	0.0029
2.000	0.1499	0.0445	0.0127	0.0031
4.000	0.1512	0.0455	0.0133	0.0033
6.000	0.1542	0.0470	0.0139	0.0034
8.000	0.1583	0.0489	0.0145	0.0036
10.000	0.1627	0.0509	0.0152	0.0038
12.000	0.1669	0.0529	0.0159	0.0040
14.000	0.1706	0.0549	0.0166	0.0042
16.000	0.1739	0.0567	0.0173	0.0044
18.000	0.1767	0.0584	0.0179	0.0046
20.000	0.1791	0.0600	0.0186	0.0047
22.000	0.1811	0.0614	0.0192	0.0049
24.000	0.1828	0.0627	0.0198	0.0051
26.000	0.1843	0.0639	0.0204	0.0053
28.000	0.1856	0.0650	0.0209	0.0055
30.000	0.1868	0.0659	0.0214	0.0056
32.000	0.1878	0.0668	0.0219	0.0058
34.000	0.1887	0.0676	0.0223	0.0059
36.000	0.1895	0.0683	0.0227	0.0061
38.000	0.1902	0.0690	0.0231	0.0062
40.000	0.1908	0.0696	0.0234	0.0063
42.000	0.1913	0.0701	0.0238	0.0065
44.000	0.1919	0.0706	0.0240	0.0066
46.000	0.1923	0.0710	0.0243	0.0067
48.000	0.1927	0.0714	0.0245	0.0068
50.000	0.1931	0.0718	0.0248	0.0068
52.000	0.1934	0.0722	0.0250	0.0069
54.000	0.1937	0.0725	0.0252	0.0070
56.000	0.1940	0.0727	0.0253	0.0071
58.000	0.1943	0.0730	0.0255	0.0071
60.000	0.1945	0.0732	0.0256	0.0072
62.000	0.1947	0.0734	0.0258	0.0072
64.000	0.1949	0.0736	0.0259	0.0073
66.000	0.1951	0.0738	0.0260	0.0073
68.000	0.1952	0.0740	0.0261	0.0073
70.000	0.1954	0.0741	0.0262	0.0074
72.000	0.1955	0.0742	0.0263	0.0074
74.000	0.1956	0.0744	0.0263	0.0074
76.000	0.1957	0.0745	0.0264	0.0075
78.000	0.1958	0.0746	0.0265	0.0075
80.000	0.1959	0.0747	0.0265	0.0075
82.000	0.1960	0.0748	0.0266	0.0076
84.000	0.1961	0.0748	0.0266	0.0076
86.000	0.1962	0.0749	0.0267	0.0076
88.000	0.1962	0.0750	0.0267	0.0076
90.000	0.1963	0.0750	0.0268	0.0076
92.000	0.1963	0.0751	0.0268	0.0076
94.000	0.1964	0.0751	0.0268	0.0076
96.000	0.1964	0.0752	0.0269	0.0076
98.000	0.1965	0.0752	0.0269	0.0077
100.000	0.1965	0.0753	0.0269	0.0077

TIME CONSTANT 0.3 MIN

TIME	OUTPUT 19	OUTPUT 18	OUTPUT 17	OUTPUT 16
0.000	0.1498	0.0443	0.0125	0.0029
2.000	0.1605	0.0458	0.0133	0.0032
4.000	0.1709	0.0487	0.0143	0.0034
6.000	0.1752	0.0517	0.0152	0.0037
8.000	0.1769	0.0546	0.0162	0.0040
10.000	0.1785	0.0572	0.0171	0.0042
12.000	0.1803	0.0594	0.0181	0.0045
14.000	0.1822	0.0613	0.0189	0.0048
16.000	0.1839	0.0630	0.0198	0.0050
18.000	0.1854	0.0644	0.0205	0.0053
20.000	0.1863	0.0657	0.0212	0.0055
22.000	0.1880	0.0668	0.0218	0.0057
24.000	0.1890	0.0678	0.0224	0.0059
26.000	0.1899	0.0686	0.0229	0.0061
28.000	0.1907	0.0694	0.0233	0.0063
30.000	0.1914	0.0701	0.0237	0.0064
32.000	0.1920	0.0707	0.0241	0.0066
34.000	0.1925	0.0712	0.0244	0.0067
36.000	0.1930	0.0717	0.0247	0.0068
38.000	0.1934	0.0721	0.0250	0.0069
40.000	0.1938	0.0725	0.0252	0.0070
42.000	0.1942	0.0729	0.0254	0.0071
44.000	0.1945	0.0732	0.0256	0.0071
46.000	0.1947	0.0734	0.0258	0.0072
48.000	0.1950	0.0737	0.0259	0.0073
50.000	0.1952	0.0739	0.0260	0.0073
52.000	0.1954	0.0741	0.0262	0.0074
54.000	0.1955	0.0742	0.0263	0.0074
56.000	0.1957	0.0744	0.0264	0.0074
58.000	0.1958	0.0745	0.0264	0.0075
60.000	0.1959	0.0747	0.0265	0.0075
62.000	0.1960	0.0748	0.0266	0.0075
64.000	0.1961	0.0749	0.0267	0.0076
66.000	0.1962	0.0749	0.0267	0.0076
68.000	0.1963	0.0750	0.0268	0.0076
70.000	0.1963	0.0751	0.0268	0.0076
72.000	0.1964	0.0751	0.0268	0.0076
74.000	0.1965	0.0752	0.0269	0.0076
76.000	0.1965	0.0753	0.0269	0.0077
78.000	0.1966	0.0753	0.0269	0.0077
80.000	0.1966	0.0753	0.0270	0.0077
82.000	0.1966	0.0754	0.0270	0.0077
84.000	0.1966	0.0754	0.0270	0.0077
86.000	0.1967	0.0754	0.0270	0.0077
88.000	0.1967	0.0755	0.0270	0.0077
90.000	0.1967	0.0755	0.0270	0.0077
92.000	0.1967	0.0755	0.0271	0.0077
94.000	0.1968	0.0755	0.0271	0.0077
96.000	0.1968	0.0755	0.0271	0.0077
98.000	0.1968	0.0755	0.0271	0.0077
100.000	0.1968	0.0756	0.0271	0.0077

TIME CONSTANT 0.26 MIN

TIME	OUTPUT 19	OUTPUT 18	OUTPUT 17	OUTPUT 16
0.000	0.1495	0.0443	0.0125	0.0029
2.000	0.1727	0.0444	0.0134	0.0032
4.000	0.2116	0.0093	0.0114	0.0033
6.000	0.2603	0.0381	0.0107	0.0032
8.000	0.2890	0.0586	0.0127	0.0033
10.000	0.2980	0.0737	0.0158	0.0035
12.000	0.2985	0.0836	0.0192	0.0041
14.000	0.2716	0.0895	0.0224	0.0047
16.000	0.2465	0.0914	0.0250	0.0054
18.000	0.2207	0.0904	0.0269	0.0061
20.000	0.1983	0.0874	0.0281	0.0067
22.000	0.1814	0.0835	0.0287	0.0072
24.000	0.1703	0.0795	0.0287	0.0076
26.000	0.1640	0.0759	0.0285	0.0078
28.000	0.1611	0.0730	0.0280	0.0079
30.000	0.1603	0.0707	0.0274	0.0079
32.000	0.1609	0.0690	0.0268	0.0078
34.000	0.1624	0.0678	0.0262	0.0077
36.000	0.1643	0.0671	0.0257	0.0076
38.000	0.1665	0.0667	0.0253	0.0075
40.000	0.1688	0.0666	0.0250	0.0074
42.000	0.1712	0.0667	0.0248	0.0073
44.000	0.1735	0.0669	0.0246	0.0072
46.000	0.1757	0.0673	0.0245	0.0071
48.000	0.1778	0.0677	0.0245	0.0071
50.000	0.1797	0.0681	0.0245	0.0071
52.000	0.1815	0.0686	0.0245	0.0070
54.000	0.1831	0.0692	0.0246	0.0070
56.000	0.1845	0.0697	0.0247	0.0070
58.000	0.1857	0.0702	0.0248	0.0070
60.000	0.1868	0.0707	0.0249	0.0071
62.000	0.1878	0.0711	0.0250	0.0071
64.000	0.1885	0.0716	0.0252	0.0071
66.000	0.1889	0.0721	0.0253	0.0072
68.000	0.1896	0.0726	0.0255	0.0072
70.000	0.1778	0.0757	0.0257	0.0072
72.000	0.1846	0.0737	0.0260	0.0073
74.000	0.1887	0.0730	0.0261	0.0073
76.000	0.1912	0.0728	0.0261	0.0074
78.000	0.1927	0.0730	0.0261	0.0074
80.000	0.1937	0.0732	0.0261	0.0074
82.000	0.1943	0.0735	0.0262	0.0074
84.000	0.1948	0.0737	0.0262	0.0075
86.000	0.1951	0.0740	0.0263	0.0075
88.000	0.1954	0.0742	0.0264	0.0075
90.000	0.1956	0.0743	0.0264	0.0075
92.000	0.1958	0.0745	0.0265	0.0075
94.000	0.1959	0.0746	0.0266	0.0075
96.000	0.1961	0.0747	0.0266	0.0076
98.000	0.1962	0.0748	0.0267	0.0076
100.000	0.1963	0.0749	0.0267	0.0076

TIME CONSTANT 0.2575 MIN

TIME	OUTPUT 15	OUTPUT 16	OUTPUT 17	OUTPUT 18
0.000	0.1495	0.0443	0.0125	0.0029
2.000	0.1740	0.0442	0.0134	0.0032
4.000	0.2476	0.0696	0.0155	0.0035
6.000	0.3107	0.0794	0.0176	0.0043
8.000	0.3633	0.0926	0.0220	0.0046
10.000	0.4000	0.1066	0.0257	0.0054
12.000	0.4169	0.1194	0.0297	0.0063
14.000	0.4204	0.1301	0.0327	0.0072
16.000	0.4065	0.1369	0.0374	0.0085
18.000	0.3802	0.1420	0.0406	0.0095
20.000	0.3455	0.1394	0.0430	0.0107
22.000	0.3067	0.1365	0.0446	0.0116
24.000	0.2682	0.1292	0.0453	0.0119
26.000	0.2330	0.1213	0.0451	0.0000
28.000	0.2065	0.1129	0.0443	0.0000
30.000	0.1863	0.1044	0.0429	0.0000
32.000	0.1744	0.0968	0.0411	0.0000
34.000	0.1684	0.0903	0.0392	0.0000
36.000	0.1627	0.0850	0.0373	0.0116
38.000	0.1605	0.0807	0.0355	0.0112
40.000	0.1596	0.0773	0.0347	0.0107
42.000	0.1597	0.0746	0.0322	0.0103
44.000	0.1604	0.0725	0.0308	0.0098
46.000	0.1616	0.0709	0.0297	0.0094
48.000	0.1631	0.0697	0.0286	0.0090
50.000	0.1645	0.0689	0.0278	0.0087
52.000	0.1657	0.0683	0.0271	0.0084
54.000	0.1666	0.0680	0.0265	0.0081
56.000	0.1706	0.0678	0.0260	0.0079
58.000	0.1725	0.0678	0.0257	0.0077
60.000	0.1743	0.0679	0.0254	0.0076
62.000	0.1761	0.0681	0.0252	0.0075
64.000	0.1779	0.0683	0.0251	0.0074
66.000	0.1795	0.0687	0.0250	0.0073
68.000	0.1810	0.0690	0.0249	0.0072
70.000	0.1824	0.0694	0.0249	0.0072
72.000	0.1837	0.0697	0.0250	0.0072
74.000	0.1849	0.0701	0.0250	0.0072
76.000	0.1860	0.0705	0.0251	0.0072
78.000	0.1870	0.0709	0.0252	0.0072
80.000	0.1880	0.0712	0.0253	0.0072
82.000	0.1888	0.0716	0.0254	0.0072
84.000	0.1895	0.0719	0.0255	0.0072
86.000	0.1901	0.0722	0.0256	0.0072
88.000	0.1907	0.0725	0.0257	0.0073
90.000	0.1912	0.0728	0.0258	0.0073
92.000	0.1916	0.0731	0.0259	0.0073
94.000	0.1919	0.0734	0.0260	0.0074
96.000	0.1921	0.0736	0.0261	0.0074
98.000	0.1922	0.0739	0.0262	0.0074
100.000	0.1919	0.0742	0.0263	0.0074

BIBLIOGRAPHY

1. Zenz, F.A. and Othmer, D.F.; Fluidization and Fluid-Particle Systems, Reinhold Publishing Corporation, New York, 1960.

2. Raghuraman, J.; Saifert, A.; Varma, Y.B.G.; Indian Chemical Journal, 4(1), 10 (1969)

3. Ryozo Toei and Takeshi Akao, Symposium on Fluidization I - Tripartite Chem. Eng'ng Conf., Montreal, September 1968.

4. Rowson, H.M., Brit. Chem. Eng'ng. 8(3), 180 (1963)

5. Avery, D.A. and Tracey, D.H., Symposium on Fluidization I - Tripartite Chem. Eng'ng Conf., Montreal, September 1968.

6. Kunii, D. and Levenspiel, O., Fluidization Engineering, John Wiley and Sons, Inc., 1969.

7. Molodov, A.A. and Ishkin, I.P.; Izv. Vyssh. Vcheb. Zav., Khim. I Khimid. Techn., 9(2), 331 (1966).

8. Agarwal, J.C., et al., CEP, 58, 85 (Nov. 1962)

9. Rylec, M. and Standart, G., Int. Chem. Eng'ng 4(4), 711 (Oct. 1964)

10. Chem. Abs., 66, 12524Z (1967)

11. Flock, W., Chemische Technik, 16(11), 647 (1964)

12. Gel'perin, N.I., et al., Int. Chem. Eng'ng, 6(1), 4 (1966)

13. Angelino, H., et al., I. Chem. E. Symposium Series No.30, Instn.Chem. Engrs., London (1968)

14. Dean, S.K., Engineering, 179(4654), 430 (April 1955)

15. Continuous Weight Measurements of Drying Flowing Products, Noble Company, Oakland, Cal., 5M-1/65

16. Kumar, R., Chemical Engineering, 76, 196 (Oct.1969)

17. Nolte, C.B., Advances in Instrumentation, 24(4), 815:1-5, 1970.

18. Sankyo Impact Line Flowmeter, Miltronics Ltd., Peterborough, Ontario.

19. De Pollier, F.A., U.S. 3,212,330, Oct.19, 1965.

20. Seyl, O.E., U.S. 3,269,181, Aug. 30, 1966.

21. Soejima, T., et al., U.S. 3,613,449, Oct. 19, 1971.

22. Kajiura, H., et al., U.S. 3,611,803, Oct. 12, 1971.

23. Tomiyasu, H., U.S. 3,742,762, July 3, 1973.

24. McCune, L.C. and Gallier, D.W., ISA Transactions 12 (3), 193 (1973).

25. Harriott, P., Process Control, P. 288, McGraw-Hill Book Co., 1964.

26. Luyben, W., et al., Transient Response of Ten Tray Distillation Column, University of Delaware, Dept. of Chemical Engineering, August 1, 1963.

27. Kunii, D., Yoshida, K., and Hiraki, I., Proceedings of the International Symposium on Fluidization, Eindhoven, June 6-9, 1967.

28. Wahl, E.R., CEP, 69 (1); 62, (1973).

29. Lapidus, L., Digital Computation for Chemical Engineers, p. 88, McGraw-Hill Book Co., 1962.